

# CONTENTS

A STUDY ON STEEL AND IRON ENTERPRISES GREEN SUPPLY CHAIN MOTIVATION.....	XUELING NIE, XIAOLIN ZHU, BAOZHI ZHANG 315
IMPROVED ALGORITHM FOR AUTOMATIC TEXT SUMMARY BASED ON WEIGHT OF SENTENCE .....	YAJUAN TANG, DEXIAN ZHANG, LIN YANG 319
MULTI-USER DETECTION BASED ON IMPORTANCE RESAMPLING PARTICLE FILTER IN IMPULSIVE NOISE.....	XIAN JINLONG, LI SHENGJIE 322
THE REALIZATION OF FOOD CORPUS BASED ON DATABASE TECHNOLOGY.....	LIN C. YANG, DEXIAN B. ZHANG, YAJUAN A. TANG 327
RE-SAMPLING REVERSE ANALYSIS ON MEASUREMENT UNCERTAINTY BASED ON BOOTSTRAP SIMULATION.....	ZU XIAN-FENG, HAN YU-QIN 331
DRIVER FATIGUE DETECTION BASED ON ACTIVE FACIAL FEATURES LOCATING.....	CAIJIAN HUA YAN ZHANG 335
MEASUREMENT OF MOISTURE CONTENT IN SOYBEAN BY NEAR-INFRARED SPECTROSCOPY TECHNIQUE.....	HUANG NAN, WANG RUOLAN, YUE JIA 340
MECHANISM OF PIER DAMAGE UNDER THE ACTION OF HIGH FILLING.....	XUE RUI, TAO YING, WU YU342
COMPUTING THE LEAST QUANTILE OF SQUARES ESTIMATION WITH AGGREGATE HOMOPOTY METHOD.....	Z. G. YAN 347
TIME SENSITIVE SOCIAL-BASED PREDICTION ROUTING PROTOCOL IN SOCIALLY-AWARE OPPORTUNISTIC NETWORKS.....	LI LIU 351
RESEARCH ON PORTFOLIO RISK PREDICTION BASED ON COPULA-GJR-SKEWT MODEL.....	WEIWU YE, ZIMING LIU 354
ANALYSIS THE AFFECTION OF INTERACTION IN TEACHING OF EXPERIMENT.....	ZHU KE 359
THE ALLOCATION OF WHEELCHAIR AT AIRPORTS PROBLEM.....	ZHANG JIN 362
DESIGN AND IMPLEMENTATION OF FIRE FIGHTING ROBOT.....	YANG. GUIKAO, LIU. HAIBO, ZHANG QING 366
SURVEY ON SOLVING LARGE-SCALE COMPLEX OPTIMIZATION PROBLEMS.....	FAHUI GU, KANGSHUN LI, LEI YANG, YAN CHEN 368
INTRODUCTION TO THE TRAINING OF YOUNG TEACHERS' TEACHING ABILITY.....	LIU. HAIBO, YANG. GUIKAO JIANG LIN 371
STUDY ON HEATING SYSTEM BY USING WATER-SOURCE HEAT PUMP TO RECYCLE WASTE HEAT IN POWER PLANTS.....	BIN YANG, LIN WANG, DEGONG ZUO, CHENGYING QI 373

# A Study on Steel and Iron Enterprises Green Supply Chain Motivation

Xueling Nie, Xiaolin Zhu, Baozhi Zhang

School of Business Administration University of Science and Technology Liaoning Anshan, China

**Abstract**—In order to ensure the green supply chain management of the steel enterprise in china implemented effectively, a motivation contract was put forward to encourage the members of the supply chain to implement "green" reformation actively. The model based on principal-agent theory and contract theory was built to distinguish members who has really reformed, and analyse the effect of the contract on supply chain members' expectation profits and efficiency. Results show that the motivation contract can not only distinguish the true "green" reformer, but also can inspires supply chain members to carry out "green" reform effectively. The steel enterprise in china can construct green supply chain system with this model.

**Index Terms**—steel enterprise, green supply chain, motivation, contract

## I. INTRODUCTION

It is an effective way to cope with environmental degradation and energy crisis for steel enterprise that implements green supply chain management. But the green supply chain's construction is based on all the members of green supply chain who have the same supply chain strategic objectives, attach the importance to environment protection, and make their actions consistent with other members. Failure to do this, the green supply chain construction will be idle. The most amount of trouble for implementing green supply chain management includes the interest conflict of members and the goal incompatibility. Especially for the steel enterprise with serious pollution, the additional costs for environmental protection will always not be burden for the members of supply chain. It has been a hard problem for implementing green supply chain management that how to make member enterprises take environmental protection as the common goal, take activities with environment factor, and maximize the overall efficiency.

As we known, the motivation theory tells us that a suitable motivation system can inspire supply chain members to implement the "green" reform. So, it is necessary to construct a motivation system to settle the problem above. In particular, the steel enterprise can make a contract with supply chain members to inspire "green" reform and constrain environment pollution.

### I. Description of Green Supply Chain Motivation Model

There are two supply chain management models used by steel enterprises. One is that the enterprise will invest, merger or control the down-stream enterprises, turn the external problems into the internal problems, and implement green supply chain management by head office's overall

control, which is an integrative management model. The other is as follows. The enterprise will realize the member coordination and controlling by the power of leader, but the members still have autonomy in management, which is a mutual independent model.

No matter which model the enterprise select, the steel enterprise must cut pollution and implement green supply chain management based on contracts and rules, the steel enterprise also must establish supply chain green environmental protection rules and contracts to control and coordinate other member enterprises, and achieve environmental protection goal. This paper established an steel enterprise green supply chain motivation model, which depended on the principal-agent theory and contract theory. the models are described as below:

- Assume that there are "n" steel distributors belonged to two different types, and the 1st type distributors will be with higher administrative efficiency and full awareness of environmental protection, and be able to carry out "green" reforming in green supply chain environmental protection request. On the contrary, the second type distributors will be with lower efficiency and lack of awareness of environmental protection, and can not finish the "green" reforming initially. The paper makes "i" represents the type of the distributors,  $i = 1, 2$ . "1" represents the 1st type, and "2" represents the second type.
- The steel suppliers will only know  $100\theta_1\%$  distributors belongs to type 1,  $100\theta_2\%$  distributors belongs to type 2, and  $\theta_1 + \theta_2 = 1$ . But the steel suppliers will be not able to distinguish what type each distributor belongs to, for its private information.
- Assume that  $x$  represents the investments in "green" reforming, which is the steel consumers' evaluation for distributor's investments in "green" reforming. Since the modern consumers now attach great importance to the steel's environmental protection character, then we may consider steel demands as a increasing function depend on  $x$ . To aid study, it assumes that demand function is a Linear deterministic random demand function, which can be describe as  $Q = qx + \xi$ . "q" is a constant, representing "green" investment influence coefficient,  $q > 0$ , " $\xi$ " represents the random demands caused by other uncertainties, whose meaning is "0", and the variance is " $\sigma^2$ ".

- "Green" cost is related to distributor's type and "green" investments. For the same type distributors, the more they invests in "green" reforming, the more cost they will increase. In order to achieve the same "green" reforming result, the type 1 distributors will cost less than type 2 distributors, which means the type 1 distributors have higher efficiency than type 2, so they have lower unit cost. This condition is called Spence-Mirrlees condition<sup>[1]</sup>, it's a key condition to distinguish the effective information<sup>[1]</sup>. It assumes the distributors "green" cost function is  $C(i, x) = k_i x^2$ .  $k_i$  represents cost coefficient,  $i = 1, 2, k_1 < k_2$ .
- " $r$ " represents the retail price of "green" steel, and it is decided by steel supplier. " $c$ " represents the unit produce cost of "green" steel that is provided by supplier. " $w$ " represents wholesale price of "green" steel that is provided by distributors,  $r > w > c$ .
- Assumes that steel supplier and distributors are risk-neutral
- The steel supplier hold a leading post in setting contract, so the distributors can only select acceptance or rejection.
- The distributors' retaining profits are " $\Pi_b^+$ ", which represents distributors' opportunity cost of contract acceptance.
- The steel supplier will give a certain compensation and motivation to the distributors to inspire them to implement "green" reforming actively. Assume that steel supplier adopts a linear transfer payment contract  $(a_i, Q_{0i})$  to motivate the distributor. it is  $T_i = a_i(Q - Q_{0i})$ . " $T_i$ " represents the total transfer payments that the supplier gives the distributors. " $Q_{0i}$ " represents the lowest sales level that type " $i$ " distributors must reach to get compensation and motivation. " $a_i$ " represents the unit transfer payments that supplier pays to the distributors whose sales more than  $Q_{0i}$  (If the sales less than  $Q_{0i}$ , it represents negative transfer payments),  $i = 1, 2$ .

II. The Model in Integrative Management Model

In this model, the supply chain take the steel supplier as coordination and controlling core, then the type of distributor will be public information. There is no information asymmetry problem, so the supply profits will be

$$\Pi_{sc,j} = n\theta_1[(r-c)Q - k_1x_1^2] + n\theta_2[(r-c)Q + k_2x_2^2] \tag{1}$$

Its expectation profits will be

$$E\Pi_{sc,j} = n\theta_1[(r-c)q - k_1x_1^2] + n\theta_2[(r-c)q + k_2x_2^2] \tag{2}$$

For " $\partial E\Pi_{sc,i} / \partial x_i = 0$ ", the supply chain optimal "green" investments will be " $x_{i,j} = (r-c)q / 2k_i, i = 1, 2$ ", and supply expectation profits will be

$$E\Pi_{sc,i} = n \sum \theta_i [(r-c)^2 q^2 / 4k_i], i=1,2 \tag{3}$$

III. THE MODEL IN INDEPENDENT MANAGEMENT MODEL

A Information Symmetry Condition

In information symmetry condition, steel supplier knows all distributors' information, so the type of distributors " $i$ " is a known constant,  $i = 1, 2$ , and the supplier's profits function is

$$\Pi_{s,f} = n \sum \theta_i [(w-c)^2 Q - T_i] \tag{4}$$

Distributors' profits function of Type  $i$  can be described as

$$\Pi_{bi,f} = (r-w)Q - k_i x_i^2 + T_i \tag{5}$$

So the expectation profits of supplier and distributors will be

$$E\Pi_{s,f} = n \sum_{i=1}^2 \theta_i [(w-c)qx_{i,f} - a_i(qx_{i,f} - Q_{0i})] \tag{6}$$

$$E\Pi_{bi,f} = (r-w)qx_{i,f} - k_i x_i^2 + a_i(qx_{i,f} - Q_{0i}) \tag{7}$$

To maximize the profits, when  $\partial E\Pi_{bi,f} / \partial x_{i,f} = 0$ , only to satisfy the condition below can type  $i$  distributors get optimal "green" investments, means that it must satisfy incentive-compatibility constraint.

$$(IC) \quad x_{i,f} = \frac{r-w+a_i}{2k_i} q \quad i=1,2 \tag{8}$$

According to (8), the distributors' optimal "green" investments are in direct proportion to "green" investment influence coefficient and unit transfer payments, and in inverse proportion to cost coefficient

To ensure distributors to accept the contract, the distributors' profits must be no less than their retaining profits " $\Pi_b^+$ ", which means it must satisfy individual rationality constraint.

$$(IR) \quad (r-w)qx_{i,f} - k_i x_{i,f}^2 + a_i(qx_{i,f} - Q_{0i}) \geq \Pi_b^+, i=1,2 \tag{9}$$

So the problem the steel supplier faced with is how to maximize the expectation profits while satisfying the incentive-compatibility constraint and individual rationality constraint. We can draw the conclusion below after computing it.

$$a_i = w - c \tag{10}$$

$$Q_{0i} = \frac{[(r-c)^2 q^2 - 4k_i \Pi_b^+]}{4k_i(w-c)} \tag{11}$$

under the above rules, type  $i$  distributors' optimal "green" investments are " $x_{i,f} = (r-c)q/2k_i$ ", and the expectation profits are " $\Pi_b^+$ ". Steel supplier's expectation profits are

$$E \Pi_{sc,f} = n \sum_i \theta_i [(r-c)^2 q^2 / 4k_i - \Pi_b^+], i=1,2 \quad (12)$$

The whole supply chain expectation profits are

$$E \Pi_{sc,f} = n \sum_i \theta_i [(r-c)^2 q^2 / 4k_i], i=1,2 \quad (13)$$

All of above show that in information symmetry condition, no matter what type the distributors belong to, they only can get the retaining profits. The additional profits of supply chain caused by increasing efficiency will be got by the steel supplier.

**B Information Asymmetry Condition**

In real business operation, usually the steel supplier will not know the type of the distributor, due to information asymmetry. To distinguish the real type of the distributors, the steel supplier may design a series of contract  $(a_1, Q_{01}), (a_2, Q_{02}), (a_3, Q_{03}) \dots$ . This paper only have two different type of distributors, and its type space is  $(1,2)$ . According to Myerson revelation principle<sup>[2]</sup>, signal space is same to type space  $(1,2)$ , the configuration function is  $(a_1, Q_{01})$  and  $(a_2, Q_{02})$ , and it will lure distributors to say the real type. Now to solve the concrete form of the configuration function.

Assume that in the above contract, type  $i$  distributors' "green" investments are  $x_{i,a}$ , and the supplier's expectation profits function will be

$$E \Pi_{s,a} = n \sum_{i=1}^2 \theta_i [(w-c)qx_{i,a} - a_i(qx_{i,a} - Q_{0i})] \quad (14)$$

Type  $i$  distributors' expectation profits function is

$$E \Pi_{bi,a} = (r-w)qx_{i,a} - k_i x_{i,a}^2 + a_i(qx_{i,a} - Q_{0i}) \quad (15)$$

Distributors are independent of supplier, so this contract must satisfy incentive-compatibility constraint, similar to (8), and it can be concluded that

$$(IC_i) \quad x_{i,a} = \frac{r-w+a_i}{2k_i} q, \quad i=1,2 \quad (16)$$

Similar to (4), to ensure distributors accepting the contract, it must satisfy distributors' individual rationality constraint.

$$(IR_i) \quad (r-w)qx_{i,a} - k_i x_{i,a}^2 + a_i(qx_{i,a} - Q_{0i}) \geq \Pi_b^+ \quad (17)$$

To ensure distributors not lying about their type, the contract must satisfy separating equilibrium condition, that is incentive-compatibility constraint.

$$(IC_3) \quad (r-w)qx_{1,a} - k_1 x_{1,a}^2 + a_1(qx_{1,a} - Q_{01}) \geq (r-w)q^2 \bullet$$

$$\frac{r-w+a_2}{2k_1} - k_1 \left( \frac{r-w+a_2}{2k_1} q \right)^2 + a_2 \left( q^2 \frac{r-w+a_2}{2k_1} - Q_{02} \right) \quad (18)$$

$$(IC_4) \quad (r-w)qx_{2,a} - k_2 x_{2,a}^2 + a_2(qx_{2,a} - Q_{02}) \geq (r-w)q^2 \bullet$$

$$\frac{r-w+a_1}{2k_2} - k_2 \left( \frac{r-w+a_1}{2k_2} q \right)^2 + a_1 \left( q^2 \frac{r-w+a_1}{2k_2} - Q_{01} \right) \quad (19)$$

Equation (18) ensure type 1 distributors not being active in pretending that they are type 2, and equation (19) ensure type 2 distributors not being active in pretending that they are type 2

To inspire distributors to implement "green" reforming actively, and enhance supply chain competitiveness, the expectation profits of type 1 distributors should be more than the profits of type 2.

$$(IC_5) \quad (r-w)qx_{1,a} - k_1 x_{1,a}^2 + a_1(qx_{1,a} - Q_{01}) \geq (r-w)qx_{2,a} - k_2 x_{2,a}^2 + a_2(qx_{2,a} - Q_{02}) \quad (20)$$

So the problem the steel supplier faced with is how to maximize the expectation profits while satisfy (16), (17), (18), (19), (20). We can draw the conclusion as below after computing it.

$$a_1 = w - c \quad (21)$$

$$a_2 = \frac{(k_1 - k_2)\theta_1 r + (k_1\theta_2 - k_1\theta_1 + k_2\theta_1)w - k_1\theta_2 c}{(k_2 - k_1)\theta_1 + k_1\theta_2} \quad (22)$$

$$Q_{01} = \frac{q^2(r-c)}{4k_2(w-c)} - \left( \frac{1}{k_1} - \frac{1}{k_2} \right) \frac{q^2(r-c)^2}{4(w-c)} \left[ \frac{k_1\theta_2}{(k_2 - k_1)\theta_1 + k_1\theta_2} \right]^2 - \frac{\Pi_b^+}{w-c} \quad (23)$$

$$Q_{02} = \frac{(k_2 - k_1)\theta_1 + k_1\theta_2}{(k_1 - k_2)\theta_1 r + (k_1\theta_2 - k_1\theta_1 + k_2\theta_1)w - k_1\theta_2 c} \bullet$$

$$\left\{ \frac{q^2(r-c)^2}{4k_2} \left[ \frac{k_1\theta_2}{(k_2 - k_1)\theta_1 + k_1\theta_2} \right]^2 - \Pi_b^+ \right\} \quad (24)$$

In above supply chain contract, the distributors' optimal "green" investments will be

Type 1:  $x_{1,a} = \frac{r-c}{2k_1} q \quad (25)$

Type 2:  $x_{2,a} = \frac{(r-c)qk_1\theta_2}{2k_2[(k_2 - k_1)\theta_1 + k_1\theta_2]} \quad (26)$

The supplier's expectation profits are

$$E \Pi_{s,a} = n \theta_1 E \Pi_{s1,a} + n \theta_2 E \Pi_{s2,a} \quad (27)$$

$$E \Pi_{s1,a} = \frac{q^2(r-c)^2}{4k_1} - \frac{q^2(r-c)^2}{4} \left( \frac{1}{k_1} - \frac{1}{k_2} \right) \bullet$$

$$\left[ \frac{k_1\theta_2}{(k_2 - k_1)\theta_1 + k_1\theta_2} \right]^2 - \Pi_b^+ \quad (28)$$

$$E \Pi_{s2,a} = \frac{q^2(r-c)^2}{4k_2} - \frac{[2k_1k_2\theta_1\theta_2 + k_1^2\theta_2(\theta_2 - 2\theta_1)]}{[(k_2 - k_1)\theta_1 + k_1\theta_2]^2} \Pi_b^+ \quad (29)$$

The distributors' expectation profits are

Type 1:

$$E \Pi_{b1,a} = \frac{q^2(r-c)^2}{4k_1} \left( \frac{1}{k_1} - \frac{1}{k_2} \right) \left[ \frac{k_1\theta_2}{(k_2 - k_1)\theta_1 + k_1\theta_2} \right]^2 + \Pi_b^+ \quad (30)$$

Type 2:

$$E \Pi_{b2,a} = \Pi_b^+ \quad (31)$$

The supply chain expectation profits are

$$E \Pi_{sc,a} = n \theta_1 E \Pi_{sc1,a} + n \theta_2 E \Pi_{sc2,a} \quad (32)$$

$$E \Pi_{sc1,a} = (r - c)^2 q^2 / 4k_1 \quad (33)$$

$$E \Pi_{sc2,a} = \frac{q^2(r - c)^2 [2k_1 k_2 \theta_1 \theta_2 + k_1^2 \theta_2 (\theta_2 - 2\theta_1)]}{4k_2 [(k_2 - k_1)\theta_1 + k_1 \theta_2]^2} \quad (34)$$

#### IV. The Analysis of Model

According to analysis above, contrasting the result in information asymmetry condition with in information symmetry condition, we can draw the conclusion as below:

- Distributors will not fulfil their environmental obligations conscientiously, for it will increase costs. Motivation measures should be taken to encourage the distributors to fulfil contract conscientiously. It is shown in the model that  $x_{i,a}(k_i) \leq x_{i,f}(k_i)$ ,  $\forall i = 1, 2$ , which means that the distributors' "green" investments in information asymmetry condition are less than in information symmetry condition.
- In information asymmetry condition, the expectation profits of supplier will be reduced. The reasons are as follows. On one hand, distributors will not fulfil environmental contract, so the optimal supply chain profits can't be achieve. On the other hand, some certain profits must be payed to distributors, if they want the distributors be able to fulfil the contract initially. It is shown in the model that  $E \Pi_{s,a} < E \Pi_{s,f}$ . It indicates that the suppliers' expectation profits in information asymmetry condition will be less than in information symmetry condition.
- In information asymmetry condition, although more investments will be caused by distributors' initial contract fulfilling, the distributors' profits will be increased, because of the supplier's motivation and compensation, which will make distributors get maximum benefit from contract. It is shown in the model that  $E \Pi_{bi,a} \geq \Pi_b^+$ ,  $\forall i = 1, 2$ . It indicates that in information asymmetry condition, the distributors' expectation profits are more than in information symmetry condition. It will be observed from  $E \Pi_{s1,a}$  that the information rent of type 1 is  $\frac{q^2(r - c)^2}{4} (\frac{1}{k_1} - \frac{1}{k_2}) [\frac{k_1 \theta_2}{(k_2 - k_1)\theta_1 + k_1 \theta_2}]^2$ , it is the profit which supplier must pay to distributors, that make the distributors tell truth.
- The distributors who have not fulfil the contract, after a comparative analysis, will find the

distributors who have fulfilled contract will be able to get more profits. Then they will decide to fulfil the contract in next period, and the motivation will come off. It will encourage distributors to strengthen "green" reforming, build up environmental consciousness, and enhance the whole supply chain competitiveness. It is shown in model that  $E \Pi_{b1,a} > E \Pi_{b2,a}$ .

- $E \Pi_{sc,a} < E \Pi_{sc,f} = E \Pi_{sc,j}$ , it indicates supply chain expectation profits are system optimal profits. The efficiency of the supply chain will be lost in information asymmetry condition, and the supply chain expectation profits are less than in information symmetry condition.

#### V. CONCLUSIONS

The research results indicated that, in information asymmetry condition, a linear transfer payment contract can encourage supply chain members to show its true type, but compared with in information symmetry condition, the investments in "green" reforming will be less, therefore the expectation profits of steel enterprise and the efficiencies of supply chain will be lower. To make supply chain members tell truth, they must be payed more expectation profits in information asymmetry condition than in information symmetry condition.

#### ACKNOWLEDGMENT

This work is supported by Liaoning provincial Federation of Social Science Circles under Grant No. 20111slktg1x-22 The Education, Department of Liaoning Province under Grant No. 2009B103 and China Society of Logistics (CSL) under Grant No. 2009CSLKT033..

#### REFERENCES

- [1] Zhang Weiyang, Game theory and information economics 1st ed. Shanghai: Shanghai People Press, 1996, pp. 167-172. (In Chinese)
- [2] Myerson J. "Incentive compatibility and the bargaining problem". *Econometrica*, 47 (1979), 47, pp. 61-73.
- [3] Giannis T. Tsoulfas, Costas P. Pappis, Stefan Minner. "An environmental analysis of the reverse supply chain of SL1 Batteries". *Resources, Conservation and Recycling*, 36 (2002), pp. 135-154.
- [4] Vincent P. Crawford, Hans Haller, "Learning how to cooperate: optimal play in repeated coordination games," *Econometrica*, vol. 58, pp. 856-869, March 1990.
- [5] Vincent P. Crawford, Uri Gneezy, and Yuval Rottenstreich, "The power of focal points is limited: even minute payoff asymmetry may yield large coordination failures," *American Economic Review*, vol. 98, pp. 1443-1458, April 2008.
- [6] Jin Yuran, "Research on the supply chain strategies of chinese enterprises under the financial crisis," *China Market*, vol. 32, pp. 12-15, August 2009.
- [7] Brian Fynes. "Environmental uncertainty, supply chain relationship quality and performance," *Journal of Purchasing & Supply Management*, vol. 10, pp. 179-190, January 2006.
- [8] Cachon G., Lariviere M. "Supply chain coordination with revenue sharing: strengths and limitations," *Management Science*, vol. 51, pp. 30-44, January 2007.

# Improved algorithm for automatic text summary based on weight of sentence

Yajuan Tang, Dexian Zhang, Lin Yang

School of Information Science and Engineering, Henan University of Technology, Zhengzhou, China

**Abstract**— Although automatic text summary based on the weight of sentence has achieved great development and advancement, the study on the improved algorithm of automatic text summary based on the weight of sentence is still inadequate, and there are some problems in the process of generating automatic text summary must be resolved. This paper aims to provide better technical support for the use of automatic text summary by analyzing improved method.

**Index Terms**—sentence weight, automatic summary, improved algorithm

## I. INTRODUCTION

Since automatic text summary appeared from the mid-twentieth century, it has made a great deal of development and progress. However, there are still some flaws and problems in the process of generating summary automatically by the computer since the generation of automatic text summary now is generally based on understanding information, selecting the main information data and generating automatic text summary. During the specific operation, the summaries generated by computer can't properly reflect full main ideas and key content in the entire article owing to failing to nicely analyze and calculate actual weights of sentences in the entire article.

When we calculate the weight of the sentences in the process of generating automatic text summary, although we consider the comparison and analysis of the similarity between the sentences, some factors like the position sentence appears in the article and their representative are frequently overlooked. However, these factors may have a profound impact. At the same time, there are some indicative words and other words sometimes in the content which may be selected as theme data of the summary. In many processes of generating automatic text summary, the feature of indicative words still fails to be taken full advantage of. This article provides better technical support to use automatic text summary through the analysis of its improved method.

## II. THE ALGORITHM FLOW OF AUTOMATIC TEXT SUMMARY

### A. The idea of generating automatic text summary

The operation process of automatic text summary algorithm can be regarded as an extraction and selection

process for some statements after integrated and carried out in accordance with the importance of sentence alignment. A kind of computer algorithm called LexRank is widely used in the processing of generating the automatic text summary. On the basis of analyzing each statement in articles and presenting them with graphics, it studies the weight of these statements. In the whole process, always throughout this algorithm process principle: if there is one sentence similar with more sentences at the same time, then, we can consider it as a sentence with a relatively high degree of importance in the text. So, it may be considered into the category of the summary [1].

### B. The process of automatic text summary algorithm

What is most widely used in the process of dealing with automatically generating text summary is vector space model. This model has been successfully applied to the famous text retrieval system named SMART[2]. It mainly presents text content and the deal query process as vector  $d_j = (w_{1,j}, w_{2,j}, \dots, w_{t,j})$  and  $q = (w_{1,q}, w_{2,q}, \dots, w_{t,q})$ .

On the basis of the assumption that there is a certain commonality about information data between text statements, compare the angle deviation from text content vector and deal query process vector so to calculate smoothly the search on keyword in the process of presenting conversion by computer. Generally, we obtain critical information by calculating cosine formula of the angle between the two vectors:

$$\cos\theta = \frac{\mathbf{d}_2 \cdot \mathbf{q}}{\|\mathbf{d}_2\| \|\mathbf{q}\|} \quad (1)$$

Among them:  $\mathbf{d}_2 \cdot \mathbf{q}$  is the product of text content vector and deal query process vector;  $\|\mathbf{d}_2\|$  is the modulus of vector  $\mathbf{d}_2$ ;  $\|\mathbf{q}\|$  is the modulus of vector  $\mathbf{q}$ . These vectors are shown in "Fig. 1".

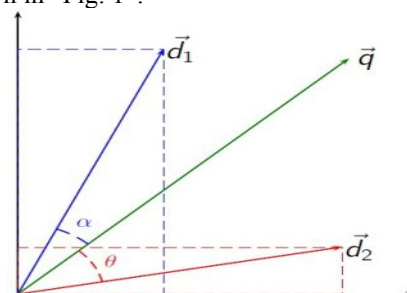


Figure 1. Vector relations

The modulus of vector is obtained by the following formula:

$$\|v\| = \sqrt{\sum_{i=1}^n v_i^2} \quad (2)$$

Among them: vector  $d$  is  $v_d = [w_{1,d}, w_{2,d}, \dots, w_{N,d}]^T$ .

$$w_{t,d} = tf_{t,d} \cdot \log \frac{|D|}{|\{d' \in D | t \in d'\}|} \quad (3)$$

Among them:  $tf_{t,d}$  is the frequency phrase  $t$  appears in the document  $d$ (a local parameter);  $\log \frac{|D|}{|\{d' \in D | t \in d'\}|}$  is a inverse document frequency(a global parameter);  $|D|$  is the total number of files in the file set;  $|\{d' \in D | t \in d'\}|$  is the number of files containing phrase  $t$ .

The cosine similarity between text content vector  $d_j$  and deal query process vector  $q$  is calculated by the following formula:

$$\text{sim}(d_j, q) = \frac{d_j \cdot q}{\|d_j\| \|q\|} = \frac{\sum_{i=1}^N w_{i,j} w_{i,q}}{\sqrt{\sum_{i=1}^N w_{i,j}^2} \sqrt{\sum_{i=1}^N w_{i,q}^2}} \quad (4)$$

In a simple phrase computing model, the weight of phrase does not include global parameters, but count on the number of phrase appearance simply:  $w_{t,d} = tf_{t,d}$ [3]. The basic process shown in “Fig. 2”.

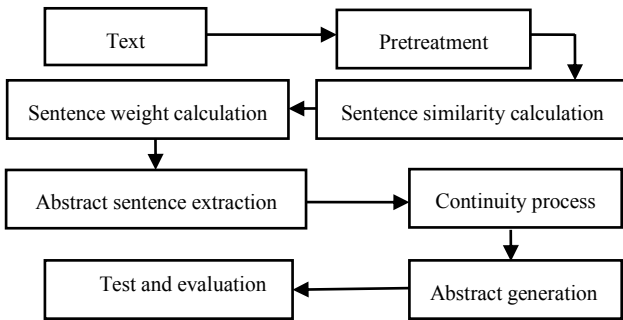


Figure 2. The basic process

### III. THE METHOD OF SENTENCE WEIGHT CALCULATION

#### A. Method One

On judging the importance of the sentences in articles, compare the degree of importance of sentences according to the analysis for location features of sentences appear in the article, keywords features, similarity of article title and sentences and directive features. Each sentence is expressed as  $T = \{T_1, T_2, \dots, T_n\}$ . Among them,  $T_i$  represents the weight of each sentence. Express  $T_i$  as  $T_i = \{t_{i1}, t_{i2}, \dots, t_{im}\}$  using weight formula. Among them,  $t_{ij}$  represents the weight information of keywords constituting a sentence. The greater the weight of each sentence in the article is, the stronger the relationship between sentences and topics is. On the contrary, the smaller the weight of each sentence in the article is, the weaker the relationship between sentences and topics is. In the way of specifying a range, find out a few of sentences which have the strongest relationship with the

content of article from these sentences to form a summary of the main content[4].

#### B. Method Two

In the specific calculation process, we can also calculate the matrix of degree of similarity in the article statement in the first place, then, calculate the specific weighting factor of individual statements in the article using computer algorithms of LexRank. The main calculation process is shown in “Fig. 3”.

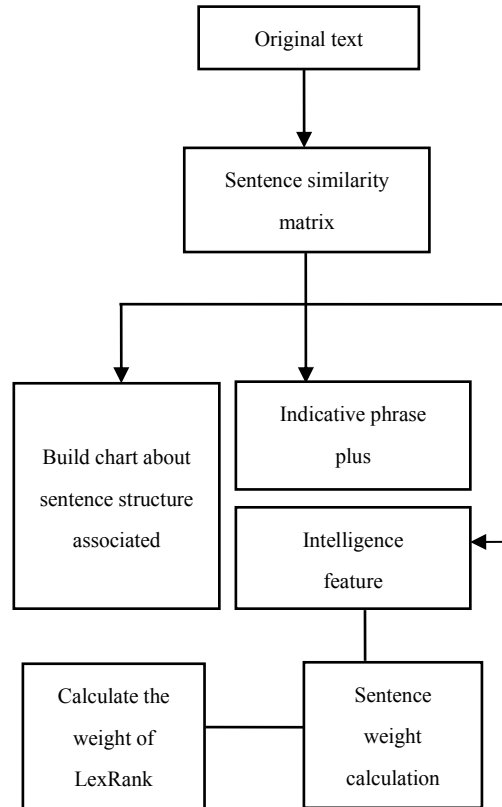


Figure3. The main calculation process

Generally speaking, it is a very important influence for the generation of automatic summary where the sentences appear in the content. We can judge importance of the sentences in articles according to whether there has regularity for the scope of the sentences appearing, location of sentences appearing, whether the words are capitalized and whether the sentences appear as title. Special keywords in articles can be obtained according to the most basic elements like time, place or person in the article as the retrieve information for generating the summary. We can judge whether the sentence about time characteristics which appear in the content can be key statement according to their position in the article. If it is appeared in the first segment, so we can select it as a key statement. Character is generally selected as key word. The occurrence of different events is in connection with different participants. Therefore, statement character is different, so articles will automatically generate different keywords. Since the importance of location is about the same with character, the sentences including location are currently selected as key statement too.

#### IV. IMPROVED ALGORITHM FOR AUTOMATIC TEXT SUMMARY BASED ON WEIGHT OF SENTENCE

In the course of the algorithm for automatic text summary based on weight of sentence, we may often encounter some statements with similar or identical meaning. Although we can establish a certain similarity matrix model, it will still cause some obstacles to the generation of automatic text summary based on weight of sentence. Therefore, we must eliminate the information data in article's jumbled statements when we study the improved algorithm of automatic text summary based on the weight of sentence. The main process is shown in "Fig. 4".

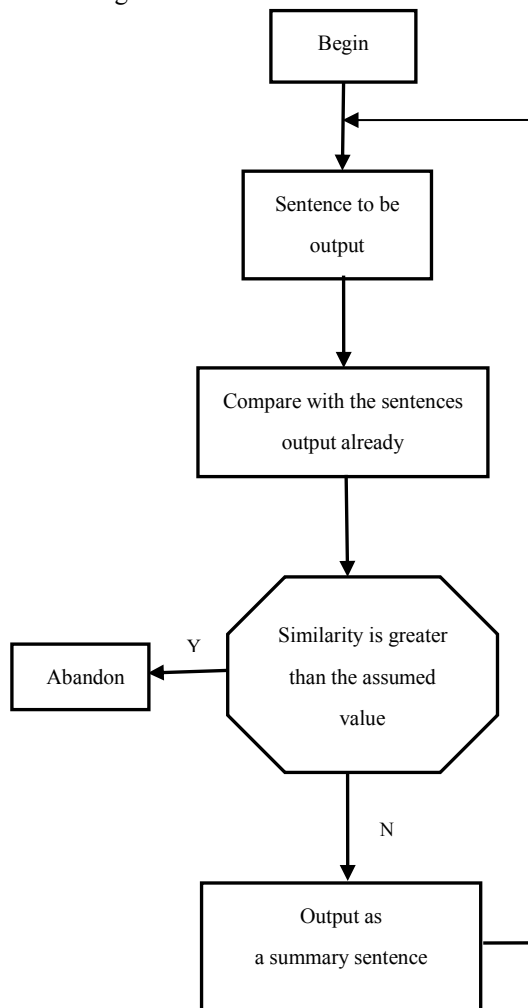


Figure4. Redundant processing steps

During the specific operation of removing jumbled information, we can improve the algorithm of automatic text summary based on the weight of sentence mainly from the following aspects:

- After calculating the specific weighting factor of individual statements in the article using the method of sentence weight analysis, arrange result data on the basis of their importance and weight so to get a sorted list of relevant candidate sentences like  $S = \{S_1, S_2, \dots, S_n\}$ , then, name collection A as the collection of summary. There is no element

among collection A.

- In the sorted list  $S = \{S_1, S_2, \dots, S_n\}$  formed in front, analyze and select the element  $S_k$  with the largest weight coefficient output as a sentence of the summary. At the same time, Suppose  $A = \{S_k\}$ ,  $S = S - \{S_k\}$  [5].
- Make a choice on  $S_k$  extracted in front according to weight proportion, we can analyze that, if there is  $S_k$  exists in the number of columns whose degree of similarity with all elements of the article in collection A are under the expected value of the original conjecture, then we can get  $A = A + S_k$ . Conversely, we can eliminate the  $S_k$ .
- In order to ensure the accuracy of the calculation process, it is necessary to repeat operating C several times until the final number of the sentences extracted is similar or same to the length assumed before.

#### V.COMCLUSION

The analysis and study on automatic text summary based on the weight of sentence can contribute to improve the operation of automatic summary. With the correlation analysis of algorithm flow of automatic text summary and improved algorithm for automatic text summary based on the weight of sentence, this article can provide a frame reference in related fields.

#### ACKNOWLEDGMENT

The authors wish to thank National High Technology Research and Development Program. This work was supported in part by a grant from it.

#### REFERENCE

- [1] Yongtao YANG, "An extraction algorithm on automatic text summary[R]". Journal of Chengdu University . 2009.
- [2] Yongtao YANG, "An extraction algorithm on automatic text summary[R]". Journal of Chengdu University . 2009.
- [3] D W Oard and etal, "A Conceptual Framework for Text Filtering", University of Maryland[R], 1996.
- [4] Xuegang ZHAN and Tianshun YAO, "Chinese classification method based on analysis of Chinese [C ]", 98 Chinese information processing International Conference. BEIJING : Tsinghua University Press, 1998.412-417.
- [5] Yongdong XU, "Study on key technology of multi-document summarization[D]", Harbin Institute of Technology, 2007.

# Multi-user Detection Based on Importance Resampling Particle Filter in Impulsive Noise

XIAN Jinlong, LI Shengjie

College of Information Science and Engineering, Henan University of Technology, Zhengzhou, 450001, Henan, P.R. China. 13991339876@vip.sina.com

**Abstract**—we proposed an importance resampling particle filter (IRPF) algorithm for adaptive multi-user detection (MUD) in synchronous code division multiple access (CDMA) system. Importance resampling strategy is adopted to improve the standard PF algorithm. The particle number is reduced through the setting of a valid sample scale. The degeneracy problem of particle filter (PF) is overcome to some extent. Simulation results indicate that IRPF has a strong ability to deal with the nonlinear system, and the bit error rate of the system and the calculation of PF are further improved after applying the adaptive resampling strategy to PF.

**Index Terms**—Particle filter, Multi-user detection, importance resampling, Non-Gaussian noise

## I. INTRODUCTION

In the code division multiple access (CDMA) system, multi-user detection is served as one of the key technologies. It is proposed originally by K. S. Schneider in 1979. This method can eliminate the multi-access interference and alleviate the near-far effect effectively. Verdu put forward the best multi-user detection method in 1986[1]. Its performance is best, but its complexity grows exponentially with the increase in the number of users. So this method is difficult to be achieved in engineering. Many researchers put forward different kinds of sub-optimal multi-user detection. The complexity is reduced. But the performance is significant lower than the optimal multi-user detection algorithm.

Multi-user detection based on particle filter is one kind of sub-optimal multi-user detection methods. The particle filter algorithm is an approximate algorithm to Bayesian estimation based on sampling theory. It combines Monte Carlo with Bayesian theory together. When the sample size is large enough, the sample set can describe the real posterior probability density function (PDF) of the state variables. This technique can be applied to non-linear non-Gaussian system. Its accuracy can approximate to the optimal estimation [2].

Usually, in the most of study about signal processing and communication, the noise is assumed to be Gaussian white noise. However, this kind of statement is not accurate. There are some peak pulses which have low probability and high amplitude in the actual system, such as atmospheric noise [3]. Laplace noise and alpha stable

noise have the above characteristics. In this paper Laplace noise and alpha stable noise are simulated non-Gaussian noise. We can prove that the applicability and effectiveness of the particle filter is well in non-Gaussian system by simulation.

This paper is organized as follows: Section 2 includes the model of the CDMA system and the presentation of two kinds of non-Gaussian noises; the application of standard particle filter algorithm for multi-user detection is presented in Section 3; the application of importance resampling particle filter algorithm for multi-user detection is presented in Section 4; Simulation results and conclusions are described in Section 5.

## II. SYSTEM MODEL

### A. CDMA SYSTEM MODEL

Consider a synchronous CDMA system with  $K$  users, and symbol interval is  $T$ . The  $k$ -th receive signal is [1][4]:

$$r(t) = \sum_{k=1}^K A_k(t)g_k(t)b_k(t) + n(t) \quad (1)$$

In the formula,  $A_k$  means the amplitude of the  $k$ -th signal;  $g_k$  means spread spectrum waveform of the  $k$ -th signal, and the value is  $\pm 1$ ;  $b_k$  means the  $k$ -th user data, the value is  $\pm 1$ ;  $n(t)$  is background noise that is selected by different type of the noise.

The cross-correlation between the signature waveforms of the  $i$ -th users and the  $k$ -th users is defined as:

$$\rho_{i,k} = \frac{1}{T_b} \int_0^{T_b} g_k(t)g_i(t)dt \quad (2)$$

In the above formula, when  $i = k$ ,  $\rho_{i,k} = 1$ ; When  $i \neq k$ ,  $0 \leq \rho_{i,k} < 1$ . As a result, we can get the output  $y_k$  of the  $k$ -th user's matched filter:

$$y_k = \int_0^T r(t)g_k(t)dt$$

$$\begin{aligned}
 &= \int_0^T \left( \sum_{k=1}^K A_k(t)g_k(t)b_k(t) + n(t) \right) g_k(t) dt \\
 &= A_k b_k + \sum_{\substack{i=1 \\ i \neq k}}^K \rho_{i,k} A_i b_i + \frac{1}{T} \int_0^{T_b} n(t) g_k(t) dt \\
 &= A_k b_k + MAI_k + z_k \tag{3}
 \end{aligned}$$

$A_k b_k$  means the signal of the  $k$ -th user;  $z_k$  is noise;  $MAI_k$  is multiple access interference (MAI) which is generated by other users.

In order to facilitate processing and analysis, the received vector can be expressed as matrix.

$$y = RAb + z \tag{4}$$

Where  $A = \text{diag}\{A_1, A_2, \dots, A_k\}$  is a diagonal matrix of received signal amplitude.  $b = [b_1, b_2, \dots, b_k]$  is user data,  $R$  is symmetric correlation matrix of  $K \times K$  order ( $\rho_{i,k} = \rho_{k,i}$ ).  $z = [z_1, z_2, \dots, z_k]^T$ , it is a complex-valued vector with independent real and imaginary components and covariance matrix equal to  $\sigma^2 R$ .

$R$  is a symmetric matrix, so Colicky factorization can be used. There is a unique lower triangular matrix  $F$  such that  $R = F^T F$ . If we apply  $F^{-T}$  to the formula (4), can we obtain [5]:

$$\bar{y} = F^{-T} y = F^{-T} FAb + F^{-T} z = FAb + \bar{z} \tag{5}$$

The covariance matrix of  $\bar{z}$  is  $\sigma^2 I$ , where  $I$  is the identity matrix. Because the noise becomes independent and identically distributed, white noise.  $\bar{y}$  is called the whitened matched filter output. Scalar expression of the received signal is as follows:

$$\bar{y}_k = \sum_{l=1}^K F_{k,l} a_l b_l + \bar{z}_k \tag{6}$$

On the basis of the spatial model, the purpose of multi-user detection is to detect signals of the users  $b_{1:k} = \{b_1, b_2, \dots, b_k\}$  from the matched filter output signals  $\bar{y}_{1:k} = \{\bar{y}_1, \bar{y}_2, \dots, \bar{y}_k\}$ .

**B. NON-GAUSSIAN NOISE SIMULATION**

In order to simplify the mathematical analysis, we often assume the noise as Gaussian noise. Usually, this assumption is reasonable. However, in practice, there are some kinds of noise that they are not happen often, but with a strong impact. These kinds of noise are not Gaussian noise, such as thunder and lightning, ice avalanches, all kinds of machine motors, neon signs, etc. do not have Gaussian nature. It is very necessary to establish a more accurate model than the Gaussian model. The following briefly discusses two models of the non-Gaussian noise.

**A. Laplace noise**

Laplace noise is one kind of non-Gaussian noise. Laplace probability density function (PDF) has an obvious smearing. This is main difference between the Laplace PDF and the Gaussian PDF. Laplace probability density function[3]:

$$\begin{aligned}
 p(x) &= \frac{1}{\sqrt{2\sigma^2}} \exp\left(-\sqrt{\frac{2}{\sigma^2}}|x|\right), \\
 &-\infty < x < +\infty \tag{7}
 \end{aligned}$$

In the formula,  $\sigma^2$  parameter is variance or power of noise.

**B. Alpha noise**

If the random variable  $X$  is subject to the Alpha stable distribution, then its characteristic function is [6][7][8]:

$$\phi(u) = \exp\{j\alpha u - \gamma|u|^\alpha [1 + j\beta \text{sgn}(u)\omega(u, \alpha)]\} \tag{8}$$

$$\omega(u, \alpha) = \begin{cases} \tan(\pi\alpha/2), \dots, \alpha \neq 1 \\ (2/\pi) \log|u|, \dots, \alpha = 1 \end{cases} \tag{9}$$

$$\text{sgn}(u) = \begin{cases} 1, \dots u > 0 \\ 0, \dots u = 0 \\ -1, \dots u < 0 \end{cases} \tag{10}$$

In the formula,  $\alpha \in (0, 2]$  is characteristic index which determines the degree of the distribution pulse characteristics.  $\alpha$  is smaller, the pulse characteristics is more obvious. When  $\alpha = 2$ , it is Gaussian distribution which mean is  $a$  and variance is  $2\sigma^2$ . In other words, the Gaussian distribution is a special case of the Alpha stable distribution. When  $0 < \alpha < 2$ , this distribution is called fractional lower order Alpha stable distribution.  $-1 < \beta < 1$  is called symmetry parameter which can control the gradient of the distribution. When  $\beta = 0$ , it is a symmetric  $\alpha$ -stable distribution, referred to as  $S\alpha S$ . When  $\alpha = 1$  and  $\beta = 0$ , this distribution is Cauchy distribution.  $\gamma$  is called scattering coefficients which can control the dispersion measure about the samples relative to the mean. It is similar to the variance of the Gaussian distribution. The noise power can be expressed approximately as  $2\gamma$ , but  $2\gamma$  is not equal completely to the true noise power. Signal to Noise Ratio (SNR) can be expresses as  $SNR = S/2\gamma$  ( $S$  is the signal power). When  $\alpha = 0$  and  $\gamma = 1$ , this distribution is called standard  $\alpha$ -stable distribution.

**III. MULTI-USER DETECTION BASED ON STANDARD PARTICLE FILTER ALGORITHM**

The particle filter is a Monte Carlo method based on Bayesian theory. Its core idea is that using the samples and their corresponding weights to express the posterior probability density function then we can use the posterior

probability density to obtain the estimated value of the state. If the samples are sampled from the posterior probability distribution, the each sample has the same weight. However, in practice the posterior probability density function  $p(b_{1:k} | \bar{y}_{1:k})$  can't be written in the typical form, so the sampling process is very difficult. Therefore, we often obtain the particles from an importance density function  $q(b_{1:k} | \bar{y}_{1:k})$ . Then the weights are defined to be [9][10][11]:

$$\omega_k^i \propto \frac{p(x_{1:k}^i | \bar{y}_{1:k})}{q(x_{1:k}^i | \bar{y}_{1:k})} \quad i = 1, \dots, N_s \quad (11)$$

The importance density function can be decomposed into:

$$q(x_{1:k} | \bar{y}_{1:k}) = q(x_k | x_{1:k-1}, \bar{y}_{1:k}) q(x_{1:k-1} | \bar{y}_{1:k-1}) \quad (12)$$

The posterior probability density function can be expressed as:

$$\begin{aligned} p(x_{1:k} | \bar{y}_{1:k}) &= \frac{p(\bar{y}_k | x_{1:k}, \bar{y}_{1:k-1}) p(x_{1:k} | \bar{y}_{1:k-1})}{p(\bar{y}_k | \bar{y}_{1:k-1})} \\ &= \frac{p(\bar{y}_k | x_{1:k}, \bar{y}_{1:k-1}) p(x_k | x_{1:k-1}, \bar{y}_{1:k-1})}{p(\bar{y}_k | \bar{y}_{1:k-1})} p(x_{1:k-1} | \bar{y}_{1:k-1}) \\ &= \frac{p(\bar{y}_k | x_k) p(x_k | x_{k-1})}{p(\bar{y}_k | \bar{y}_{1:k-1})} p(x_{1:k-1} | \bar{y}_{1:k-1}) \\ &\propto p(\bar{y}_k | x_k) p(x_k | x_{k-1}) p(x_{1:k-1} | \bar{y}_{1:k-1}) \quad (13) \end{aligned}$$

So, if we know  $p(x_{1:k-1} | \bar{y}_{1:k-1})$ , can we obtain  $p(x_{1:k}^i | \bar{y}_{1:k})$  through new samples. By substituting (13) with (11) and (12), we will get importance weights updated formula is:

$$\begin{aligned} \omega_k^i &\propto \frac{p(\bar{y}_k | x_k^i) p(x_k^i | x_{k-1}^i) p(x_{1:k-1}^i | \bar{y}_{1:k-1})}{q(x_k^i | x_{1:k-1}^i, \bar{y}_{1:k}) q(x_{1:k-1}^i | \bar{y}_{1:k-1})} \\ &= \omega_{k-1}^i \frac{p(\bar{y}_k | x_k^i) p(x_k^i | x_{k-1}^i)}{q(x_k^i | x_{1:k-1}^i, \bar{y}_{1:k})} \quad (14) \end{aligned}$$

For the standard particle filter algorithm, we choose the a priori probability density function as the importance density function.

$$q(x_k^i | x_{1:k-1}^i, \bar{y}_{1:k}) = p(x_k^i | x_{k-1}^i) \quad (15)$$

By substituting (14) with (15), the formula can be simplified as:

$$\omega_k^i \propto \omega_{k-1}^i p(\bar{y}_k | x_k^i) \quad (16)$$

Weights are normalized:

$$\omega_k^i = \omega_k^i / \sum_{i=1}^{N_s} \omega_k^i \quad (17)$$

When the process of algorithm is finished for the all users, we can estimate the posterior probability density function through the particles set and its corresponding weights set  $\{x_{1:K}^i, \omega_{1:K}^i\}_{i=1}^{N_s}$ . For example, the marginalized posterior probability density function  $p(x_k | \bar{y}_{1:k})$  can be expressed as:

$$p(x_k | \bar{y}_{1:K}) \approx \sum_{i=1}^{N_s} \omega_K^i \delta(x_k - x_k^i) \quad (18)$$

In the formula,  $\delta(\cdot)$  is the Dirac delta function.

If we defined two vectors,  $x_k = [x_k^1, x_k^2, \dots, x_k^{N_s}]^T$ ,  $\omega_k = [\omega_k^1, \omega_k^2, \dots, \omega_k^{N_s}]^T$ . According to the Maximum A Posterior (MAP) rule, we have

$$b_k = \text{sign}(x_k^T \omega_k) \quad (19)$$

With the increase of the iterations, weight of the particles concentrate gradually on a small number of particles and most of the particles weights are very small. This problem is called the degradation of the particle. The degeneracy implies that a large computational effort is devoted to updating particles whose contribution to the approximation to  $p(x_k | \bar{y}_{1:k})$  is almost zero. Re-sampling technique was introduced to solve degeneracy[12]. The basic idea of resampling is sampling  $N_s$  times from the posterior probability density function

$p(x_k | \bar{y}_{1:K}) \approx \sum_{i=1}^{N_s} \omega_K^i \delta(x_k - x_k^i)$ , then we can obtain

the new sample set  $\{x_k^{i*}\}_{i^*=1}^{N_s}$ . The weights are set to be  $\omega_k^{j*} = 1 / N_s$ .

In summary, the steps of multiuser detection based on particle filter are as follows [13][14][15]:

Step 1: Sampling for the k-th user, making  $x_k^i : q(x_k | x_{1:k-1}^i, \bar{y}_{1:k})$ .

Step 2: According to equation (14) to calculate the weights of the particles.

Step 3: Normalizing the weights according to equation (17).

Step 4: Resampling for the particles.

Step 5: According to equation (19) to estimate the signals of the k-th user.

Step 6: Turn to step1, and estimating the signals of the next user.

#### IV. MULTI-USER DETECTION BASED ON IMPORTANCE RESAMPLING PARTICLE FILTER.

There is a defect that is the degradation phenomenon in Particle filter algorithm. With the increase of the iterations, weight of the particles concentrate gradually

on a small number of particles and most of the particles weights are very small. This problem is called the degradation of the particle. The degeneracy implies that a large computational effort is devoted to updating particles whose contribution to the approximation to  $p(x_k | \bar{y}_{1:k})$  is almost zero. An effective measure to overcome the degradation phenomenon is to select appropriate and effective sampling scale  $N_{eff}$ , it is also a measure of the degradation phenomenon, defining  $N_{eff}$  for:

$$N_{eff} = \frac{N}{1 + \text{var}(\omega_k^i)} \quad (20)$$

Which,  $\omega_k^i$  by the formula (14) and (17) determine,  $\text{var}(\omega_k^i)$  for  $\omega_k^i$  variance.  $N_{eff}$ 's general values can not be calculated exactly, but can be approximated by the following formula:

$$N_{eff} = \frac{1}{\sum_{i=1}^{N_s} (\omega_k^i)^2} \quad (21)$$

By formula (20) shows that  $N_{eff} \leq N_s$ ,  $N_{eff}$  smaller, more serious degradation. Thus increasing the number of particles  $N_s$  degradation problems can be solved, but it will increase the amount of calculation and influence real-time of this algorithm.

In this paper, the importance resampling is to overcome the degradation. The importance resampling purpose is to reduce the number of particles smaller weights, only concentrate on the particles having a maximum priority value. The basic method is through the posterior probability density of discrete approximation

expression  $p(x_k / y_{0:k}) \approx \sum_{i=1}^{N_s} \omega_k^i \delta(x_k - x_k^i)$  re-M

samples, Generating a new set of particles  $\{x_k^{*i}\}_{i=1}^M$ , such that  $p(x_k^{*i} = x_k^i) = \omega_k^i$ . Because resampling are independent and identically distributed, weights are re-set to  $\omega_k^i = 1/M$ . At first setting a threshold  $N_{threshold}$ .

When  $N_{eff} = 1 / \sum_{i=1}^{N_s} (\omega_k^i)^2 < N_{threshold}$ , resampling.

Then we have no need to resampling at every moment, it can adaptively decide whether to re-sample. The complexity of the algorithm can be reduced to a certain extent.

In summary, the steps of multiuser detection based on particle filter are as follows :

Step 1: Sampling for the k-th user, making  $x_k^i : q(x_k^i | x_{1:k-1}^i, y_{1:k})$ .

Step 2: According to equation (14) to calculate the weights of the particles.

Step 3: Normalizing the weights according to equation (17).

Step 4: According to above resampling for the particles.

Step 5: According to equation (19) to estimate the signals of the k-th user.

Step 6: Turn to step1, and estimating the signals of the next user.

### V. SIMULATION RESULTS AND CONCLUSIONS

Analyze the performance of the multi-user detection based on importance resampling particle filter algorithm by simulation. Consider a synchronous CDMA system with 5 users, 50000 information bits, 31-bit gold spread-spectrum code and the user power partial value is 10. Channel noises include Gaussian noise, Laplace noise and Alpha stable noise. The range of signal to noise ratio (SNR) for all users is -4~10 dB. The total number of particles is 50.  $N_{threshold}$  is 5.5.

Figure1: When the signals are interfered by Gaussian noise, we can find that the performance of the IRPF algorithm is better than the PF algorithm. The research results have important reference value for the research of MUD system.

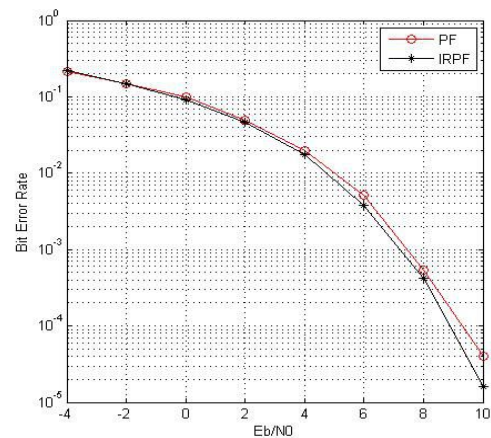


Figure1. The BER of PF detection and IRPF detection

Figure2: This figure analyzes the error code performance of IRPF detection aiming to Gaussian noise, Alpha stable noise and Laplace noise. It can be seen from the Figure 3 that the error code performance of the Gaussian noises and the Laplace noise are almost the same. The error code performance of the Alpha stable noises slightly weakened. It is due to the true power of the Alpha stable noise is not  $2\gamma$ . But, in the simulation, we assume that his power is  $2\gamma$ . The result also proves that the applicability of the importance resampling particle filter algorithm is well in the non-Gaussian system. In other words, this algorithm has a strong robustness. Therefore, this algorithm has practical reference value.

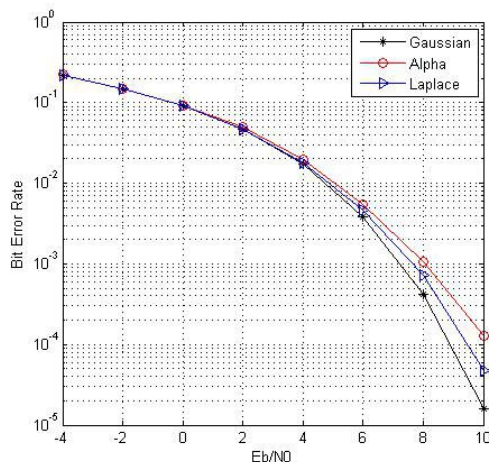


Figure 2. BER of IRPF detection under three kinds of noise

#### ACKNOWLEDGMENT

Supported by the Scientific Research Fund of Henan University of Technology

#### REFERENCES

- [1] Verdu, "Minimum probability of error for asynchronous Gaussian multiple-access channels", *IEEE Trans. Inform. Theory*, vol. IT-32, pp.85-96, 1986.
- [2] Zhu Zhiyu, *The particle filter algorithm and its application*, Science Press, China, 2010.
- [3] Steven M.Kay Edited, translated by Peng-fei Luo, *Statistics based on signal processing: estimation and detection theory*, Electronic Industry Press, China, 2006.
- [4] Dou zhongzhao, Lei xiang, *CDMA Wireless Communications Theory*, Tsinghua University Press, China, 2004.
- [5] Hou Rui, Zhang Santong, Zhu Gang, "CDMA Multiuser Detection Using Unscented Particle Filtering" 2007 International Conference on Wireless Communications, Networking and Mobile Computing, *WiCOM 2007*, pp.902-905, 2007.
- [6] ZHANG Xianda, BAO Zheng, *Communication Signal Processing*, National Defence Industrial Press, China, 2000.
- [7] Xian Jinlong, Li Jianwu. "Multi-user Receiver Based on MMSE Criteria in Laplace Noise and Alpha-stable Noise", 2010 WASE International Conference on Information Engineering, *ICIE 2010*, vol.4, pp.38-41, 2010.
- [8] Xiaodong Wang, H.Vincent Poor, translated by ZHENG Baoyu, *Wireless Communication Systems Advanced Techniques for Signal Reception*, Electronic Industry Press, China, 2005.
- [9] Tsakalides, Panagiotis, Nikias, Chrysostomos L, "Wideband array signal processing with alpha-stable distributions", *IEEE Military Communications Conference MILCOM*, vol.1, pp.135-139, 1995.
- [10] Hu Shiqiang, Jing Zhongliang, *Principles and Applications of particle filter*, Science Press, China, 2010.
- [11] Zhimin CHEN, Yuming BO, Panlong WU, Mingfeng YIN, "Quasi-Monte Carlo Particle filter Fault Prognosis Algorithm Based on GRNN", *JCIT*, vol.7, no.7, pp.96-103, 2012.
- [12] Fan Zhou, Zhen Qin, Chunjing Xiao, Shuquan Li, Wei Jiang, Yue Wu, "Tracking Moving Object via Unscented Particle Filter in Sensor Network", *JDCTA: International Journal of Digital Content Technology and its Applications*, vol.5, no.12, pp.77-84, 2011.
- [13] Liang Yan, Pan Quan, Yang Feng, Zhang Lei, *Modern estimation theory and application of complex system*, Science Press, China, 2009.
- [14] Farid Mousavi Pour, S. Seyedtabaai, "Iterative Kalman Versus Rao-blackwellized Particle Filter in Speech Enhancement", *IJACT: International Journal of Advancements in Computing Technology*, vol.3, no.5, pp.234-242, 2011.
- [15] Lin Qing, Yin Jian Jun, Zhang Jian Qiu, Hu Bo. "Gaussian sum particle filter methods for non-linear non-Gaussian methods", *Systems Engineering and Electronics*, vol.32, No.12, pp.2493-2499, 2010.

**Xian Jinlong** obtained the B.S. and M.S. degree from Beijing University of Science and Technology Beijing in 1987 and 1990. He received his Ph.D in Communications Engineering from Beijing University of Posts and Telecommunications in 2000. He is an associate professor in the College of information science and engineering, Henan University of Technology. His research interest includes wireless communication network, the key technology of the fourth generation mobile communication and digital signal processing.

**Li Shengjie** received his B.S. degree in Electronic information science and technology from Henan University of Technology in 2009 and 2013. He is currently working towards his M.S. degree in Signal and information processing at Henan University of Technology. His current research interest includes wireless communication network and multi-user detection technology

# The Realization of Food Corpus based on Database Technology

Lin C. Yang, Dexian B. Zhang and Yajuan A. Tang

School of Information Science and Engineering, Henan University of Technology, Zhengzhou, China

**Abstract**— Since the 1990s, the corpus is rapidly developing, the corpus-based linguistics has yielded fruitful results in the research of linguistics and computer science, and corpus building also got wide attention all over the world, but the development of food information corpus and other special corpus are lagging behind. This article describes the definition and role of the corpus, leads to the construction of the importance of food corpus. Starts from the food corpus's definition, design, collection, annotation and the selection of retrieval software and so on, then with computer and database technology proposes the idea for the construction of food corpus. Research and built food corpus provides a rich new field for the development of linguistics and food related research.

**Index Terms**— food corpus, computer, database technology, build

## I. INTRODUCTION

Corpus building began in the 1960s, rise rapidly after the 1980s, countries began to establish various sizes and forms of the corpus, their respective forms are increasingly precise, construction began corpus has been highly in all areas of the world attention. Establish corpus, norms not only become an important foundation of modern linguistics studies [1], but as other specialized academic research in the field of medicine, architecture, law, English and other premises guaranteed.

This paper essentially start from the corpus to study linguistics as a theoretical basis, computer software engineering and database as guidance, drawing on the experience of other areas of the corpus study on the establishment of food corpus proposed solutions to problems you may encounter and building a database technical methods are discussed.

## II. THE CORPUS AND THE FOOD CORPUS

For the corpus linguists have different definitions, such as Sinclair thinks "Corpus is selected and sorted according to specific linguistic standard language use material collection, samples to use as a language". Atkins and Clear think "Corpus is made up of a large collection of written or spoken, and through the computer storage and handling". This paper thinks corpus is: according to certain principles of linguistics, using computer and database technology to collect snippets of text or oral language, supplemented artificial deep processing to build an electronic text library.

Special corpus is defined as collecting a particular field of corpora to built ideal library collection [2].

Currently, there are special corpus mostly small, mostly concentrated in the computer range [3,4], medical [5], the law[6] and a variety of common language , collected from multiple sources corpus newspapers and magazines, dictionaries books, etc., so that the information is not comprehensive enough .

Thus, the food corpus is defined as gathering a lot of food information on the text to real performance characteristics food exclusive collection of corpora under with aid of the database technology.

## III. BASIC IDEA OF BUILDING THE FOOD CORPUS

### A. The Development Process Of Building Food Corpus.

A high quality expected library construction should not only master the linguistics, computational science, but also needs to statistics, copyright, knowledge management, and other professional disciplines. This means that the corpus construction would be a huge task. its realization needs scientific and standardized design.

1. Requirements analysis phase. Consulting all kinds of literature and books to build a comprehensive understanding of the corpus, which could clear information requirements, processing requirements, security and integrity of corpus, so that building a database to determine the scope of application.
2. Design phase. Built on the corpus of scientific and reasonable structure design, detailed design.
3. Implementation phase. Design corpus storage structure, configure the computer hardware and software systems, to determine the researchers conducted methodical building a database in accordance with the objectives and design requirements analysis.
4. Maintenance phase. Ensure the food corpus is expected that the library can be built by continuity, and ensure its restoration and expansion in future.

### B. Detailed Design The Building Of Food Corpus.

For the size of the corpus of grain design, generally speaking if the conditions permit should be the bigger the better, but with the development of science and technology, real-time, dynamic development of language itself began, corpus should also with the dynamic development, therefore, the construction of the corpus should be constantly expanding process.

Food corpus structure diagram is shown in figure (1).

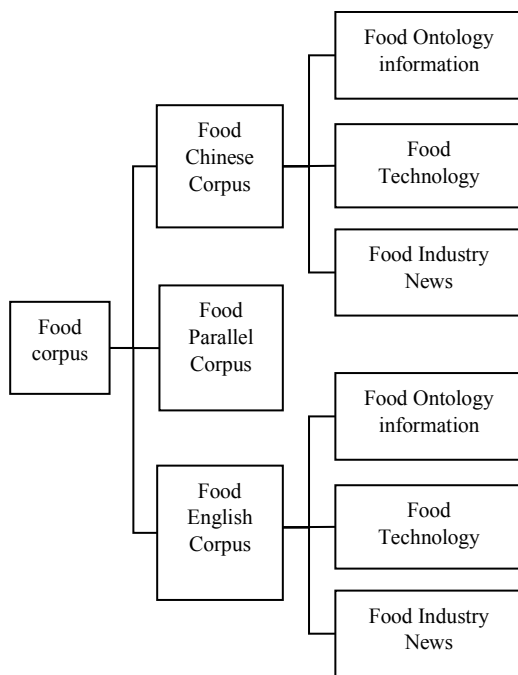


Fig1. Food corpus structure diagram

#### 1. Food Chinese Corpus

- Food ontology information, which includes cereals, legumes, oilseeds and all variety of animal or plant products and other nutrients which can sustain human life.
- Food technology, which includes prevention on food production capacity, infrastructure, storage methods, such as insects and other biological hazards.
- Food industry news, which includes the body extending from the food live on food, such as food supply and demand, prices, policy, accidents, security and situation monitoring.

#### 2. Food English Corpus

In China, the research of English corpus developed rapidly in the 1990s, such as SWECCL, COLSEC, CLES, CEEC, JDEST [7]. Currently, there is a professional English corpus has been built, such as Legal English Corpus and Medical English Corpus[8]. For example, National Language Committee has built computer professional bilingual corpus, etc[9]. Food corpus building through the real food English text to the response of the characteristics of English food information, which cannot only provide real natural language materials for food education, food translation and food language study, but also provides reliable information for the public opinion monitoring network.

#### 3. Food Parallel Corpus

Mona Baker has pointed out that "In the professional disciplines, a professional in the field of Chinese-English parallel corpus will be based on the existing machine translation system performance, the better to achieve professional results in the English translation of the article" [10]. Food parallel corpus refers to double corpus

of English and Chinese. Currently parallel corpus has been built is not fully covered, the scope of application is not widespread, so professional food parallel corpus construction have great prospects for development.

#### IV. BASIC METHODS OF BUILDING THE FOOD CORPUS

The food corpus is mainly related to the data of corpus collection, corpus cleaning, corpus processing, retrieval and data sharing. The basic process of building the food corpus is shown in figure(2).

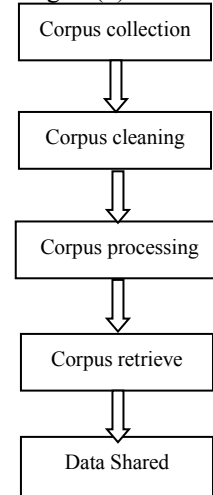


Fig2. The basic process of building food

##### A. Corpus collection

The data of food corpus include the entity and virtual information. Entity information including food-related professional books, newspapers, academic journals and other text resources. Virtual information is electronic resources which translated from website, the network library, database, CD, video, etc. Acquisition process mainly through manual keyboard input, identifying scanning and combination of these two methods. Such as the existing reference corpus can be used directly and some precious raw file or video can use artificial recognition, such as manual input method, so that ensure the corpus collected comprehensive and has higher availability.

##### B. Corpus cleaning

Corpus cleaning process is the key for building a corpus. Copious amounts of text or scanning it is downloaded over the network, there are a variety of formats, so not only to the text in the link of finishing backup, more important is the text of the specification of the finishing. Usually use some software to replace the specifications of the text, such as "Text Sorting Device" and so on [9].

##### C. Corpus processing

The corpus processing of building food corpus including word segmentation, corpus annotation, corpus retrieve and parallel corpus aligned processing.

##### 1. The corpus segmentation

Clean text word is add spaces after the English character to facilitate late annotation and retrieval. There are lots of ways to deal with ambiguity phenomenon in the process of word segmentation, such as “Phrase structure method”, “Expert system”, “Markov models”. The current mainstream of automatic word segmentation technology is based on forward and reverse maximum matching string matching algorithm, which is based on positive maximum matching algorithm flow chart is shown in figure (3).

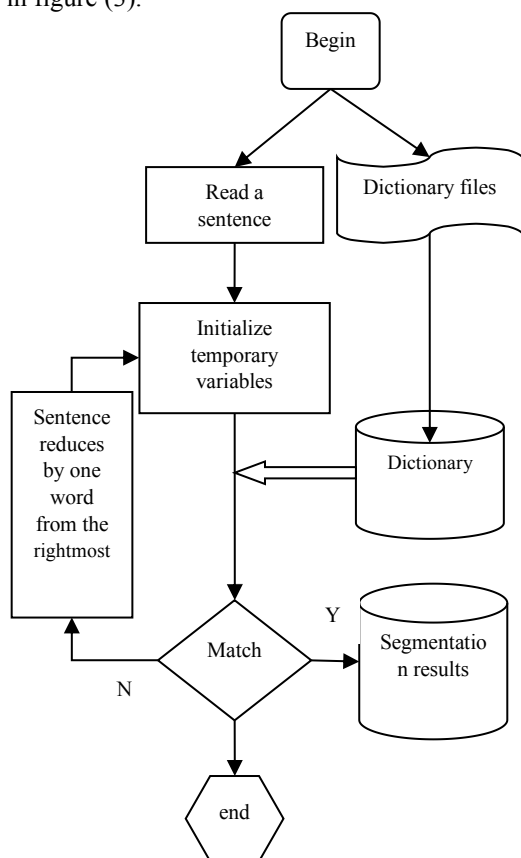


Fig3. Forward maximum matching string matching algorithm

2. The corpus annotation

High-quality corpus needs for multi-level corpus annotation. Corpus annotation is that every word in the text label attribute of the word. There are 26 basic parts of speech marks and four proper nouns mark in Tag set [11].

Currently, there are parts of corpus annotation software, such as CLAWS, ICTCLAS\_Win, and they could POS assigned code for corpus. Using artificial computer aided method when further processing of food corpus.

3. The corpus retrieve

With the development of computer technology, corpus should be like a database operation and convenient operation. Currently, the existing corpus retrieval software, such as Wordsmith Tools, Concordance, Mono-concord and WordCrucher, among Micro-concord for open software, DOS-based platform Tact 2.1, there are Wconcord,

Concap, Mlct-concordancer, Wordpilot, Antconc, Paraconc also could use convenient [12].

In the retrieval phase grain corpus construction, pre-mature mentioned above can be used to retrieve the software, the latter with the corpus of continuous improvement and professional food information, the software will probably not meet the demand, then consider the development of special use to retrieve software.

4. Parallel corpus aligned processing

Align the corpus is divided into paragraphs, sentences, clauses, phrases and words in a few different levels. Current Studies have bilingual automatically align technology mainly for the sentence and its internal structure, the method used is usually based on the length of terms, or the length, vocabulary hybrid approach [13].

V. THE APPLICATION PROSPECT OF THE FOOD CORPUS

Food information corpus will have the following characteristics: the first, building corpus according the linguistic theoretical guidance to achieve construction of professional services for food professional purpose, so it is not the corpus of mechanical accumulation. The second, text of corpus is continuously professional information, under the auxiliary treatment of computer technology to store by electronic text. Third, food corpus not only is a kind of idea or a research method, but also it is a new research idea.

For food corpus, it mainly professional food language research, such as food professional teaching outline word set, term extraction, dictionary compilation, problem sets and written examination and so on. Grain corpus should implement corpus resource sharing, platforms can be online index, query and other functions, used for food grain network public opinion, intelligence analysis, and other professional research in the field of information collection, allowing researchers to accurately according to the food prices changes, output and natural factors such as grain realistic situation to make the most effective means. In short, the use of food corpus can be summarized in two points: first, the rich grain of language study linguistics; Secondly, food grain and related professional research accuracy and lay a solid foundation.

VI. CONCLUSION

Food corpus based on database technology not only can enrich the linguistics research, and can meet the demand of food related professional information collection. Although food corpus building may spend a lot of manpower, material resources, will maybe a huge project. However, with computer and database technology, machine translation and other related technologies are maturing, I believe that food corpus building will become a new area of research, its application will be completed and just around the corner.

## VII. REFERENCE

- [1] Ting-Ting HE: *Corpus research[D]*. Central China normal university. 2003
- [2] Mao-Cheng LIANG, Wen-Zhong LI, Jia-Xin XU: *Corpus Application Tutorial[H]*.2010
- [3] Shehzad W. *Announcement of the principal findings and value addition in Computer Science research papers [J]* . Ibérica, 2010( 19) : 97-118.
- [4] Claveau V, Marie — Claude L'Homme . *Discovering and organizing noun — verb collocations in specialized corpora using inductive logic programming [J]* . International Journal of Corpus Linguistics, 2006,11( 2) : 209-243.
- [5] William I A . *Semantico — syntactic environments of the verbs show and demonstrate and Spanish mostrar and demostrar in a bilingual corpus of medical research articles[J]*. International Journal of Corpus Linguistics, 2008,13( 1) : 38-74.
- [6] Wanner L, Bohnet B, Giereth M, et al. *The first steps towards the automatic compilation of specialized collocation dictionaries[J]*. Terminology 2005,11( 1) : 43-80.
- [7] Zhang-Yong YE: *Construction and application of English Corpus [J]*: State and reflection, Ningbo Vocational and Technical College.2014,18(1)
- [8] Ping-Xin QIN: *Architecture English Corpus building ideas, methods and application [J]*. Guangdong University of Technology (Social Science Edition) .2009.9 (3)
- [9] Ai-Hua DONG: *Special purpose corpus construction, application , problems and development trend [J]*. Beijing Institute of Graphic Communication. 2013, 21(5)
- [10] [America] Lewis Kaplan *World Photography Masters biography series--Laszlo Moholy Nagy [M]* . translate by Han-Qin LU. Hangzhou . Zhejiang photography publishers.2010
- [11] Shi-Wen YU, Hui-Ming DUAN, Xue-Feng ZHU. *Peking University Modern Chinese Corpus basic processing specification [J]* Chinese Information Technology, 2002,16 ( 5 ) : 49-64
- [12] Wen-Zhong LI, Hui-Zhong YANG, Nai-Xing WEI. *Corpus indexing tool. An introduction to corpus linguistics[C]*. Shanghai: Shanghai foreign language education press, 2002.
- [13] Fei-Fan LIU, Jun ZHAO, Bo XU. *Building Large-Scale Domain Independent Chinese-English Bilingual Corpus and the Researches on Sentence Alignment [J]*.

# Re-sampling Reverse Analysis on Measurement Uncertainty Based on Bootstrap Simulation

ZU Xian-feng, HAN Yu-qin

First Aeronautical College of Air Force/ Department of Aeronautical Mechanical Engineering, Xinyang, China

**Abstract**—In order to resolve the puzzle of measurement uncertainty evaluation on source signals in measurement chains, according to reverse analysis idea and Monte Carlo (MC) simulation for distribution propagation, the re-sampling reverse analysis for uncertainties distribution is presented. The method extends the samples numbers by the bootstrap re-sampling, realizes distribution simulation from output to input and reverse process of MC simulation, integrated the estimation of probability density function (PDF) with small samples and the uncertainty evaluation. It can indirectly accomplish the uncertainty evaluation from testing signals to source signals. The result of verification experiment and simulation shows the validity and the feasibility of the re-sampling reverse analysis for uncertainty distribution because of the adaptability of uncertainty parameters from the reverse analysis and practical verification.

**Index Terms**—measurement Uncertainty, reverse Analysis, bootstrap re-sampling, Monte Carlo simulation

## I. INTRODUCTION

Technology needs progress, while metrology comes first. So metrology and calibration play an important role in scientific research. Metrology is an examination on test which is a more advanced test. Uncertainty is the objective inherent nature of things that exists in a variety of social phenomena, natural phenomena and engineering practice [1]. A measurement result is only complete if it is accompanied by a statement of the measurement uncertainty. In fact, input uncertainties and output uncertainties usually exist in actual systems [2] [3]. For the measurement chains, the calibration includes two aspects: output accuracy on source signals and measurement accuracy of the test channel [4]. The automatic test based on on-station calibration used analog equivalent device. Because source signals can not be tested directly, there is difficulty in evaluation of measurement uncertainty on source signals.

According to reverse analysis idea in structural engineering [5] [6], the re-sampling reverse analysis for uncertainty distribution is presented based on uncertainty distribution and Monte Carlo (MC) simulation for distribution propagation. The method which extends the samples numbers by the bootstrap calculates the estimation of probability density function (PDF) with samples. The error of source in measurement chain is traced through MC simulation. The probability distribution with source signals is evaluated and then the

measurement uncertainty is determined. Therefore reverse analysis for uncertainty from output to input is realized and the uncertainty of source signals is evaluated indirectly.

## II. BOOTSTRAP RE-SAMPLING WITH SMALL SAMPLES

Small sample is a common case when the calibration signals are acquired artificially. The small sample is that measurement data is less than thirty. Because of error in samples, it makes a large deviation in distribution fitting. Bootstrap re-sampling is used to extend the samples numbers. Then obtain the probability density function of sample by method of best square approximation [7].

Bootstrap method is first proposed as a statistical method for augmented samples by Efron in 1979. In the case of small data samples, Bootstrap method is a useful tool which is used for the evaluation on accuracy of estimated variable and parameters verification [8].

Bootstrap method is that an empirical distribution  $\hat{F}_n$  from independent population samples  $X$  is used to replace unknown population distribution  $F$ . Suppose random samples  $X = (x_1, x_2, \dots, x_n)$  come from unknown population  $F$ ,  $R(X, F)$  considered as a pre-selected random variable is the function of  $X$  and  $F$ . Distribution of  $R(X, F)$  is estimated according to sample observations  $X = (x_1, x_2, \dots, x_n)$ . The method is as follows:

- Empirical distribution function  $\hat{F}_n$  for sub-sample is constructed from sample observations  $X = (x_1, x_2, \dots, x_n)$  and  $\hat{F}_n$  in each point  $x_i$  has equal probability.
- Sample  $X^* = (x_1^*, x_2^*, \dots, x_m^*) \sim \hat{F}_n$  from  $\hat{F}_n$ . It's considered as Bootstrap sample.
- Distribution of  $R(X, F)$  is used to replace  $R^* = R(X^*, \hat{F}_n)$  distribution. It's considered as Bootstrap sample. It has been proved that when  $m$  is large enough Bootstrap sample can represent population distribution and statistical characteristics from original sample.

The usual methods for calculating Bootstrap distribution and estimator include calculation directly, MC method and the Taylor law. With the development of computer technology, it's convenient to compute Bootstrap statistics by MC method. Obviously it's more accurate and reliable to determine the PDF of the original samples with extended Bootstrap samples.

### III. RE-SAMPLING REVERSE ANALYSIS FOR UNCERTAINTY DISTRIBUTION

The re-sampling reverse analysis for uncertainty distribution is based on the foundation of uncertainty distribution. The essentiality is converse process of distribution propagation by MC simulation. Uncertainty distribution of the source signals will be calculated by the way of re-sampling reverse analysis from uncertainty distribution of measurement result. The basic principle is shown as Figure 1.

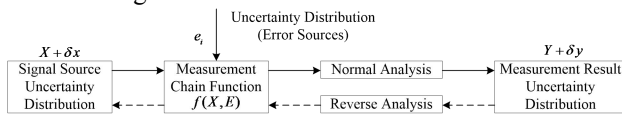


Figure 8. Uncertainty distribution with re-sampling reverse analysis.

Suppose function model of measurement chains, which are established by standard source signals and verification experimental data, is shown as following:

$$Y + \delta y = f(X + \delta x, e_i). \quad (1)$$

Which,  $X$ 、 $Y$  is input vector and output vector in system.  $\delta x$ 、 $\delta y$  are values of uncertainty distribution.  $e_i$  is uncertainty distribution of all error sources in measurement chains. It can be calibrated by standard experiment or traceability, also can be obtained by relevant technical specifications. Uncertainty distribution with re-sampling reverse analysis method is to implement as follows:

- Fit the uncertainty distribution of vector  $Y$  from measured samples. Different fitting way of PDF is used in different size of sample.
- Sample value  $y_1$  of output vector  $Y$  and sample value  $e_{i1}$  of all random error sources  $e_i$  are produced with MC simulation based on probability distribution.
- Sample value  $x_1$  of a corresponding input vector  $X$  is got in a reverse way by system model or inverse function.
- Repeat the above steps and re-sample in a reverse way  $M$  times. The sample value of  $X$  is got as sets  $x_k (k = 1, 2, \dots, M)$ .
- $x_k$  which is the sample value of vector  $X$  is used to define probability distribution of uncertainty. Thus the uncertainty and confidence interval of vector  $X$  can be calculated.

### IV. RE-SAMPLING REVERSE ANALYSIS OF SOURCE SIGNAL

#### A. Experiment Step

To apply re-sampling reverse analysis method, source signals and test signals are regarded as a linear transfer relationship combined with Bootstrap re-sampling. And verify the delivery channels in laboratory to determine the gain and offset. Re-sample reverse analysis for a particular source. Assess the size of uncertainty and output distribution character. The main steps are as follows:

- Verify the delivery channel of value between source signals and test signals. Therefore obtain transfer function is shown as following:

$$y = Gx + D = 0.1662x + 0.0681. \quad (2)$$

- Evaluate the error distribution character of delivery channel. The gain error is 67ppm here. Assumed to be uniform distributed, the offset error is 0.00038V. Assumption is normal distribution.
- Connect excitation source signal, start measurement and then obtain the measurement sample. Determine and remove the gross error in the sample by some principle and select raw sample data which capacity is 40.
- Extend sample to size of 200 using Bootstrap method. And then convert the domain of sample data range to [0, 1]. Get the PDF of raw sample data by square approximation method and restore the domain later.
- Apply re-sampling reverse analysis for uncertainty distribution simulation. Sample the output value, the gain error and offset error of delivery channel respectively by existing probability distribution, uniform distribution and normal distribution from sample. Calculate the corresponding input value using the following relationship :

$$x(i) = [y(i) - (D + \delta_D(i))] / (G + \delta_G(i)). \quad (3)$$

- Re-sample 1000 times. The false input sampled data of 1000 source signals can be got. After converting the domain, square approximation method is used to obtain the PDF.
- The average value, standard uncertainty, expanded uncertainty, confidence probability and covering factor can be calculated through PDF of false input sample. And make its quantitative description of the probability distribution.
- Re-sampling reverse analyze by reverting raw sample data directly so as to compare the effect of Bootstrap method.

#### B. Sample of Raw Sample Data

The output of raw measurement sample data which passing through the delivery channel from source signals is shown in Table 1. Carry on re-sampling reverse analyze for uncertainty.

TABLE I.  
RAW MEASUREMENT SAMPLE DATA OF SOURCE SIGNALS

raw measurement sample data of source signals (Unit: V)				
5.8760	5.8847	5.8849	5.8815	5.8781
5.8763	5.8855	5.8845	5.8810	5.8778
5.8772	5.8859	5.8841	5.8806	5.8771
5.8783	5.8860	5.8837	5.8802	5.8768
5.8794	5.8859	5.8833	5.8798	5.8765
5.8807	5.8857	5.8828	5.8793	5.8763
5.8820	5.8855	5.8824	5.8789	5.8761
5.8834	5.8852	5.8820	5.8785	5.8760

C. PDF Curve of Output Sample

The PDF curve which is fitted from initial or Bootstrap output sample shown in figure 2:

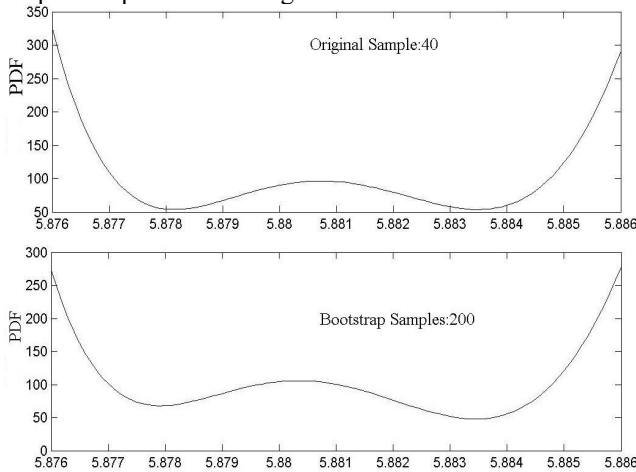


Figure 8. PDF curve of output sample with source signals.

D. PDF Curve of Input Source Signal

After using Re-sampling reverse analyze, the PDF curve which got from input source signals is shown in figure 3:

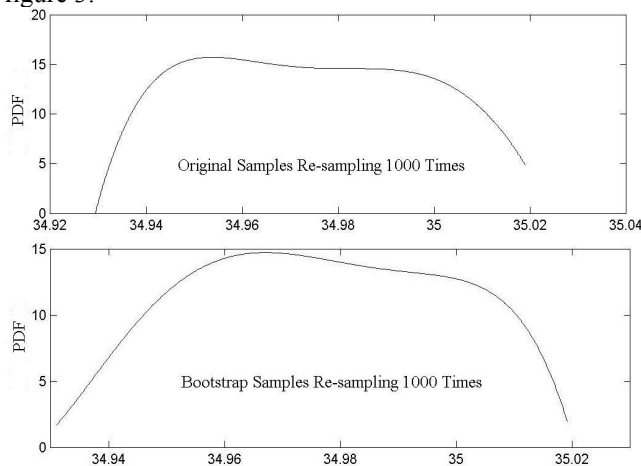


Figure 8. PDF curve of input source signals.

E. Coefficient of Sample PDF Curve

The best square approximation polynomial coefficient of output sample PDF for source signal are:

Original = [3.2584 -33.695 144.82 -256.98 189.28 -43.758]

Cbootstrap = [2.7386 -28.279 133.83 -258.93 208.58 -55.162]

Accordingly, the best square approximation polynomial coefficient of input sample PDF for source signal are:

Coriginal = [-0.15644 14.941 -57.553 98.917 -76.396 20.521]

Cbootstrap = [0.14908 3.8662 10.514 -60.112 84.476 -38.724]

V. SOURCE SIGNALS UNCERTAINTY EVALUATION

Measurement result and its uncertainty will be estimated and evaluated after fixing PDF of measurement data sample. Certainly, the PDF determined based on measurement of the sample need to carry on fitting test. The common way includes K-S and  $\chi^2$  test method. The former is applicable to small sample, and the latter is applicable to big sample.

Assume the PDF estimation of measurement sample is  $\hat{f}(x)$ , Correspondingly the measurement result is:

$$\hat{x} = \int_a^b x \hat{f}(x) dx . \tag{4}$$

Standard uncertainty of measurement result is:

$$u = \sqrt{\int_a^b (x - \hat{x})^2 \hat{f}(x) dx} . \tag{5}$$

Coverage factor is assumed as  $k$ , and then the expanded uncertainty is:

$$U = ku . \tag{6}$$

The confidence is calculated by following formula under the condition of symmetrical distribution.

$$P = \int_{\hat{x}-ku}^{\hat{x}+ku} \hat{f}(x) dx . \tag{7}$$

Integral interval of above formula with asymmetrical distribution is :  $[\hat{x} - (1 + \alpha)ku, \hat{x} + (1 - \alpha)ku]$ , which  $\alpha$  is asymmetrical coefficient under the condition of asymmetrical distribution. It can be fixed by skew and peak coefficient of sample. The detail is shown in reference [9]. The mean, standard uncertainty, expanded uncertainty, confidence interval and coverage factor of source signals can be calculated by the PDF of input signals. And the parameters are compared with the actual test result as shown in table II.

TABLE II.  
SOURCE UNCERTAINTY PARAMETERS COMPARED WITH THE ACTUAL TEST RESULT

Signal parameter	Source signals		
	Raw data Re-sample	Bootstrap Re-sample	actual test result
Sample mean	34.9735	34.977	34.9762
Standard uncertainty	0.0227	0.0217	0.0220
95% Confidence	[34.9351,	[34.937,	[34.9322,

interval	35.0126]	35.013]	35.0202]
Coverage factor	1.6952	1.8267	2
Extended uncertainty	0.0385	0.0397	0.0440

## VI. CONCLUSION

From the probability distribution and related uncertainty parameters based on above re-sampling reverse analyze, we can see:

- The source signal is close to rectangular distribution, the coverage factor should be in between 1.6 and 1.8. It's in accordance with character of rectangular distribution. For GUM uses the coverage factor of 2.0, normal distribution is assumed. As a result, confidence interval and extended uncertainty will bring large deviation.
- The re-sampling distribution result which extends sample size and fits PDF with Bootstrap has a small difference between the actual test values. The fitting results are satisfied.
- The uncertainty of sample distribution evaluation is more accurate and useful, which can calculate confidence interval and extended uncertainty conveniently.

The parameters based on bootstrap simulation are close to actual test result. Therefore the effectiveness and feasibility of re-sampling reverse analysis for uncertainty distribution are verified.

## REFERENCES

- [1] Yuran Liu, Mingliang Hou and Yanglie Fu, "Uncertainty Time Series' Multi-Scale Fractional-Order Association Model," *Journal of Computers*, vol.7, No.11 (2012), pp.2617-2622, November 2012.
- [2] Jiexin Zhang, "A Fast New Cryptographic Hash Function Based on Integer Tent Mapping System," *Journal of Software*, vol.6, No.6 (2011), pp.1154-1162, June 2011.
- [3] Xinyu Wang, Hongxing Wang and Junwei Lei, "Synchronization of Uncertain Chaotic Systems with Unknown Response Systems," *Journal of Computers*, vol.8, No.1 (2013), pp.178-185, January 2013.
- [4] ZU Xian-feng, PAN Meng-chun, and LUO Fei-lu, "Signal-oriented On-station Calibration System for Missile Weapon Testing Equipments," *8th International Conference on Electronic Measurement & Instruments (ICEMI'2007, Xi'an)*, vol. I, pp. 129-133, August 2007.
- [5] HE Yu-ao and MA Zhuo-jun, "Structural Parameter Identification Based on Genetic Algorithm and Extract Sample Back-Analysis Method," *JOURNAL OF TIANJIN UNIVERSITY*, China, Vol.35, No.5, Sep. 2002, pp.541-545(in Chinese).
- [6] WU Xiao-hui and SONG Hong-wei, "Recent status and prospect of reverse analytical method used in geotechnical engineering," *Mining Engineering*, China, Vol.1, No.5, Oct. 2003, pp.29-33(in Chinese).
- [7] D.N. Politis, "Computer-Intensive Method in Statistical Analysis," *IEEE Signal Processing Magazine*, January 1998, pp.39 - 55.
- [8] Zoubir A.M and Boashan B, "the Bootstrap and its Application in Signal Processing," *IEEE Signal Processing Magazine*, January 1998, pp.56 - 76.
- [9] LIN Hong-hua, "Statistical calculation on non-normal distribution error," *Space Navigation Measurement Technology*, China, Vol.16, No.5, August 1996, pp.6 - 15(in Chinese).

**ZU Xian-feng** was born in Anhui Province, China, in 1974. He received his B.S. degree from Northwestern Polytechnical University, Xi'an, China, in 1997. He received his M.S. degree and Ph.D. degree in Instrumentation Science and Technology from National University of Defense Technology, Changsha, China, in 2002 and 2008, respectively. He is working in First Aeronautical College of Air Force, China. His research interests include military metrology and military automatic test system.

**HAN Yu-qin** was born in Shaanxi Province, China, in 1975. She received her B.S. degree from Northwestern Polytechnical University, Xi'an, China, in 1997. She received her M.S. degree in Mechatronics Engineering from Xidian University, China, in 2013. She is currently a teacher of First Aeronautical College of Air Force, China. Her research interests include aeronautical ordnance and smart instrumentation.

# Driver Fatigue Detection Based on Active Facial Features Locating

Caijian HUA and Yan ZHANG

School of Computer Science, Sichuan University of Science and Engineering, Zigong, China

**Abstract**—Driver fatigue is a major cause of traffic accidents. The vision-based driver fatigue detection is one of the most prospective commercial applications of facial expression recognition technology. The facial feature recognition is the primary technique issue in it. Major challenges that arise are fast movements of eyes and mouth, changes in pose and lighting variations. In this paper, an active facial feature locating technology is presented for facial features detection of features extracted using active shape models. The fatigue detection consists of three levels of tasks: face detection, facial expression information extraction, and fatigue characterization measurement. The model used and characterization methodology showed efficient to detect fatigue using the active approach of the cases.

**Index Terms**—driver fatigue detection, facial feature locating, active shape model

## I. INTRODUCTION

Currently, driver fatigue has been widely accepted as a significant factor in a variety of transportation accidents[1]. Although it is difficult to determine the exact number of accidents due to fatigue, it is much likely to be underestimated. The effect of fatigue on driving performance has been widely studied from physiologists and transportation experts. Fatigue has been proved to be a main cause of road accidents and pushed automotive corporations, since late 90s, toward the development of on-board intelligent safety systems, useful to evaluate in real time the driver's state of vigilance [2,3].

Driver fatigue detection should detect whether the driver is tired, such as dozing or sleeping, so as to generate a warning alarm to alert the driver[4]. Fatigue measurement is a significant problem as there are few direct measures, with most measures of the outcomes of fatigue rather than of fatigue itself. In the last decade many researchers have been working on the development of the monitoring systems using different techniques. The best detection of primary drowsiness and inattention is the measurement of brain-waves, heart rate and pulse [5]. These techniques are intrusive, since they need to attach some electrodes on the drivers, causing annoyance to them. Some representative projects in this line are the MIT Smart Car [6], and the ASV (Advanced Safety Vehicle) project performed by Toyota, Nissan[2]. Other techniques monitor eyes and gaze movement using a helmet or special contact lens, which are still not acceptable in the practice [7]. A driver's state of vigilance can also be characterized by indirect behaviors of the

vehicle like lateral position, steering wheel movements. Although these techniques are not intrusive, they are subjected to several limitations as the vehicle type, driver experience, geometric characteristics and state of the road [8]. People in fatigue show some visual behaviors easily observable from changes in their facial features like eyes, head and face. Computer vision can be a natural and non-intrusive technique to monitor driver's vigilance[9-11]. Facial expression detection on the other hand gives an accurate detection with minimal impact on the driver[12-14]. As human eyes and mouths express the most direct reaction when dozing or sleeping, eye closure and opening mouth rank detection are widely used as the basis for the driver fatigue detection by researchers, such as to calculate the fatigue associated parameters as PERCLOS, AECS and YawFrec[15-18].

The detection and tracking of faces, eyes and mouths in video sequences is a basic problem in computer vision[19-21]. In the recent years, digital image processing and computer vision techniques on human faces have been used in many applications, such as face recognition, face analysis, eyes detection, gaze tracking etc. Among all these research, the first step is usually to locate the face. Feature based face detection methods utilize some well-known knowledge on human faces e.g, relative location of the eyes, nose and mouth in a face etc, to classify the image as a face. Various classifiers are based on the neural networks, Principal Component Analysis (PCA) and Support Vector Machines (SVM) [22].

This paper work proposes a fatigue detection system based on the computer vision techniques, where they are being analyzed by the visual characterizes of the driver face, from the variations that present the facial features, specially those in regions shape of the eyes and mouth. Those features are detected by using comprehensive techniques as Active shape models (ASMs), which from the a-priori object knowledge (face to be analyzed) and being help by a parametric model (79 facial points landmarked scheme), allow to estimate the object shape with a high precision level. ASMs bring the advantage of handle with problems as noise, occlusions, illumination changes and elements that could add variations to the analyzed image background. From the detected features, it is possible to perform eye closure and opening mouth rank measurement, to calculate the fatigue associated parameters as PERCLOS, AECS and YawFrec.

## II. ACTIVE LOCATING FACIAL FEATURES

Automatic and accurate location of facial features is difficult. The variety of human faces, expressions, facial hair, glasses, poses, and lighting contribute to the complexity of the problem. Concerning face localization, very robust techniques have been developed in late 90s based on neural networks. In 2004, Viola and Jones [23] proposed a new algorithm based on integral images and robust classification that achieves very good results and guarantees high performance. Both these approaches belong to the image-based subclass of the face detection techniques. More recently also feature-base approaches demonstrated a reasonable level of efficiency.

ASMs is a commonly used technique for facial feature extraction[24-25]. This technique is similar to the Active Contour Model, or snakes, but has the advantage that instances of an ASM can only deform in the ways found in its training set. ASM also allows considerable variability in shape modeling, but the model is specific to the class of target objects or structures that it intends to represent.

### A. Active Shape Models

The classical ASM is characterized by its use of the Mahalanobis distance on one-dimensional profiles at each landmark and a linear point distribution model. Training determines the characteristics of the profile and point distribution models.

A landmark represents a distinguishable point present in most of the images under consideration. A set of landmarks forms a shape. Shapes are represented as vectors: all the  $x$ -followed by all the  $y$ -coordinates of the points in the shape. A shape model is described by  $n$  landmark points that represent the important positions in the object to be represented. These points are generated based on a set of training shapes. Each training shape  $x$  is represented as a shape vector, which is a collection of landmark points called a point distribution model

$$x = (x_0, y_0, x_1, y_1, \dots, x_k, y_k, \dots, x_{n-1}, y_{n-1})^T \quad (1)$$

Where  $T$  represents the transpose operation, and  $(x_k, y_k)$  are the coordinates of the  $k$ th landmark point.

The training shapes are all aligned by translation, rotation and scaling for minimizing the sum of squared distances between their corresponding landmark points. Then, the mean shape  $\bar{x}$  and the deviation of each training shape from the mean are calculated. Principal component analysis (PCA) is then applied to capture most of the shape variations. Therefore, a shape model can be approximated as follows:

$$x \approx \bar{x} + Pb \quad (2)$$

Where  $P=(p_1 p_2 \dots p_t)$  is the matrix whose columns are the first  $t$  eigenvectors with the largest eigenvalues arranged in descending order, and  $b=(b_1 b_2 \dots b_t)^T$  is a weight vector for the  $t$  eigenvectors, referred to as the shape parameters. When fitting the shape model to an object, the value of  $b_i$  is constrained to lie within the range  $\pm 3$  standard deviations. This can ensure that this range of the shape parameters can represent most of the

shape variations in the training set. The number of eigenvectors  $t$  to be used is determined such that the eigenvectors can represent a certain amount of the shape variations in the training shapes, usually ranging from 90% to 95%. The desired number of eigenvectors  $t$  is given by the smallest  $t$  which satisfies

$$\sum_{i=1}^t \lambda_i \geq 0.95 \sum_{i=1}^N \lambda_i \quad (3)$$

Where  $N$  is the total number of eigenvectors available.

### B. Locating Facial Features

A straight forward way to improve the mean fit is to increase the number of landmarks in the model. Fitting a landmark tends to help fitting other landmarks, so results are improved by fitting more landmarks than are actually needed. Search time increases roughly linearly with the number of landmarks. The landmark scheme used by us consists of 79 facial points as shown in Figure 1.

Figure 8. Landmarking scheme used in our ASM implementation

The classical ASM uses a one-dimensional profile at each landmark, but using two-dimensional profiles can give improved fits. Instead of sampling a one dimensional line of pixels along the whisker, we sample a square region around the landmark. Intuitively, a 2D profile area captures more information around the landmark and this information if used wisely should give better results. A set of landmarks forms a shape. The ASM starts the search for landmarks from the mean shape aligned to the position and size of the face determined by a global face detector. We locate facial features by locating landmarks using active shape model, including the location of the left eye pupil, the right eye pupil and the mouth.

## III. FATIGUE CHARACTERIZATION MEASUREMENT

As mentioned in the earlier section, ASM model will be used to estimate the shape of the subject's face and with this get the 79 facial points that make up the parametric model. These points will be used to determine the movements and variations in shape of the regions of eyes and mouth, on which there will be realized the measurement of three parameters PERCLOS, AECS and YawnFrec. PERCLOS and AECS are measurements that characterize the movement of the eyelids. PERCLOS has been already validated and it has been that is the parameter most adapted to detect the fatigue [26]. AECS is a good indicator of fatigue, and it has been defined as the necessary quantity of time to close or open completely the eyes. The degree of eye closure is characterized by the shape of the pupil, it has been observed that when the eyes are closed, the pupil is occluded by the eyelids doing that his form makes to itself more elliptical. The degree of eye closure is computed as the ratio between the axis of the pupil's ellipse and with this one a record takes in the time to obtain the PERCLOS [27]. Otherwise, studies have shown that a person tired AECS is typically different from that of an alert person [28].

Figure 8. The ocular and mouth regions represented by SAM

A fatigued person is characterized by few expressions show because there is minimal activity of facial muscles, with the yawning or opening the mouth the most common expression. Monitoring the movements of the lips can be detected on open mouth position, provided that the features around the mouth to deviate from its closed configuration. The opening of the mouth is computed as the ratio between of its height and width. This measurement is used to estimate the YawFrec. The Figure 1 shows the landmarks chosen to analyze the subject's fatigue.

*A. Eyelid Movement Characterization*

To calculate PERCLOS and AECS, there has been propose to follow the pupil steadily and determinate the eye closure rank in an accumulative way on time, by using the axis reason on the pupil ellipse. An individual eye closure is defined as the difference of time between two moments to which the pupil size is 20% or less compared to the normal size. One individual closure velocity is defined as the time period where the pupil size is between 20% and 80% compared to the nominal pupil size. In order to realize those measurements, it is proposed to apply the described methodology on [5], with the difference not to be calculated the eye closure rank using its ellipse reason, but using the eye vertex defined on the 79 points landmarking scheme model(fig.1). More specifically using the 24, 25, 26, 27,28, 29, 30 and 31 eyelid vertex for the left eye and 16, 17, 18, 19, 20, 21, 22 and 23 for the right.

The distance  $D(i,j)$  between landmarks  $i$  and  $j$  is defined as

$$D(i, j) = \sqrt{(x_i - x_j)^2 + (y_i - y_j)^2} \quad (3)$$

According to the polynomial shape of the eyes and mouth, the eye closure rank is calculated by

$$C_{LeftEye} = \frac{D(25 - 31) + D(26 - 30) + D(27 - 29)}{3} \quad (4)$$

$$R_{OpenMouth} = \frac{D(41 - 43) + D(40 - 44) + D(39 - 45)}{3 \times D(32 - 38)} \quad (5)$$

From the Equations 4 and 5, when the eye closure rank is less or equal to 20% of maximum distance between the eyelid, it is considered that the eyes are closed. According to the work accomplish on [29], if the eyes are close during 5 consecutive frames, it could be considered as the diver falling sleep.

*B. Lips Movement Characterization*

To calculate the mouth opening frequency, is necessary to know the mouth opening rank, which is represented by the mouth's high and the width reason. The mouths high is represented by the distance between upper lip and

down lip, and the mouths width is represented by the distance between the left corner and the right one. The opening rank graphic is known as the YawnFrec and this can be seen as peaks yawns To perform the mouth opening rank measurement, it is proposed to use the mouth vertexes gotten by the 79 facial points landmarking scheme (fig.1). More specifically there must be use the vertexes that would define the mouth extremes (right 32, right 38, up 39, 40 and 41, and down 43, 44 and 45).

The mouth opening is defined as

$$C_{RightEye} = \frac{D(19 - 21) + D(18 - 22) + D(17 - 23)}{3} \quad (6)$$

Through the work on [30], if the mouth opening rank is above 0.5 in more than 20 consecutive frames, it could be consider as the driver yawning.

IV. EXPERIMENTS AND ANALYSIS

*Data Collection*

In order to test the effectiveness of the proposed approach, a USB industrial Camera has been installed in a car, as shown in figure 3. This camera allows the recording of several minutes of video during typical driving situations.

We collected data from 6 acquisition sessions of the same driver in different moments of the day and various conditions of ambient light. The user was driving both wearing glasses or not, without caring about the position of the seat and of the camera such as fig.4. Each session consists of 3 minutes of video recording, manually classified as follows:

- (1) About one minute of normal driver behavior: the driver looks at the road straight-away or to rear view mirrors;
- (2) About one minute of simulated fatigue effects: the driver closes the eyes and simulates nodding;
- (3) About one minute of distracted behavior: the driver looks up, down or laterally.

The proposed driver fatigue detection algorithm is tested on Intel Pentium, 2.9 GHz CPU with 2.0 GB RAM with OpenCV2.0 equipped with Microvision MV-1300UM camera as a video source to capture the images in real time. The format of the input video is 45fps @ 640 \* 480 true color.



(1) Camera set (2) sample frame captured

Figure 8. Fig.3 Camera set and sample frame captured



Figure 8. Samples of frame with normal attention states and inattentive states

### B. Results

As detailed in the previous section, the proposed approach is composed of three processing blocks. In the first block, each video frame (a  $640 * 480$  pixels true color image, see figure 4) is passed to the Viola-Jones detector. The resulting region of interest is cropped around the center of the region, giving rise to a small frame of fixed dimension ( $320 * 320$  pixels). If the detected ROI is smaller than  $320 * 320$  pixels, remaining pixels are set to zero.

In the second processing block, the active shape model choose takes in input the extracted ROIs and computes the 79 points landmarks used different for locating facial feature, including locating the eyes and mouth regions. The landmarks locate the facial feature. In our test, we use the 1D profile model and 2D profile model respectively in the same test data images.

In the third processing block, the eyelid and lips movement characterization are measured using the choose landmarks.

The algorithm was tested on various persons with different size, shape and color of eyes, skin color, facial hairs and gender. For small head movements, the algorithm rarely loses track of the eyes and has a tolerance on head rotation of up to 30 degrees in azimuth. The result of the facial features locating for fatigue detection of algorithm is shown in Table 1.

Table 1 summarizes the results of our list experiment using active shape models on the test data sets respectively. We compared our scheme against two other implementations, 1D classical ASM (that uses only 1D profiling and the Mahalanobis distance metric) and stacked ASM (that uses a two stage ASM approach with 1D profiling used list followed by 2D profiling and the Mahalanobis distance metric).

TABLE III.  
FATIGUE DETECTION ACCURACY OF 1D AND 2D PROFILING ASMS

Accuracy	1D profiling	2D profiling
Normal Behavior	94.5%	96.4%
Fatigue Behavior	90.2%	92.3%
Distracted Behavior	89.7%	93.6%

All models were trained on the same set of images. On the 1D profile model, our implementation outperformed the classical ASM algorithm by slightly average 91.3% on normal behavior, fatigue behavior and distracted behavior fitting error and the average normalized fitting error and was more accurate than stacked ASM by 8.18% on both counts. Similar results were obtained on the 2D profile model test, where our method was 3% more accurate than 1D profile conventional ASM.

### V. CONCLUSION

This paper was presented the characterization of fatigue based on the facial feature locating using active shape models. The analyzed regions correspond to the eyes and the mouth on which detection and tracking of features is done using the 79 points landmarking scheme. The results show that the estimation of the points is exact and complies with the requests for this type of systems. Through quantitative analysis evaluated the robustness of the ASM model in feature detection, which is maintained in nominal range pose. The used model and the methodology of characterization showed efficiency to detect the fatigue in 94.2% of the evaluated cases. In addition, due to high accuracy in detecting and characterizing features proposed to estimate parameters associated with fatigue as the PERCLOS, AECS and YawFrec to determine the presence of this, the designed system has great potential for detect fatigue in the early stages, being of great interest in vial research prevention.

### ACKNOWLEDGMENT

This work was supported by the Scientific Research Foundation of Sichuan University of Science and Engineering (Grant No. 2012RC22), Sichuan Provincial Department of Education Fund (Grant No.13ZB0139 and No. 14ZB0217) and Key Laboratory for Enterprise Information and IOT Measurement and Control Technology of the education department of Sichuan province Open Fund (Grant No.2013WYY04).

### REFERENCES

- [1] Hancock, P.A., Verwey, W.B. "Fatigue, workload and adaptive driver systems". *Accid. Anal. Prev.* 29(4),1997, pp. 495-506.
- [2] A. Kircher, M. Uddman, J. Sandin. "Vehicle control and drowsiness", *Technical Report VTI-922A*, Swedish National Road and Transport Research Institute, 2002.
- [3] The role of driver fatigue in commercial road transport crashes. European Transport Safety Council, Brussels 2001.
- [4] Qiong Wang, Jingyu Yang, Mingwu Ren, Yujie Zheng. Driver Fatigue Detection: A Survey. *Proceedings of the 6th World Congress on Intelligent Control and Automation*, Dalian, China, 2006.
- [5] Ji, Qiang, and Xiaojie Yang. "Real-time eye, gaze, and face pose tracking for monitoring driver vigilance". *Real-Time Imaging* 8.5, 2002, pp. 357-377.

- [6] J. Healey, and R. Picard, "SmartCar: detecting driver stress," *in Proc. 15th Int. Conf. Pattern Recognition*, Barcelona, Spain, vol. 4, 2000, pp. 218-221.
- [7] Anon, "Perclos and eyetracking: Challenge and Opportunity," *Applied Science Laboratories*, Bedford, MA, 1999.
- [8] H. Ueno, M. Kaneda, and M. Tsukino "Development of drowsiness detection system," *in Proc. Vehicle Navigation and Information Systems Conf.*, 1994, pp.15-20.
- [9] X. Liu, F.L. Xu, and K. Fujimura, "Real-time eye detection and tracking for driver observation under various light conditions," *in Proc. Intelligent Vehicle Symp., Versailles*, France, 2002, pp. 344-351.
- [10] H. Gu, Q. Ji, and Z.W. Zhu, "Active facial tracking for fatigue detection," *in Proc. Workshop on Application of Computer Vision*, Orlando, 2002, pp. 137-142.
- [11] Saradadevi, Mandalapu, and Preeti Bajaj. "Driver fatigue detection using mouth and yawning analysis." *International Journal of Computer Science and Network Security*, 8.6, 2008, pp. 183-188.
- [12] [13] Liu, Weiwei, Haixin Sun, and Weijie Shen. "Driver fatigue detection through pupil detection and yawing analysis." *Bioinformatics and Biomedical Technology (ICBBT)*, International Conference on. IEEE, 2010.
- [13] Senaratne, Rajinda, et al. "Comparing two video-based techniques for driver fatigue detection: classification versus optical flow approach." *Machine Vision and Applications*, 22.4, 2011, pp. 597-618.
- [14] Tang, Jie, et al. "Driver fatigue detection algorithm based on eye features." *Fuzzy Systems and Knowledge Discovery (FSKD)*, 2010 Seventh International Conference on. Vol. 5. IEEE, 2010.
- [15] D.F. Dinges, and R. Grace, "PERCLOS: A valid psychophysiological measure of alertness as assessed by psychomotor vigilance," *US Department of Transportation, Federal highway Administration*. Publication Number FHWA-MCRT-98-006.
- [16] Rajinda, S., David, H., Vanderaa, B., Halgamuge, S. "Driver fatigue detection by fusing multiple cues". *Proceedings of the 4th International Symposium on Neural Networks*, 2007, pp.801-809.
- [17] Smith, P., Shah, M., da Vitoria Lobo, N. "Determining driver visual attention with one camera". *IEEE Transactions on Intelligent Transportation Systems* 4, 2003, pp. 205-218.
- [18] Bergasa, L.M., Nuevo, J., Sotelo, M., Barea, R., Lopez, M. "Real-time system for monitoring driver vigilance". *IEEE Transactions on Intelligent Transportation Systems* 7, 2006, pp. 63-77.
- [19] Castrillón, Modesto, et al. "A comparison of face and facial feature detectors based on the Viola-Jones general object detection framework." *Machine Vision and Applications*, 22.3, 2011, pp. 481-494.
- [20] Ding, Liya, and Aleix M. Martinez. "Features versus context: An approach for precise and detailed detection and delineation of faces and facial features." *Pattern Analysis and Machine Intelligence*, IEEE Transactions, 32.11, 2010, pp. 2022-2038.
- [21] Maglogiannis, Ilias, Demosthenes Vouyioukas, and Chris Aggelopoulos. "Face detection and recognition of natural human emotion using Markov random fields." *Personal and Ubiquitous Computing*, 13.1, 2009, pp. 95-101.
- [22] CM Bishop, "Pattern recognition and machine learning", *Springer Science Business Media*, 2006.
- [23] Viola Paul, Jones, Michael J, "Robust Real-Time Face Detection". *International Journal of Computer Vision*, 57.2, 2004, pp. 137-154.
- [24] Andrew Blake, Michael Isard. "Active Contours: Active shape models", *Springer London*, 1998, pp. 25-37.
- [25] Kwok-Wai Wana, Kin-Man Lama, "An accurate active shape model for facial feature extraction". *Pattern Recognition Letters*, Volume 26, Issue 15, 2005, pp. 2409-2423.
- [26] Dinges, D.F., Mallis, M., Maislin, G., Powell, J. "National Highway Traffic Safety Administration: Evaluation of techniques for ocular measurement as an index of fatigue and the basis for alertness management", No. HS-808 762, 1998.4.
- [27] Zhu, Z., Ji, Q., Lan, P, "Real time non-intrusive monitoring and prediction of driver fatigue", *IEEE Trans. Veh. Technol.*, 53, 2004, pp. 1052-1068.
- [28] Ji, Q., Yang, P, "Real time visual cues extraction for monitoring driver vigilance", *In: ICVS*, 2001, pp. 107-124.
- [29] Dong, W.H., Wu, X. "Driver fatigue detection based on the distance of eyelid", *In: IEEE Int. Workshop VLSI Design and Video Technology*, Suzhou, 2005, pp. 28-30.
- [30] Wang, T., Shi, P. "Yawning detection for determining driver drowsiness", *In: Proceedings of 2005 IEEE International Workshop on VLSI Design and Video Technology*, 2005, pp. 373-376.

**Caijian HUA** received the M.S. degree in computer science from Southwest University of Science and Technology, Mianyang, China, in 2005, the Ph.D. degree in instrument science and technology from the Sichuan University, Chengdu, China, in 2012.

He is currently a lecture with the School of Computer Science, Sichuan University of Science and Engineering, Zigong, China. His areas of research include computer vision, information fusion, and pattern recognition. His latest research focuses on face detection and recognition, facial expression analysis, image segmentation, object tracking, and active information fusion for monitoring human fatigue.

# Measurement of moisture content in soybean by near-infrared spectroscopy technique

Huang Nan, Wang Ruolan and Yue Jia

Henan University of Technology (HAUT) Food Institute, Grain storage and security of Ministry of education, Engineering Center, National Engineering Laboratory of grain storage and transportation, ZhengZhou, China

**Abstract**—The model of determining soybean moisture was built using near-infrared spectroscopy(NIRS) and the Foss XDS system as the analyzer the influences on the model of factors such as the mathematics methods and optics treatment methods were studied the calibrations of the moisture content in soybean were also performed the results showed that the best factors were SNV only for optic treatment method and 1.4.4.1 for mathematics method. The correlation coefficient(1-VR) was 0.9907, the average determination coefficient of validation( $R^2$ ) was 0.9937, the square error of cross(SEC) was 0.0966, the square error of cross validation(SEVC) was 0.1272, and the standard error of prediction(SEP) was 0.135. This model could substitute for tradition chemical method to determine the moisture content in soybean.

**Index Terms** —near-infrared ,spectroscopy ,soybean ; moisture

## I. INTRODUCTION

Near-infrared spectroscopy technique is applied to analysis grain composition has a long history nearly 50 years. The technique has been widely used all over the world because of its many advantages such as Non-destructive, simple operation, large processing quantity, objective and accurate, fast and no pollution. Near-infrared spectroscopy technique established the relationship between the absorption spectrum and the content of substance, test material such as protein, carbohydrate, moisture etc. All above are based on using OH, C, and NH groups in the near infrared region(800~2500nm) of frequency doubling and sum frequency absorption. In recent years, with the development of computer technology and chemometrics method, near infrared detection is getting more and more attention, especially the grain and oil and its products has got relatively rapid development.

Water is an important index of the quality of soybean, however it can be pretty time consuming by using conventional standards to determine the moisture of soybean, so, establish the near infrared standard model which is a rapid science and reasonable detection method. In this paper, using near infrared diffuse reflectance spectrum analyzer, scanning 150 soybean samples spectrum in different areas from Henan, Liaoning and Inner Mongolia, and using the conventional standard method to detect the water content of all samples, establish the near infrared model of soybean moisture and verify the accuracy of the model which laid the

foundation of near infrared spectroscopy technique in study on the quality of soybean in China.

## II. MATERIALS AND METHOD

### A. materials

Soybean samples which come from Henan, Lioaning, Inner Mongolia

### B. Instrument

The FW-135 type publisher, XDS type FOSS NIR spectrum analyzer

### C. Test method

1. GB/T 5497-1985
2. Near infrared analysis method
3. Spectral collection

Near infrared spectra collected is performed simultaneously with the conventional detection, and completed within the same day. Crushed samples passing through 40 mesh sieve, and use of nature packing method. Each sample was repeated 2 times by loading the sample. To overcome the inhomogeneity, we taking the average spectral collection method after scanning each loading sample. The scanning wavelength range of 400~2498nm, scanning for 32 times. One of the samples' near infrared spectroscopy as shown in figure 1.

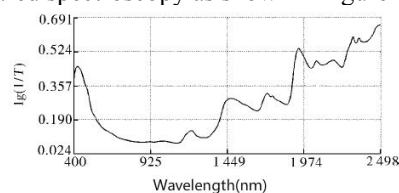


FIGURE.1 Wavelength

### 4. The establishment of mathematical model of NIRS

Choose 100 samples as calibration sample to set correction model, sample moisture distribution shown in figure 2. By using WIN ISI calibration software to set up the model of soybean moisture content. And analysis the influence on model results condition, the spectral scattering process, mathematical processing parameters so that select the optimum model parameters.

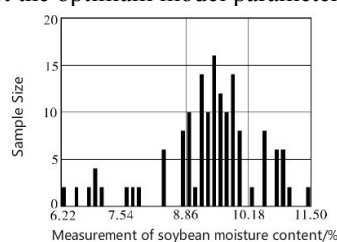


FIGURE2. Measurement of soybean moisture content

5. Model Test

Model test using two methods: internal cross validation and external validation. Internal cross validation is in turn eliminate sample group of one or more samples, with the remaining samples to modeling and forecasting removed sample composition. By comparing the difference between the rejection samples prediction value and actual value. Thus determine the accuracy of prediction model. External validation is choosing a number of independent samples, through comparing the differences between the prediction value of independent samples and actual analysis value to determine the model's forecast accuracy.

III. RESULTS AND DISCUSSION

A. Analysis of the results of calibration moisture content of soybean samples

The results of determination of moisture content of samples one shown in table 1. The table 1 shows that the determination error of all samples was less than 1.03%. The amplitude of the water content in the sample is large, basically covering the varieties of soybean moisture content, and also, with a good sample representation.

Table 1 effects of samples' moisture content

sample	sample size	average value	maximum value	minimum value	standard deviation
calibration sample	100	9.342	11.502	5.708	1.225
verification sample	40	8.968	11.466	5.681	1.364

B. Effects of modeling parameter

The main parameters that influence model are the optical processing method and mathematical method of near infrared spectroscopy, optical processing, None optical processing, standard normal treatment combined to bias technology, standard normal treatment, Deviation technology, standardized multiplicative scatter correction, weighted scatter correction, inversion of multiple scatter correction.

The mathematical treatment method: select of 0.0.1.1, 1.4.4.1 two mathematic methods as effect factors to investigate the 14 calibration equation of model.

Table 2 Moisture content calibration equation parameters

Scattering processing technology	Mathematical treatment	1-VR	R <sup>2</sup>	SEC	SECY
None	0.0.1.1	0.9758	0.9875	0.1362	0.2054
SNV and Detrend	0.0.1.1	0.9813	0.9896	0.0993	0.1806
SNV Only	0.0.1.1	0.9801	0.9853	0.1479	0.1853
Detrend Only	0.0.1.1	0.9804	0.9914	0.1155	0.1424
Standard WSC	0.0.1.1	0.9835	0.9911	0.1176	0.1702
Weighted WSC	0.0.1.1	0.9891	0.9725	0.2034	0.2313
Inverse WSC	0.0.1.1	0.9859	0.9922	0.1099	0.1596
None	1.4.4.1	0.9898	0.9926	0.1068	0.1382
SNV and Detrend	1.4.4.1	0.9902	0.9936	0.1266	0.1315
SNV Only	1.4.4.1	0.9907	0.9939	0.0967	0.1273
Detrend Only	1.4.4.1	0.9835	0.9889	0.1302	0.1711
Standard WSC	1.4.4.1	0.9902	0.9935	0.1008	0.1306
Weighted WSC	1.4.4.1	0.9881	0.9928	0.1043	0.1445
Inverse WSC	1.4.4.1	0.9897	0.9933	0.1022	0.1339

C. Analysis model of internal cross validation and external validation results

1. The results of internal cross validation

Model of internal cross validation results as shown in table 3. As can be seen from table 3, there are good results of soybean moisture content by using near infrared spectroscopy, the interactive calibration coefficient of determination reached as 0.9908. Calibration coefficient of determination is 0.9939, standard error is 0.0967, interactive calibration standard error is 0.1273.

Table 3

SEC	R <sup>2</sup>	SECY	1-VR
0.0966	0.9939	0.1272	0.9906

2. Results of external inspection

The calibration model external inspection results as shown in table 4.

Table 4 Results of external inspection

sample size	ANL	LAB	R <sup>2</sup>	SEP	T	T0.05
40	8.892	8.968	0.991	0.137	0.547	2.02

Table 4 shows that the T test value of the measured value and predicted value did not reach significant level, the test effect shows in figure 3.

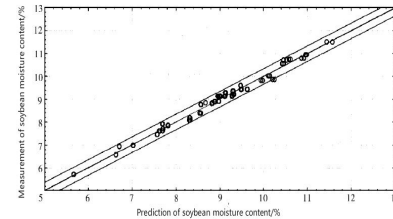


FIGURE3. Prediction of soybean moisture content

As you can see from figure 3, the correlation of measured values and predicted values is very high. The results illustrate the near infrared spectroscopy technology can be used in detecting the moisture content of soybean.

IV. CONCLUSION

This paper uses the near infrared spectroscopy technology to established near infrared analysis of soybean moisture content model, and validates the accuracy of detection model.

The experimental results shows that, the correlation among the sample forecast value and the measurement value is very high. This technology can totally be used as a method for the determination soybean moisture content. It can also replace the conventional standard methods in studying the rapid evaluate the soybean quality.

REFERENCE

- [1] DELW ICHE S R. Protein content of single kerne ls of wheat by near-infrared reflectance spectroscopy. J Cereal Science, 1998, 27: 241- 254.
- [2] Kovalenko I V, Rippke G R, Hurburgh C R. Measurement of soybean fatty acids by near-infrared spectroscopy: Linear and nonlinear calibration methods. Journal of the American Oil Chemists' Society, 2006, 5(83).
- [3] Roberts C A, Ren C, Beuselinck P R, etal. Fatty acid profiling of soybean cotyledons by near-infrared spectroscopy. Applied Spectroscopy, 2006, 11(60).
- [4] Dondee S, Meeso N, Soponronnarit S, etal. Reducing cracking and breakage of soybean grains under combined near-infrared radiation and fluidized-bed drying. Journal of Food Engineering, 2010, 1(104).
- [5] Dondee S, Meeso N, Soponronnarit S, etal. Reducing cracking and breakage of soybean grains under combined near-infrared radiation and fluidized-bed drying. Journal of Food Engineering, 2010, 1(104).
- [6] Nielsen D C. Forage soybean yield and quality response to water use. Field Crops Research, 2011, 3(124).

# Mechanism of Pier Damage under the Action of High Filling

Xue Rui<sup>1</sup> \*, Tao Ying<sup>2</sup>, Wu Yu<sup>1</sup>

<sup>1</sup>School of Civil Engineering and Architecture, Chongqing Jiaotong University, Chongqing, 400074

<sup>2</sup>CCTEG Chongqing Engineering Co., LTD., Chongqing, 400016

**Abstract:** High filling behind bridge abutment is very common. Because of higher filling, subsidence and deformation which occur over time lead to weakening of integral strength, consequently the stability and security of nearby bridge structure will be affected. Against the background of some continuous steel structure bridge, this thesis adopts ABAQUS finite element software to conduct contacting nonlinear analysis on No. 7 pier of this continuous steel structure bridge, research on causes of its cracks, analyze respective influence on this pier due to damage mechanism of pier, pile foundation and cushion cap, factors including volume-weight, elasticity modulus, Poisson's ratio, cohesive force and internal friction angle of soil mass, and original topographic conditions, and mainly focus on variation laws of horizontal displacement and stress calculation results of all points on the pier.

**Keywords:** High filling; pier, consolidation settlement, lateral displacement, status nonlinearity

## I. OVERVIEW

Spoil phenomenon is very common in practical engineering projects, and the spoil will generate unbalanced soil pressure on one side of the pier, thus the pier will bear vertical load, horizontal load, oblique load or moment of force, thus, there may be larger lateral deformation, which directly influences the stability of the pier [1]. Generally speaking, when soil is in an unstable status, lateral displacement of soil mass is more dangerous than vertical settlement, especially for concrete bridge piers. The bearing capacity for horizontal load hasn't been considered during design process of piers, so that researches on damage mechanism of piers under the action of filling and influences of filling on safety performance of the entire bridge are of great importance [2].

### *Action mechanism of high filling on piers*

Actions of high filling means that apply a load on original foundation soil, the load will increase vertical load and generate a horizontal thrust on a part of the pier above ground. Influence of ground filling on adjacent

pile(s) is a complex question, which is mainly manifested in two aspects: 1. Unstable status of filling leads to a tendency that soil mass will slide down along original ground to squeeze the pier, thus the pile will bring about additional displacement and bending moment of pile body, even shear failure. 2. Filling causes deformation of consolidation settlement of soil mass around the pier, soil mass will have downward displacement relative to the pile, thus downward force of negative friction appears in pier body, which increases axial load of the pier and produces additional settlement, and usually the settlement is nonuniform, which goes against superstructure [3].

## II. PROJECT PROFILE OF NO. 7 PIER OF SOME CONTINUOUS STEEL STRUCTURE BRIDGE

General information of this continuous steel structure bridge: Central elevation of bridge floor is 220m, overall width of bridge floor is 20m, net width of carriageway is 15m, and width of sidewalk is 2\*2.5m. This bridge is a continuous steel structure bridge of steel tube concrete composite truss with three 120m spans and two 75.4m side spans. General layout of this bridge is shown in figure 2-1.

No. 7 pier of this continuous steel structure bridge is located at K0+678 point of Tianxian Lake No.12 land block bank-protection engineering in comprehensive treatment engineering of Zhuxi River. No. 7 pier adopts H-type reinforced concrete structure, and uses the foundation type of socketed pile, while foundation bearing stratum is moderately weathered bed rock. There are 3-level bank-protection side slopes to south and west side of No.7 pier, which forms concave landform because of unloading. General site terrain is high in the north and east but low in the south and west, and it's mainly the stratum including artificial filling, broken and silty clay, alluvial-diluvial sand pebble soil and the Upper Shaximiao Formation of Middle Jurassic. Site soil layer has large thickness, loose structure, poor engineering geological conditions, abundant underground water and medium-complexity hydrogeological conditions.

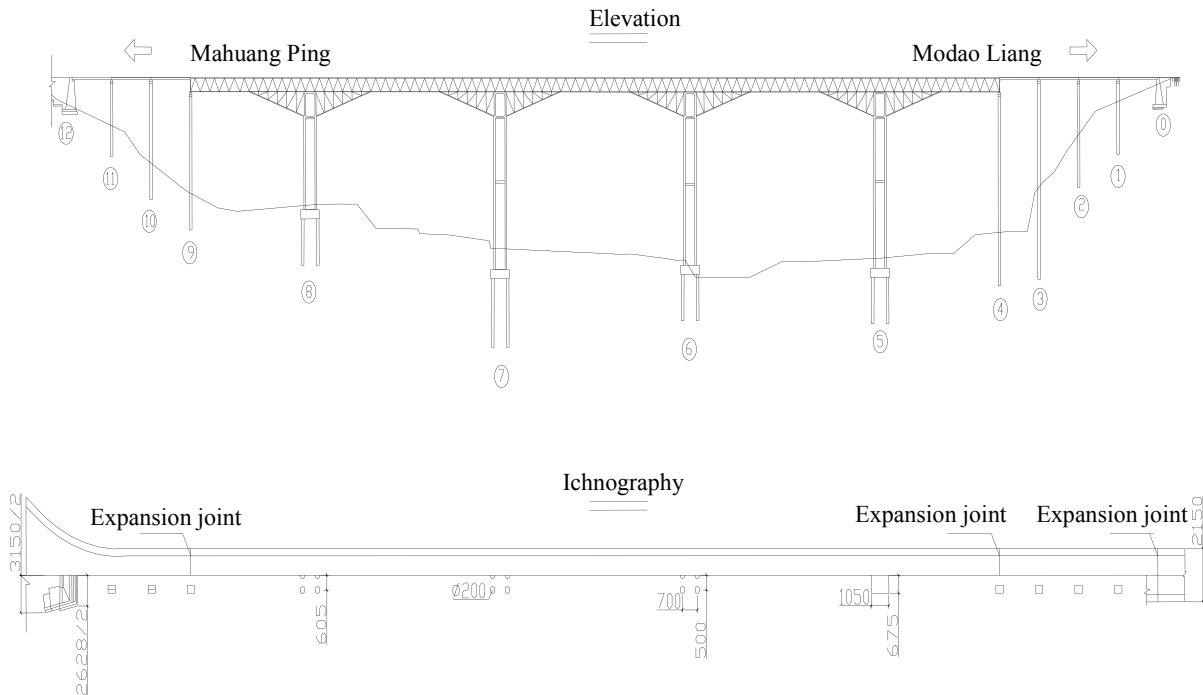


Figure 2-1 General layout of some continuous steel structure bridge

### III. MODEL CALCULATION AND ACTUAL DISEASE ANALYSIS

For No.7 pier of some continuous steel structure bridge, the height of central straining beam is 0.8m, pier height is 62.408m, cushion cap dimension is 13.5m\*10.5m\*3.5m, and underneath the cushion cap is pile foundation whose length is 24.5m, and diameter is 2m. 200m is adopted both in longitudinal and lateral direction to conduct model calculation for high filling.



Figure3-1 Spatial model for the pier

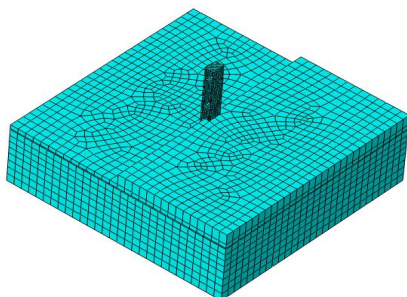


Figure3-2 Spatial model for pile soil of the pier

Only actions of high filling and gravity to the pier are considered in this model, and vertical load of

superstructure is out of question. Results of stress and horizontal displacement calculated in this model is shown in Figure 3-3~Figure 3-6.

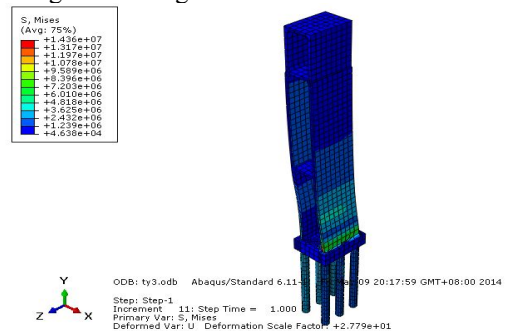


Figure 3-3 Mises stress diagram of pier pile

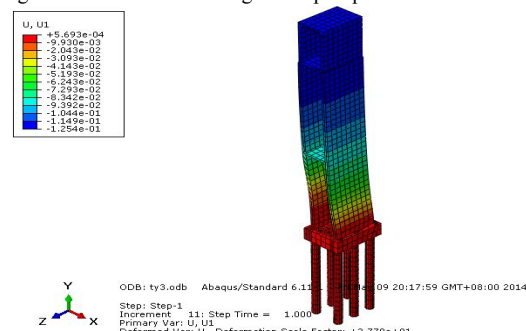


Figure 3-4 Horizontal displacement (U1) diagram of pier pile

From Figure 3-3 Mises stress diagram of pier pile, we can see that maximum stress is located at the position where right-side thin-wall pier of No. 7 pier is connected with the cushion cap, and the maximum value is 14.36MPa.

From Figure 3-4 Horizontal displacement (U1) diagram of pier pile and Figure 3-5 Mises stress diagram of cushion cap pile foundation, we can see that the displacement of cushion cap and pile foundation is very small, but the displacement of pier is bigger, and the

maximum value is 12.54cm, which coincides with cracks existing in No. 7 pier. Maximum actual observed displacement of No. 7 pier is 11.91cm, which is close to calculation results. Under the actions of high filling, displacement of the pier reaches up to 12.54cm, which shows that high filling has great influences on the displacement of the pier, and it's the main factor of pier displacement. At the lowest straining beam under the pier, horizontal displacements of vertical thin-wall piers both to the left and right side are inconsistent, thus incongruous deformations lead to phenomena of cracks in straining beam. Stress of cushion cap is shown in Figure 3-6, stress of cushion cap is distributed unevenly, maximum stress is concentrated in connection locations with upper bridge pier, and maximum stress value is 8.66Mpa. This phenomenon of stress concentration results in cracks of cushion cap, and the fact is also certified by damage observation results of No. 7 pier.

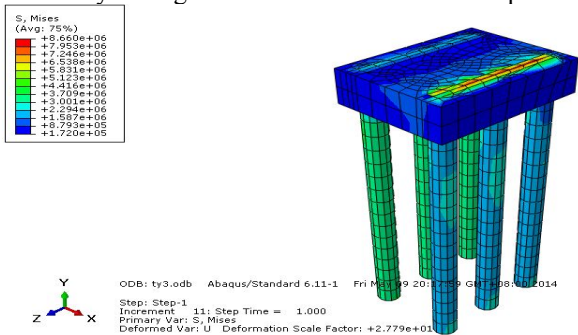


Figure 3-5 MISES stress diagram of cushion cap pile foundation

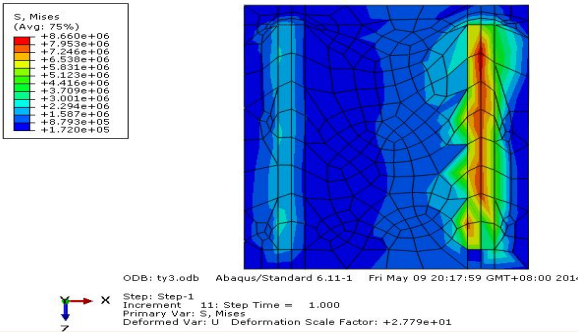


Figure 3-6 MISES stress diagram of cushion cap

IV. PARAMETER ANALYSIS OF SOIL MASS CALCULATIONS

Many factors have influences on pile-soil interactions, such as geometrical shape and height of soil mass, material parameter of the filling, shape of original landform, pile diameter of the pier, and all established finite element models. Influence analysis of these factors on pile soil is required to accurately analyze the damage mechanism of piles under the actions of high filling. Utilizing ABAQUS finite element software, this thesis conducts analysis on the influences of various soil mass models and original landform conditions on pile soil, and discusses influencing rules of horizontal displacement and stress of piers.

Constitutive model of soil mass material in this thesis adopts extended Mohr-coulomb model, and in this model there are 5 related parameters, which are volume-weight of soil mass  $\gamma$ , elasticity modulus E, Poisson's ratio  $\nu$ ,

internal friction angle  $\phi$  and cohesive force c respectively. Here analysis on various factors is conducted.

4.1. Influences of volume-weight of soil mass

Volume-weight values of soil mass are 10kN/m<sup>3</sup>, 20kN/m<sup>3</sup>, 30kN/m<sup>3</sup>, which are adopted to analyze influences of different volume-weight of soil mass on the pier.

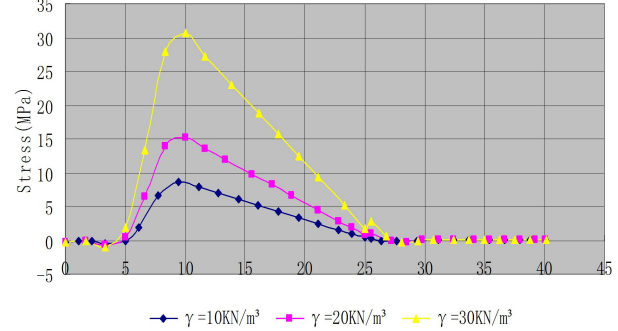


Figure 4-1 Influences of soil mass volume-weight on maximum primary stress of the pier

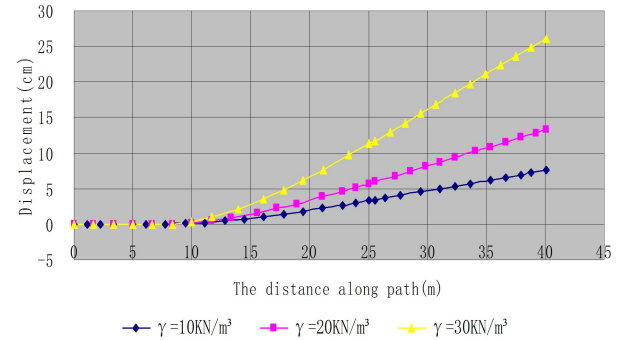


Figure 4-2 Influences of soil mass volume-weight on horizontal displacement (U1) of the pier

From Figure4-1~Figure 4-2, we can see that horizontal displacement increases along with the increase of soil mass volume-weight. This is because when soil mass volume-weight increases, vertical load of subsoil mass will increase, lateral deformation of soil mass will enlarge, downward tendency of soil mass will be bigger, thus anti-skid force of the pier will also increase accordingly. When soil mass volume-weight increases, soil pressure suffered by the pier will also increase [4].

4.2. Influences of elasticity modulus of soil mass

Elasticity modulus values of soil mass are 10MPa, 20MPa, and 30MPa, which are adopted to analyze influences of different elasticity modulus of soil mass on the pier.

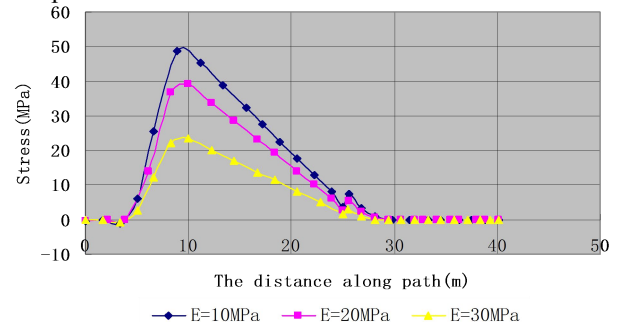


Figure 4-3 Influences of soil mass elasticity modulus on primary stress of the pier

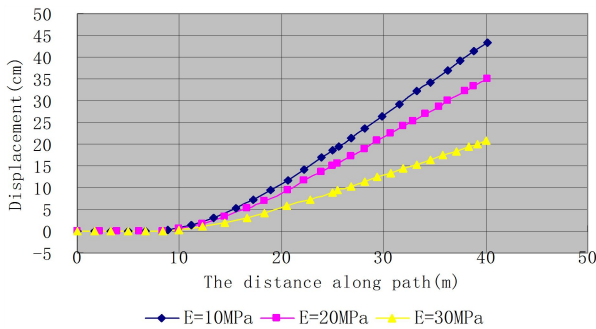


Figure 4-4 Influences of soil mass elasticity modulus on horizontal displacement (U1) of the pier

Theoretically, if the elasticity modulus is bigger, lateral deformation of soil mass, soil pressure suffered by the pier and horizontal displacement will be smaller; On the contrary, if the elasticity modulus is smaller, lateral deformation of soil mass, soil pressure suffered by the pier and horizontal displacement will be bigger. Results simulated by finite element software is shown in Figure 4-3 and Figure 4-4, and we can see that along with the increase of elasticity modulus, maximum primary stress and horizontal displacement of the pier will be smaller. This also shows that simulated results are consistent with the theory [5].

4.3. Influences of Poisson's ratio of soil mass

Poisson's ratio values of soil mass are 0.2, 0.3 and 0.4, which are adopted to analyze influences of different elasticity modulus of soil mass on primary stress and horizontal displacement of the pier.

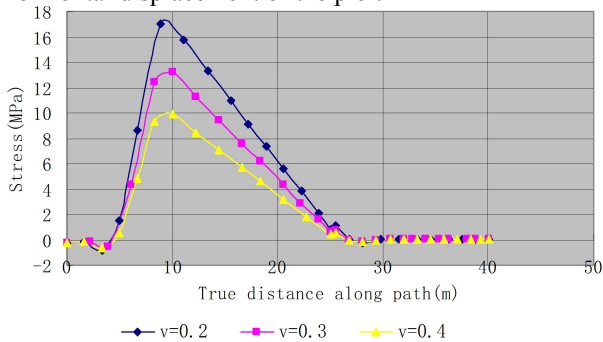


Figure 4-5 Influences of soil mass Poisson's ratio on primary stress of the pier

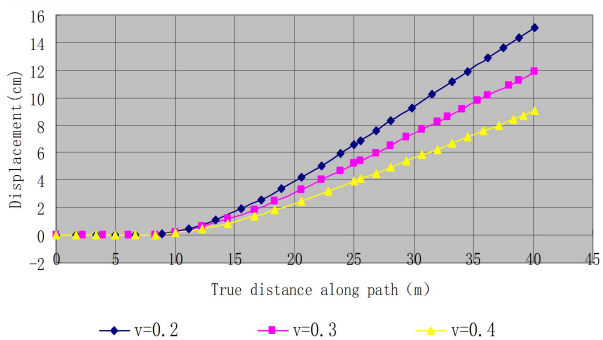


Figure 4-6 Influences of soil mass Poisson's ratio on horizontal displacement (U1) of the pier

displacement (U1) of the pier

From Figure 4-5, we can see that when the value of Poisson's ratio is 0.2, 0.3 or 0.4, distribution rules tend to consistency: Along with the increase of Poisson's ratio, primary stress of the pier becomes smaller. From Figure 4-6, we can see that horizontal displacement (U1) of the pier becomes smaller with the increase of Poisson's ratio.

4.4. Influences of cohesive force of soil mass

Cohesive force values of soil mass are 32kPa, 42kPa and 52kPa, which are adopted to analyze influences of different cohesive force of soil mass on primary stress and horizontal displacement of the pier. Theoretically, influences of cohesive force on plastic deformation of soil mass is very big, if the cohesive force is bigger, the plastic deformation will be smaller, and stability of soil mass increases along with the increase of cohesive force. This shows that influences of cohesive force on the stability of soil mass are very big.

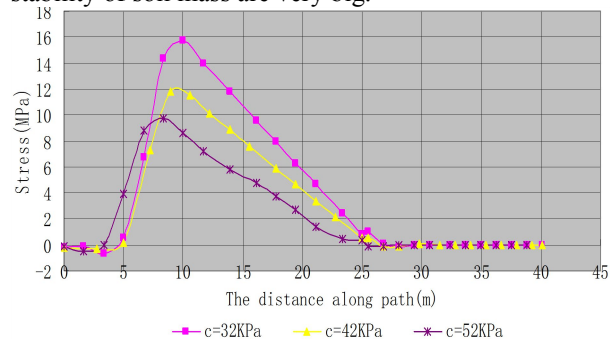


Figure 4-7 Influences of soil mass cohesive force on maximum primary stress of the pier

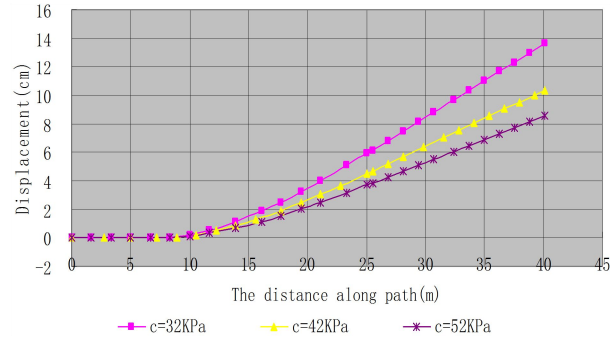


Figure 4-8 Influences of soil mass cohesive force on horizontal displacement (U1) of the pier

From Figure 4-7, we can see that the pier has similar deformation shapes under different cohesive forces, and horizontal displacement (U1) of the pier decreases with the increase of cohesive force. From Figure 4-8, we can see that for variational cohesive forces, soil pressure of the pier has similar distribution patterns, which are all similar to parabola. Soil pressure has different action ranges on the pier, if the cohesive force is bigger, the soil pressure becomes closer to the end of pier; when cohesive force of soil mass materials increases, maximum soil pressure acted on the pier gradually turns towards to the end of pier. Meanwhile, we can see that with the increase of cohesive force, maximum soil pressure acted on the pier decreases, and relative

horizontal displacement of the pier also decreases. Results of numerical simulation totally coincide with the theory, which verifies that if the cohesive force of soil mass is bigger, the status of soil mass will be more stable, soil pressure acted on the pier will become smaller and displacement of the pier will also be smaller [6].

#### 4.5. Influences of internal friction angle of soil mass

With other conditions unchanged, internal friction angle values of soil mass are  $15^\circ$ ,  $17.5^\circ$ , and  $20^\circ$ , which are adopted to analyze influences of different internal friction angle of soil mass on primary stress and horizontal displacement of the pier.

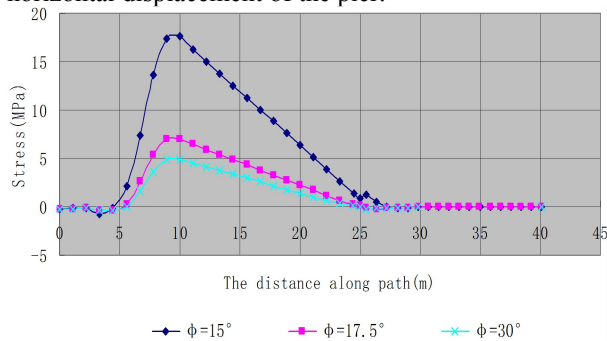


Figure 4-9 Influences of soil mass internal friction angle on maximum primary stress of the pier

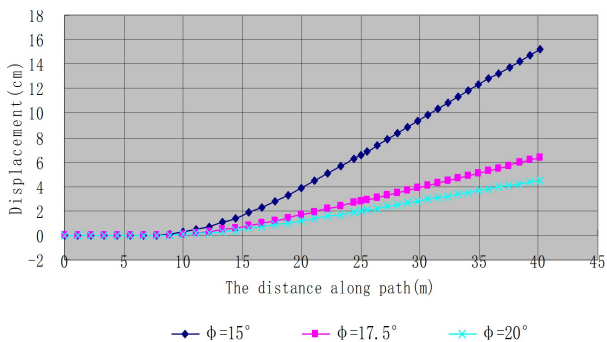


Figure 4-10 Influences of soil mass internal friction angle on horizontal displacement (U1) of the pier

Obviously, the stability of soil mass have been greatly influenced by the friction angle, the bigger the friction angle is, the more stable the soil mass will be. Figure 4-9~Figure 4-10 give out different friction angle, maximum primary press suffered by the pier, and the situation of horizontal displacement. It's shown that influences of friction angle and cohesive force on the stress and displacement characteristics of the pier are also obvious; but what's different is that the bigger the friction angle is, the smaller the soil pressure suffered by the pier will be. Besides, the location where there is the maximum primary stress is also greatly influenced by the friction angle; If the friction angle is smaller, the distribution scope of soil pressure suffered by the pier will be bigger; When the friction angle is very big, the soil mass will be in a stable status under the action of friction force, and the stress suffered by the pier will be smaller, which is just the reverse of influences of cohesive force.

## V. CONCLUSION

This thesis introduces action mechanism of high filling on the pier, utilizes ABAQUS finite element software to conduct status nonlinear analysis to No. 7 pier of some bridge from a project case, and compares analysis results with actual damages of No. 7 pier. And then it finds the influence rules on primary stress and horizontal displacement of the pier from many aspects, including soil mass  $\gamma$ , elasticity modulus  $E$ , Poisson's ratio  $\nu$ , internal friction angle  $\phi$  and cohesive force  $c$ .

## References

- [1] Liu Jianwu, Han Dunzan, Li Fei, Jiao Chen. Force analysis and solutions of piles of bridges under the actions of soil pressure [J]. *Journal of highway and transportation research and development (Application version)*, 2011, 75(3): 60-63.
- [2] Liang Fayun, Yu Feng, Li Jingpei, Yao Guosheng. Influence analysis of horizontal displacements on load bearing behavior of nearby existing pile foundation [J]. *Rock and Soil Mechanics*, 2010, 31(2):449-454.
- [3] Yao Guosheng. *Pile model tests and numerical analysis of existing axial load under the lateral displacement of soil mass* [D]. Shanghai, Tongji University, 2009.
- [4] Huang Longxian, Yang Hugen. Force analysis of pier with variable box-type cross-section of reinforced concrete in filling. [J] *Journal of Chongqing Jiaotong University*. 2006, 8: 44-48.
- [5] Liu Chengyu. *Soil mechanics (Second edition)* [M]. China Railway Publishing House.1990.
- [6] Chen Xizhe, Ye Jing. *Foundation of soil mechanics (Fifth edition)* [M]. Tsinghua University Press, 2013.

# Computing the Least Quantile of Squares Estimation with Aggregate Homotopy Method

Z. G. Yan

Accounting School, Jiangxi University of Finance and Economics, Nanchang, Jiangxi, PR China

**Abstract**—The difficulty in computing the least quantile of squares (LQS) estimate, which minimizes the  $\tilde{m}$  smallest squared residual for a given data set, is due to the nondifferentiation and many local minima of the objective function. In this paper, based on aggregate homotopy method, we present an algorithm to compute LQS estimate not only valuable for linear model, but also for nonlinear regression. Numerical experiments illustrate the efficiency of our algorithm.

**Index Terms**—least quantile squares, multiple linear regression, nonlinear regression, min-max-min problem, aggregate homotopy.

## I. INTRODUCTION

Rousseeuw(1984, [1]) defined the LQS estimator. For observed data points  $(u_i, v_i) \in R^p \times R, i = 1, 2, \dots, m$ , the regression model is given by:

$$u_i = f(v_i, x) + r_i, \quad i = 1, 2, \dots, m, \quad (1)$$

where  $x$  is an unknow parameter vector and  $r_i$  are unknow errors. For a given estimate  $x$ , we denote the residuals as  $r_i(x) = u_i - f(v_i, x)$ . The LTS estimator is defined as

$$x^* = \arg \min_{x \in R^p} r_{(\tilde{m})}^2(x), \quad (2)$$

where  $r_{(1)}^2(x) \leq \dots \leq r_{(m)}^2(x)$  is the rearrangement of all the square residuals.

Several algorithms have been proposed to LQS estimate. For the linear model, the typical exact algorithm is proposed by Stromberg in [2]. Under the Haar condition assumption, computes the Chebyshev fit to each  $p+1$  element subset. The fit with the least  $\tilde{m}$ th smallest squared residual is the exact value. Because of the complexity of computing Chebyshev fit to all  $(p+1)$ -element subsets, this algorithm is feasible only for  $m \leq 50$  and  $p \leq 5$  ([2]). Since for slightly big data set the exact algorithm is infeasible or takes too long time, LQS regression is mostly computed by an approximate algorithm, called PROGRESS, proposed by Rousseeuw and Leroy in [1]. This algorithm calculates the exact fit to  $p$ -element subset chosen randomly. This procedure is repeated many times, and the fit with the least  $\tilde{m}$ th smallest squared residual is retained. This algorithm can also be used for nonlinear model by computing the Chebyshev fit to many  $\tilde{m}$ -subsets. Although with satisfying speed, the convergence of PROGRESS is not

guaranteed and the result is even not a stationary point usually (see [3]).

In this paper, we don't decompose the problem but transform it to a min-max-min problem, then solve it by aggregate homotopy method ([4]). The structure of the paper is as follows. We first establish min-max-min problem for LQS estimate, and analyse its properties. Next, we adopt aggregate homotopy method to solve it. At last, we show the performance of our algorithm by several examples.

## II. MIN-MAX-MIN PROBLEM FOR LQS ESTIMATE

In this section, we offer a min-max-min representation for LQS estimate. Let  $a = \{a_1, \dots, a_m\}$  be a finite set of real numbers and  $a_{(\tilde{m})}$  be the  $\tilde{m}$ th smallest element among them. Because  $a_{(\tilde{m})}$  can be represented as

$$a_{(\tilde{m})} = \max_{I \in \mathfrak{S}_{m-\tilde{m}+1}} \min_{i \in I} a_i, \quad (3)$$

where  $\mathfrak{S}_{m-\tilde{m}+1}$  is the set of all  $(m-\tilde{m}+1)$ -subsets of the index set  $N = \{1, \dots, m\}$ . Denote  $k = m - \tilde{m} + 1$ , LQS estimate may be rewritten as such min-max-min problem

$$\min_{x \in R^n} \{F(x) = \max_{I \in \mathfrak{S}_k} \min_{i \in I} r_i^2(x)\}. \quad (4)$$

According to [4], suppose  $r_i \in C^h (h \geq 1)$ , if  $F(x)$  is locally lipschitz at  $x^*$  and  $F(x)$  attains its local minimum at  $x^*$ , then there exist  $\alpha_i \geq 0, i \in \mathfrak{S}_k$  and  $\beta_i \geq 0, i \in I$ , such that

$$\begin{cases} \sum_{I \in \mathfrak{S}_k(x^*)} \alpha_I \sum_{i \in I(x^*)} \beta_i \nabla r_i^2(x^*) = 0, \\ \sum_{I \in \mathfrak{S}_k(x^*)} \alpha_I = 1, \sum_{i \in I(x^*)} \beta_i = 1, \alpha_I \geq 0, \beta_i \geq 0, \end{cases} \quad (5)$$

where

$$\begin{aligned} \mathfrak{S}_k(x^*) &= \{I \in \mathfrak{S}_k : F(x^*) = \min_{i \in I} r_i^2(x^*)\}, \\ I(x^*) &= \{i \in I : \min_{i \in I} r_i^2(x^*) = r_i^2(x^*)\}. \end{aligned} \quad (6)$$

(5) is the generalized KKT system of (4) and the point satisfying (5) is called the generalized KKT point of (4).

## III. ALGORITHM AND ITS CONVERGENCE

In this section, we introduce aggregate homotopy method to solve (4).

As to the nonsmooth function  $g(x) = \max_{1 \leq i \leq m} g_i(x)$ , based on maximum entropy principle, X. S. Li deduced a smooth function in [5], called aggregate function, to approximate  $g(x)$ . Let  $t > 0$ , the mostly used aggregate function is defined as

$$g(x,t) = t \ln \left[ \sum_{i=1}^m \exp \left( -\frac{g_i(x)}{t} \right) \right], \quad (7)$$

and  $g(x,t) \rightarrow g(x)$  a.s.  $t \rightarrow 0^+$  :

$$g(x) \leq g(x,t) \leq g(x) + t \ln m.$$

Later in [4], to smooth  $g(x) = \max_{1 \leq i \leq m} \min_{1 \leq j \leq l_i} g_{ij}(x)$ , B. Yu

proposed a hierarchical aggregate function

$$g(x,t) = t \ln \left[ \sum_{1 \leq i \leq m} \exp \left( -\frac{\phi_i(x,t)}{t} \right) \right],$$

where

$$\phi_i(x,t) = t \ln \left[ \sum_{1 \leq j \in l_i} \exp \left( -\frac{g_{ij}(x)}{t} \right) \right],$$

and  $g(x,t) \rightarrow g(x)$  a.s.  $t \rightarrow 0^+$ . Hence, we can define

$$F(x,t) = t \ln \left[ \sum_{i \in \mathfrak{S}_k} \exp \left( -\frac{\phi_i(x,t)}{t} \right) \right], \quad (8)$$

where

$$\phi_i(x,t) = t \ln \left[ \sum_{i \in I} \exp \left( -\frac{r_i^2(x)}{t} \right) \right], \quad (9)$$

to smooth  $F(x)$  defined in (4). Then, aggregate homotopy method can be adopted to solve this problem.

**Theorem 1 ([4], Theorem 3)** *If  $r_i^2(x) \in C^h (h > 2)$  satisfying the following assumption 1: There exist  $M > 0, \bar{x} \in R^n$ , such that for all  $\|x - \bar{x}\| \geq M$ , it has*

$$\nabla r_i^2(x)^T (x - \bar{x}) > 0, i = 1, 2, \dots, m.$$

Choose a small constant  $\theta \in (0, 1]$ , then for almost all  $x^0 \in R^n$ , aggregate equation

$$H(x,t) \equiv (1-t) \nabla_x F(x, \theta t) + t(x - x^0) = 0, \quad (10)$$

determines a smooth curve  $\Gamma$ , which starts from  $(x^0, 1)$  and approaches to the plane  $t = 0$ . Moreover, if  $(x^*, 0)$  is a limit point of  $\Gamma$  on the hyperplane  $t = 0$ , then  $x^*$  is a generalized KKT point of (4).

The Predictor-Corrector method (see [6] for details) is usually adopted to numerically trace the homotopy path  $\Gamma$ . Moreover, to reduce the computation cost, truncated aggregate homotopy method has been proposed in [7] to trace the homotopy path efficiently for nonlinear programming. Here, we can also use the truncated aggregate technique. For each iteration point  $(x,t) \in R^n \times R$ , choose a parameter  $\varepsilon > 0$ , denote

$$\begin{aligned} N(x, \varepsilon) &= \{i \mid |r_i^2(x) - r_{(\tilde{m})}^2(x)| \leq \varepsilon, 1 \leq i \leq m\}, \\ N^-(x, \varepsilon) &= \{i \mid r_i^2(x) - r_{(\tilde{m})}^2(x) \leq -\varepsilon, 1 \leq i \leq m\}, \\ \mathfrak{S}_k &= \{I \subset N(x, \varepsilon) \mid \#(I) = k'\}, \end{aligned} \quad (11)$$

where  $k' = \#(N(x, \varepsilon)) - (\tilde{m} - \#(N^-(x, \varepsilon))) + 1$ , and the symbol  $\#(I)$  denotes the capacity of set  $I$ . Then aggregate function value  $F(x,t)$  is approximately equal to

$$F^{\mathfrak{S}_k}(x,t) = t \ln \left[ \sum_{i \in \mathfrak{S}_k} \exp \left( -\frac{\phi_i(x,t)}{t} \right) \right], \quad (12)$$

where

$$\phi_i(x,t) = t \ln \left[ \sum_{i \in I} \exp \left( -\frac{r_i^2(x)}{t} \right) \right], \quad (13)$$

Moreover, since computing the Jacobi and Hessian of  $F(x,t)$  is very expensive, we can use the Jacobi and Hessian of  $F^{\mathfrak{S}_k}(x,t)$  to reduce the computation cost greatly.

Now, we consider adopting the truncated aggregate technique to trace the homotopy path  $\Gamma$  efficiently. For conciseness, we write  $v = v(x,t)$ .

**Algorithm 1** (Truncated aggregate homotopy algorithm for LQS)

*Data.*  $\theta > 0, x^0 \in R^n, t_0 = 1$ .

*Parameters.* Initial steplength  $h_0 > 0$ ; tolerance  $t_{tol} = 10^{-7}$ ,  $t_c = 10^{-6}$ ,  $H_{tol} = \min\{10^{-3}, 1/t\}$ ; maximum steplength  $h_{max}$ ; maximum inner iteration number  $N_{in}$ ; truncated parameter  $\varepsilon > 0$ .

*Step 0.* Unit tangent vector  $d^0, k = 0, i = 0$ .

(Predictor step)

*Step 1.* If  $0 \leq t_k \leq t_{tol}$ , end the procedure; else go to Step 2.

*Step 2.* If  $k > 0$ , compute  $d_k = \frac{v^k - v^{k-1}}{\|v^k - v^{k-1}\|}$ . If  $t_k > t_c$ , go

to Step 3, else go to Step 4.

*Step 3.* Set  $v^{k,0} = v^k + h_k d^k, i = 0$ , go to Step 5.

*Step 4.* Let  $h_k = \frac{t_{tol} - t_k}{d_{n+1}^k}$ , and  $v^{k,0} = v^k + h_k d^k$ , then correct

$v^{k,0}$  on the hyperplane  $t = t_{tol}$ .

(Corrector step)

*Step 5.* If  $t_{k,i} \notin [0, 1]$ ,  $h_k = 0.5h_k$ , set, go to Step 2; else, let  $v = (x,t) = (x^{k,i}, t_{k,i})$ , go to Step 6.

*Step 6.* Compute  $F^{\mathfrak{S}_k}(x, \theta t)$  according to (11)-(13). If  $\|R_{k,\varepsilon}(v)\| \leq H_{tol}$ , where

$$R_{k,\varepsilon}(v) = \begin{bmatrix} H_\varepsilon(v) \\ d^{k^T} (v - v^{k,0}) \end{bmatrix},$$

with  $H_\varepsilon(v) = (1-t) \nabla_x F^{\mathfrak{S}_k}(x, \theta t) + t(x - x^0)$ , go to Step 7; else go to Step 8.

*Step 7.* Set  $v^{k+1} = v^{k,i}, h_{k+1} = \begin{cases} \min\{1.5h_k, h_{max}\}, & i < 3, \\ h_k, & \text{else,} \end{cases}$

$k = k + 1$ , go to Step 1.

*Step 8.* If  $i \geq N_{in}$ , set  $h_k = 0.5h_k$ , go to Step 3; else, obtain  $v^{k,i+1}$  using truncated aggregate iteration,

$$v^{k,i+1} = v^{k,i} - DR_{k,\varepsilon}(v^{k,i})^{-1} R_{k,\varepsilon}(v^{k,i}),$$

set  $i = i + 1$ , and go to Step 5.

In theory, the global convergence of above truncated aggregate homotopy algorithm is guaranteed if  $\varepsilon$  is sufficiently small. The relative proofs for truncated aggregate algorithms have been given in [7] and some other papers. Here, we will not discuss it but aim to introduce the good application effect of our algorithm.

#### IV. NUMERICAL EXPERIMENT

In this section, we give some numerical results, comparing Algorithm 1 (TAH) with some other algorithms, such as the PROGRESS algorithm and exact algorithm proposed by Stromberg in [2] to show the efficiency of our algorithm.

In example 1, 2 and 4,  $\bar{m}$  is set as the integer proximal to  $(m + p + 1) / 2$  ([2]). In example 3, it is set as the number of non-outliers. During the computation in Algorithm 1, we set parameters  $h_0 = 0.1$ ,  $h_{max} = 0.3$ ,  $\theta = 0.1$ . The parameter  $Num$  denoting the running numbers of Chebyshev fitting procedure for randomly subsets in PROGRESS algorithm is set as 10000. All the computations are done by running MATLAB 7.6.0 on a laptop with AMD Turion (tm) 64 × 2 Mobile Technology TL-58 CPU 1.9 GHz and 896M memory.

**Example 1.**[Regression through the origin, [2]] Fit the data in Table 1 by a simple linear regression through the origin. Here  $n = 1, p = 1, m = 10, \bar{m} = 5$ . Because it is a small problem with  $C_m^p = 10$ , each line passing through the origin and one point of the set is calculated in PROGRESS. However, it still can't obtain the global solution to LQS estimate. In this experiment, our algorithm is executed five times for different initial points  $x^0$  randomly generated from  $[0, 1]$ , and while  $x^0 = 0.6672$ , it obtains the global solution  $x^* = 0.3848$ .

**Example 2.**[Cloud seeding data, [8]] This data summarizes the results of a cloud seeding experiment done in Florida in 1975. The data is fit using a multiple linear regression model with six explanatory variables and an intercept. For this example and the followings, our algorithm is performed ten times with different initial points roughly produced by proximate algorithm in low computation cost. PROGRESS is also repeated ten times, and in each time, the number of  $p$ -subset chosen randomly for exact fit is 3000.

**Example 3.** Initial data set is generated firstly according to  $y = -2.1323x_1 + 1.4356x_2 + 0.7854x_3 - 5.2496x_4 + 7.2158x_5 - 4.5424x_6 - 6.0012x_7 + \delta$ , where  $\delta \sim N(0, 0.1^2)$ . Then data set is obtained by increasing the absolute error of 20% points. Because exact algorithm can't deal with so large problem, we only compare our algorithm with PROGRESS.

**Example 4.** Consider rotated paraboloid data in [9]. Data points are generated similarly to the prescription used in [9]: produce point  $(v_i^1, v_i^2, u_i) \in R^3$  on an unrotated paraboloid, add error item to  $u_i$ , and make rotations and translation. So, for a given data  $(v_i^1, v_i^2, u_i)$ , we should consider transformation

$$(\bar{v}_i^1, \bar{v}_i^2, \bar{u}_i, 1) = (v_i^1, v_i^2, u_i, 1)T(x_1, x_2, x_3, x_4, x_5),$$

where  $T(x_1, x_2, x_3, x_4, x_5) = A(x_3, x_4, x_5)B(x_1)C(x_2)$ , and  $A, B, C$  are defined as follows:

$$A = \begin{pmatrix} 1 & 0 & 0 & 0 \\ 0 & 1 & 0 & 0 \\ 0 & 0 & 1 & 0 \\ x_3 & x_4 & x_5 & 1 \end{pmatrix}, \quad B = \begin{pmatrix} 1 & 0 & 0 & 0 \\ 0 & \cos(x_1) & \sin(x_1) & 0 \\ 0 & -\sin(x_1) & \cos(x_1) & 0 \\ 0 & 0 & 0 & 1 \end{pmatrix},$$

$$C = \begin{pmatrix} \cos(x_2) & 0 & -\sin(x_2) & 0 \\ 0 & 1 & 0 & 0 \\ \sin(x_2) & 0 & \cos(x_2) & 0 \\ 0 & 0 & 0 & 1 \end{pmatrix}.$$

Then residual  $r_i(x) = \bar{u}_i - x_6((\bar{v}_i^1)^2 + \bar{v}_i^2)$ . Because exact algorithm in [2] can't deal with nonlinear model, we only compare our algorithm with PROGRESS. Especially, for this nonlinear model, initial  $x^0$  in PROGRESS is set as the least squares estimate for the entire data set.

From above numerical results, it can be seen that for small linear model, such as example 1, our algorithm is comparable to exact algorithm in fitting result and the runtime is acceptable. When  $n, \bar{m}$  are enlarged a few, such as example 2, compared with exact algorithm taking more than one hour to get global solution, the advantage of our algorithm is embodied fully that it is able to attain the same estimate within only a few seconds. Moreover, for large linear problem and nonlinear model, our algorithm can obtain good solution within acceptable time while exact algorithm is infeasible. Compared with PROGRESS, the solution obtained by our algorithm is always better. In addition, for some complex nonlinear model, such as example 4, our algorithm is superior to PROGRESS not only in fitting result but also in runtime because the later also need Newton iteration in the exact fit to  $p$ -subsets.

TABLE I.  
DATA FOR EXAMPLE 1

$v$	1	2	3	4	5	1	2	3	4	5
$u$	0.3320	0.6590	0.9888	1.3194	1.6495	0.6596	1.3192	1.9815	2.6289	3.3011

TABLE II.  
PERFORMANCE OF THREE ALGORITHMS

Example	$m$	$n$	$\bar{m}$	$r_{(\bar{m})}^2(x^*)$			CPU Time		
				TAH	Exact algorithm	PROGRESS	TAH	Exact algorithm	PROGRESS

1	10	1	5	<b>0.0755</b>	<b>0.0755</b>	0.1070	0.0940	<b>0.0160</b>	<b>0.0150</b>
2	24	7	15	<b>0.1375</b>	<b>0.1375</b>	0.2452	<b>1.7820</b>	>3600	<b>1.3600</b>
3	200	7	167	<b>0.3463</b>	–	0.4282	<b>0.9530</b>	–	1.3289
4	40	6	21	<b>0.0191</b>	–	0.0323	<b>3.0470</b>	–	6.4840

## ACKNOWLEDGMENT

I thank Y. Xiao for valuable discussion. This work was supported by the National Natural Science Foundation of China (11126172).

## REFERENCES

- [1] P. J. Rousseeuw and A. M. Leroy, *Robust Regression and Outlier Detection*. John Wiley: New York, 1987.
- [2] A. J. Stromberg, "Computing the exact least median of squares estimate and stability diagnostics in multiple linear regression," *SIAM J. Sci. Comput.*, 14(6), pp. 1289-1299, 1993.
- [3] H. Barreto and D. Maharry, "Least median of squares and regression through the origin," *Computational Statistics & Data Analysis*, vol. 50, pp. 1391-1397, 2006.
- [4] G. X. Liu, *Aggregate homotopy methods for solving sequential max-min problems, complementarity problems and variational inequalities*. PhD thesis, Jilin university: China (in Chinese), 2003.
- [5] X. S. Li, "An aggregate function method for nonlinear programming," *Science in China (A)*, 34(2), pp. 1467-1473.
- [6] E. L. Allgower and K. Georg, *Numerical Path Following*, in: Handbook of Numerical Analysis, Vol. 5, ed P. G. Ciarlet and J. L. Lions: North-Holland, pp 3-207, 1997.
- [7] Y. Xiao, H. J. Xiong, B. Yu, "Truncated aggregate homotopy method for nonconvex nonlinear programming," *Mathematics Methods and Software*, 29(1) pp 160-176, 2014.
- [8] R. D. Cook and S. Weisberg, *Residuals and Influence in Regression*. Chapman-Hall, London, 1982.
- [9] Y. Xiao, B. Yu, D. L. Wang, "Truncated smoothing Newton method for  $L_\infty$  fitting rotated cones," *Journal of Mathematical Research & Exposition*, 30(1) pp 159-166, 2010.

# Time Sensitive Social-based prediction routing protocol in Socially-aware Opportunistic Networks

Li Liu

Shandong Jiaotong University, Jinan 250023, China.

**Abstract**—Mobile devices are popular used in people's life. Generally, most of portable mobile devices are carried by people. Thus, the mobility of mobile devices is influenced heavily by people's social relationship. Socially-aware Opportunistic Networks are used in intermittently connected networks by use of store-carry-and-forward fashion. It is mainly based on social relationship to design solutions for problem such as routing protocol or data dissemination. In this paper, we exploit social relationship about friendships information among people and use them to predict the contact opportunities. We present Friend-based Prediction routing protocol (FBP) and establish experiment based on ONE. The simulation results show that the efficiency of FBP outperforms Epidemic and PROPHET in higher delivery ratio, lower overhead and shorter average latency.

**Index Terms**—Opportunistic Networks; Friendship; Routing Protocol.

## I. INTRODUCTION

Thanks to the proliferation of portable devices and mobile transmission technologies, several ubiquitous applications and services have been developed recently. Recently, short transmission wireless technologies such as Bluetooth and WiFi have been exploited as a promising solution to lighten the overload. Mobile nodes can form Opportunistic Networks [1] or DTNs [2] which are characterized with intermittent connection due to nodes' mobility. It is the key problem in routing field to predict future contact probability through studying nodes' mobility property.

As the main carriers of mobile devices, humans are usually regarded as mobile nodes in networks which their social properties have big influence to their mobility. Socially-aware Opportunistic Networks are mainly based on social relationship to design solutions for problem such as routing protocol or data dissemination.

In socially-aware Opportunistic Networks, mobile nodes utilize opportunistic contact opportunity to deliver messages using store-carry-and-forward fashion. When a source node wants to deliver a message to a destination node, several intermediate nodes may be selected to help the forwarding process hop by hop. Usually, the node which has more probability to meet the destination node is prior selected.

Many social properties are exploited to found the regularity of people's mobility and predict the appropriate intermediate nodes as forwarders. The community is

popular used in these works. People with some social relationships (such as family member, friendships, colleagues or same interests etc.) are formed community. Members in same community have more opportunities to meet than in different communities. However, it is difficult to detect and maintain community structure. Sometimes, mobile nodes only record parts of community information related with themselves.

In this paper, we utilize friendship among mobile nodes and their contact records to predict the future meet probability. Friendship is one of the social relationships which are easy to obtain and maintain. Generally, we record our friend information in mobile devices. And friends can meet more frequently. These friends are direct-friends. Additionally, we take contact history into consideration. When a mobile node NA deliver a message successfully to another node NB, NB is recorded as second-friend of NA.

## II. RELATED WORK

Routing in Opportunistic Networks is challenging due to lacking of end-to-end connection between source node and destination node. In recent few years, lots of researches about social related strategies have been proposed to solve the routing problem.

Bubble Rap [5] defines k-clique community from contact graph and hierarchical ranking tree to guide routing. Nodes which can reach each other through a series of adjacent k-cliques form a community. In addition, MOPS [6] and LocalCom [7] construct communities based on neighboring relationship from nodes' encounter histories. MOPS considers not only the direct but also the indirect neighboring relationship. LocalCom presents a metric named similarity to construct the neighboring graph which considers the encounter frequency, encounter length, separation period in the encounter history.

Our work in this paper aims to find a more easily maintain standard to predict the future contact opportunities. FBP utilizes direct-friend information and second-friend information stored in mobile nodes to predict the meet probability to destination node in order to improve the delivery efficiency.

## III. SYSTEM MODEL AND IMPLEMENT

### A. System Model

Friend information is common used in reality. So our routing protocol FBP is fit to the people’s reality life such as students in school, colleagues in company. In this section, we give the system model. We assume there are N mobile nodes with short transmission wireless technologies such as Bluetooth or WiFi. Each node need to maintain their direct-friend information and second-friend information. For the direct-friend information, people can input them into the mobile device and maintain manually. For the second-friend information, the FBP routing protocol is responsible to store and maintain. And the mobility of mobile devices is regular through time. In one word, the structure of mobile node is consisted of two parts, as shown in Fig 1.

Structure of Mobile Node			
direct-friend		second-friend	
ID	degree	ID	degree
1	18	6	12
4	3	9	5
.....		.....	

Fig.1 The Structure of Mobile Node

Direct-friend and second-friend shares same structure which is constructed of value-pair (ID, degree). Where ID represent the friend node and the degree indicate the contact strength of the friendship between two nodes. The difference between them is that the degree of direct-friend is based on contact times. The more contact times in a time window, the higher the degree is. So the degree of direct-friend is computed by using Eq. (1) as follows. Where T is a time window, n is the meet times between two nodes in T.

$$deg = \sum_{t=0}^T n \tag{1}$$

On the contrary, the degree of second-friend is based on the successful delivery times. Considering the fewer successful delivery times, we do not limit the time window for degree of second-friend. Thus, the degree of second-friend is based on Eq. (2) as follows.

$$deg = \sum n \tag{2}$$

Finally, an evaporation process is necessary for the degree by (3).  $\gamma$  and k is evaporation factor.

$$deg\_new = deg\_old * \gamma^k \tag{3}$$

**B. System Implement.**

In FBP, mobile nodes record and maintain not only direct-friend information but also second friend information according to contact times in a time window and successful delivery respectively. When two nodes are in transmission range, they exchange message according to FBP, which consists of 4 steps. For implicitly

description, we assume the transmission is happened between node NA and NB. And we give the detailed introduction from NA’s aspect. NB does the same process as NA.

1) NA firstly checks whether the NB is his friend. If NB is one of friends, NA maintains the degree for NB in direct-friend. Otherwise, go to 2).

2) For each message in NA, NA checks whether NB is the destination. If NB is the destination, the message is delivered to NB. On the same time, NA maintain the second-friend information. Otherwise, go to 3).

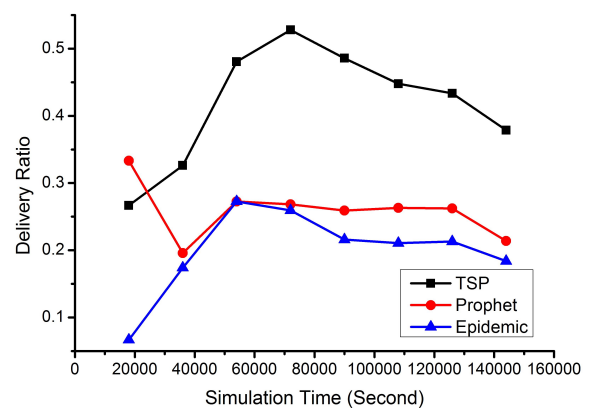
3) NA and NB exchange the message list. The message list consists of the destination information (ND) and current meet probability. For example, message in message list of NB has a meet probability between NB and ND (supposed PBD), which is mainly based on degree in (ND, degree) in NB. For each message, FBP compute the meet probability between NA and ND, supposed PAD. If PAD > PBD, the message is decided to deliver from NB to NA.

4) Start the transmission process until beyond the transmission range.

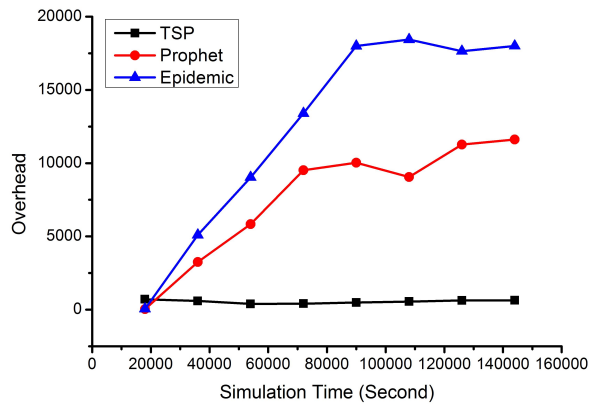
**IV. SIMULATION**

In the simulation, we use real data set collected by an opportunistic mobile social application MobiClique during SIGCOMM2009 conference [10]. The experiment is carried out through the Opportunistic Network Environment (ONE) Simulator [11]. The nodes are fixed direct-friend information at the beginning. The messages with 10 hours TTL are generated randomly.

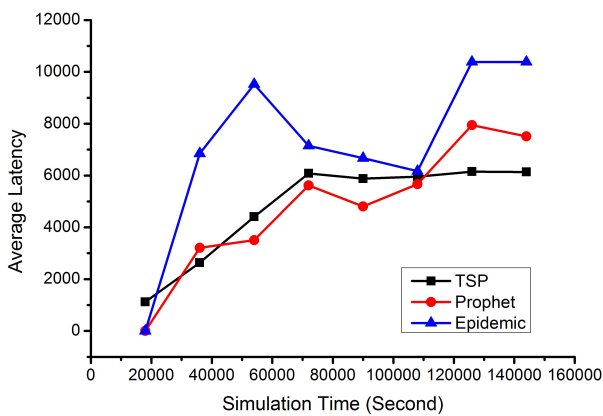
We compare the effectiveness of our FBP with two 'non-oblivious' routing protocols: Epidemic and PROPHET. Epidemic adopts a simple flooding method which copies the messages to every encounter that has not received a copy. Epidemic obtain highest delivery ratio if buffer size is unlimited. However, it produces highest overhead due to huge number of copies. PROPHET is prediction-based routing which predicts and selects the forwarders by the use of history encounter records. It supposes that nodes meet in history will have more opportunity to meet in the future. For PROPHET, we use the default parameters provided by ONE.



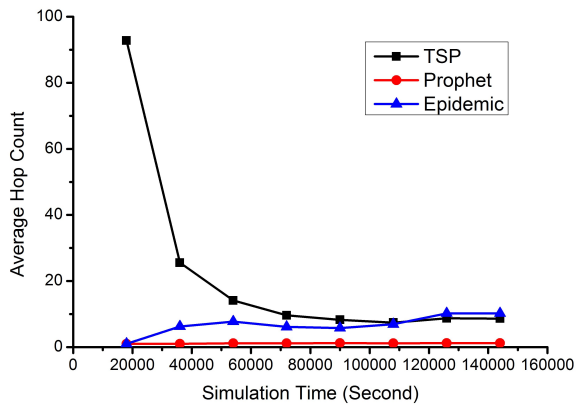
(a) Delivery Ratio



(b) Overhead



(c) Average Latency



(d) Average Hop Count

Fig.2 Efficiency Comparison

In Fig 2, we show comparison of all algorithms in terms of delivery ratio, overhead ratio and average latency under different simulation times respectively. The simulation times are designed at 6 hour interval. That is 6,12, 18, 24, 30, 36 hours. As shown, the performance of FBP outperforms Epidemic and PROPHET. In Fig 2, the delivery ratio of FBP is far higher than Epidemic and PROPHET. For example, in 12 hours, FBP forwards 26.33% , which is much higher than Epidemic with 14.7% and PROPHET 10.7%. In Fig 3, the overhead of FBP is 12.8, which is much lower than Epidemic with 716 and PROPHET 959. In Fig 4, the average latency of FBP is 2523, which is close to Epidemic with 2846 and PROPHET 1273.

V. CONCLUSION

In this paper, we present a routing protocol in socially-aware Opportunistic Networks, named friend based prediction (FBP) . In FBP, each mobile device records and maintains direct-friend information and second-friend information respectively. And based this information, FBP predict the higher meet probability to the destination node as forwarder in order to improve the efficiency. The simulation shows that FBP obtains the predicted results.

ACKNOWLEDGEMENTS

This work was financially supported by the Shandong Jiaotong University Science Research Foundation (Z201305).

References

- [1] M. Conti, S. Giordano, M. May, and A. Passarella, "From opportunistic networks to opportunistic computing," *Communications Magazine*, vol. 48, no. 9, pp. 126–139, 2010.
- [2] C. M. A. M. Khabbaz and W. Fawaz, "Disruption-tolerant networking: A comprehensive survey on recent developments and persisting challenges," *IEEE Commun. Surveys & Tutorials*, vol. 14, no. 2, pp. 607–640, 2012.
- [3] A.Vahdat and D. Becker, "Epidemic routing for partially connected ad hoc networks," *Technical Report CS-200006*, 2000.
- [4] A. Lindgren, A. Doria, and O. Schel'en, "Probabilistic routing in intermittently connected networks," *SIGMOBILE Mob. Comput. Commun.*
- [5] *Rev.*, vol. 7, no. 3, pp. 19–20, jul 2003. H. Pan, J. Crowcroft, and E. Yoneki, "Bubble rap: Social-based forwarding in delay-tolerant networks," *Mobile Computing*, vol. 10, no. 11, pp.1576–1589, 2011.
- [6] [6] F. Li and J. Wu, "Mops: Providing content-based service in disruptiontolerant networks," *Distributed Computing Systems*, 2009. 29th IEEE International Conference on, pp. 526–533, June 2009.
- [7] L. Feng and W. Jie, "Localcom: A community-based epidemic forwarding scheme in disruption-tolerant networks," *6th Annual IEEE Communications Society Conference on*, pp. 1–9, 2009.
- [8] E. Bulut and K. Szymanski, B, "Friendship based routing in delay tolerant mobile social networks," *Global Telecommunications Conference, 2010 IEEE*, pp. 1–5, 2010.
- [9] L. Gao, M. Li, A. Bonti, W. Zhou, and S. Yu, "Multidimensional routing protocol in human-associated delay-tolerant networks," *IEEE Transactions on. Mobile Computing*, vol. 12, no. 11, pp. 2132–2144, 2013.
- [10] A.-K. Pietil'ainen, E. Oliver, J. LeBrun, G. Varghese, and C. Diot, "Mobiclique: middleware for mobile social networking," *Proceedings of the 2nd ACM workshop on Online social networks*, pp. 49–54, 2009.
- [11] A. Ker'anen, T. K'ark'ainen, and J. Ott, "Simulating mobility and dtns with the one," *Journal of Communications*, vol. 5, no. 2, pp. 92–105, 2010.

# Research on Portfolio Risk Prediction based on Copula-GJR-Skewt Model

Weiwu Ye\*, Ziming Liu

College of Information, South China Agricultural University, Guangzhou, China

**Abstract**—For diversified investment portfolio risk prediction, using thick tail GJR-Skewt model depicts a single asset, biased characteristics, as well as non-linear correlation structure Copula model depicts a diversified investment portfolio, simulates the random distribution of financial assets by the Monte Carlo method combined with rolling time window method, the future of venture capital portfolios to-sample empirical results show that dynamic prediction. Copula-GJR-Skewt model to predict the risk of asset returns can achieve satisfactory results. In the VaR forecasting performance to GJR-Skewt model as the edge of the distribution function, even if there is a system error, but also to obtain optimal predictions. Preset residuals obey biased distribution of students, the prediction is better than normal VaR and traditional Garch-Guassian model predictive capability is the worst.

**Index Terms**—Portfolio Risk; Prediction; Copula-GJR-Skewt; System

## I. INTRODUCTION

It is expected that authors will submit carefully written and proofread material. Careful checking for spelling and grammatical errors should be performed.

For diversified investment portfolio risk prediction, using thick tail GJR-Skewt model depicts a single asset, biased characteristics, as well as non-linear correlation structure Copula model depicts a diversified investment portfolio, simulate the random distribution of financial assets by the Monte Carlo method, combined with rolling time window method, the future of venture capital portfolios to-sample empirical results show that dynamic prediction, Copula-GJR-Skewt model to predict the risk of asset returns can achieve satisfactory results. In the VaR forecasting performance to GJR-Skewt model as the edge of the distribution function, even if there is a system error, but also to obtain optimal predictions; preset residuals obey biased distribution of students, the prediction is better than normal VaR; traditional Garch-Guassian model predictive capability worst [1-2].

According to Markowitz's mean-variance efficient frontier portfolio theory, investors should hold a diversified investment co. If the portfolio of industry concentration is high, weakening the ability to reduce risk. INDUSTRIAL ENGINEERING found that there was a significant negative relationship between industry concentration and Fund Performance Fund's investment portfolio. Characteristics of different industries, correlation between different sectors, investors should rational allocation of sectors, lower or higher risk

portfolio which industries? At different stages in the stock market cycle, lower portfolio risk, or if a higher relative relationship will change, that if you want to replace the industry portfolio investors? This is of great concern to investors.

Easy to describe the characteristics of an industry, but the relationship between the industry and the distribution of non-industry due to the nonlinear yield normality, so a linear model or multivariate normal distribution model does not work, use more academic research Copula model. Han Xuelian relationship with Gumbel-Copula Function of Public Utilities Index and Industrial Index, draw a strong correlation between the two indices during the bull market to bear market correlation conclusion, a combination of both valid [3]. Liu Qiongfang Underperformance using the two-parameter fit Copula stock returns related to real estate and finance industry structure, and found two industries when tail dependence is higher than the active during the market downturn [4], it is not by reducing the risk of their portfolio. Chen Yinzong, inter ECHNOLOGY Shenzhen Industry tail correlation analysis in Clayton-Copula and Gumbel-Copula function, the results show that in addition to the service sector, have a significant correlation between asymmetric tails of other industries [5].

With the development of Copula theory, dynamic Copula model is presented and reflected a strong advantage. A. Dias Copula function in conjunction with the GARCH time series data fitting, the model results are more accurate measure. Luo Fu Yan, when Deng Guangming estimated using varying Copula Shanghai, Shenzhen index portfolio VaR, a better [6].

From the above analysis, the current research portfolio sector allocation of risk or to focus on a few industries, or remain at the level of static analysis. In order to provide investors with more investment reference, we further expand on the basis of previous studies, in order to cover over the whole of Shenzhen industry sector index (13 categories A total of nine categories of 22 industries) for the study, with time variable Copula-GJR-Skewt model captures the nonlinear relationship between dynamic industry, dynamic computing portfolio value at risk VaR, stock market analysis at different stages of the cycle, changes in portfolio risk of a variety of industries. In order to make the model fit best effect, and with the results of the static Copula model comparison, the paper in the choice of Copula function, also studied in three time-varying function and six static Copula Copula function [7-9].

II. COPULA THEORY

Copula function to decompose the joint distribution of the variables is clearly structured in two parts, namely the variables related to the structure of their edges between distribution and describe the relationship between variables. According to Sklar theorem continuous distribution of binary variables X, Y joint distribution function H, the edge of the variable distribution of F (x) and G (y), there is always a condition of Copula C, satisfy:

$$H(x, y) = C(F(x), G(y)) \tag{1}$$

Normality Copula and t-Copula belongs Elliptical Copula, which is characterized by the distribution function of radial symmetry. Gumbel, Clayton and Frank are Archimedean Copula, which Gumbel-Copula and Clayton-Copula asymmetric, the former on the tail correlation sensitive, which is sensitive to the lower tail correlation. Frank Copula can describe the negative correlation between variables. Joe Patton at the JC Copula function based on the improvement is proposed for the upper and lower end are sensitive and symmetrical SJC Copula. Correlation between financial market will change with changes in the external environment, and therefore become Copula and variable structure Copula when Patton also proposed. In the time-varying Copula model, it is assumed to obey the dynamic evolution equation parameters related to time, according to correspondence between the parameters and the

correlation coefficient, the dynamic evolution equation parameters established by the evolution of the correlation over time [10].

Varying normality Copula correlation coefficient  $\rho$  change its relationship with the parameters as follows:

$$\tilde{\Lambda} = \frac{1 - e^{-x}}{1 + e^{-x}} \tag{2}$$

$$\rho_t = \tilde{\Lambda}(\omega_\rho + \beta_\rho \rho_{t-1} + \alpha_\rho \times 1/10 \sum_{i=1}^{10} \Phi^{-1}(u_{t-i}) \Phi^{-1}(v_{t-i})) \tag{3}$$

Logistic transformation is modified, it makes  $\rho_t$  maintained in the range (-1, 1).

T-Copula of time-varying correlation coefficient  $\rho_t$  and freedom when  $k_t$  change their upper and lower tail correlation  $\tau^U, \tau^L$  relationship:

$$k_t = \frac{1}{\log_2(2 - \tau^U)}, \gamma_t = \frac{1}{\log_2 \tau^L} \tag{4}$$

$$\tau^U = \tau^L = 2T_{\rho_t, k_t}(-\sqrt{k_t + 1} \sqrt{\frac{1 - \rho_t}{1 + \rho_t}}; k_t + 1) \tag{5}$$

III. COPULA-GJR-SKEWED MEASURE VAR MODEL APPROACH

In mathematical expressions VaR VaR is  $VaR_\alpha = \inf \{l \in R: P(L > l) (1 - \alpha)\}$ , where,  $\alpha \in (0,1)$  is the confidence level,  $l$  is the minimum VaR portfolio value

that meets the future holds for the probability of more than 1 period not to exceed the actual loss  $L (1 - \alpha)$ . VaR is a good way to measure portfolio risk, it's estimated that there are historical simulation methods, analysis and Monte Carlo simulation method. Rosen-berg and Schuermann use Copula theory of market risk, credit risk and operational VaR aggregation risk. Ye May Copula method using high-frequency dependence structure analysis yields rising losing streak and estimate VaR [11].

Copula model with portfolio risk measure VaR is the key to accurately characterize the distribution and use of the right edge of the Copula function. Firstly, determine the marginal distribution of the industry index returns, and then choose the best time-varying and static Copula function calculates all industry index pairwise combinations of dynamic and static final value at risk VaR using a Monte Carlo simulation.

A. Determine of the Marginal Distribution

Financial time series usually present autocorrelation and conditional heteroskedasticity and showed a fat tail, volatility clustering and leverage. Varying variance describing AR (1) -GARCH (1, 1) model can capture and conditional heteroskedasticity autocorrelation time series, depicts the characteristics of volatility clustering, but the leverage is not well reflected. Further introduction of leverage can capture GJR establish AR (1) -GJR (1, 1) model. GJR of  $\gamma$  measures the leverage effect, when  $\gamma = 0$ , GJR model degenerates into a GARCH model. Assuming the normalized residuals obey Skewt biased distribution, for obedience AR (1) -GJR (1, 1) model yields [12].

Financial time series usually present autocorrelation and conditional heteroskedasticity and showed a fat tail, volatility clustering and leverage. Varying variance describing AR (1) -GARCH (1, 1) model can capture and conditional heteroskedasticity autocorrelation time series, depicts the characteristics of volatility clustering, but the leverage is not well reflected. Further introduction of leverage can capture GJR establish AR (1)-GJR (1, 1) model. GJR of  $\gamma$  measures the leverage effect, when  $\gamma = 0$ , GJR model degenerates into a GARCH model. Residuals obey biased assumptions of Skewt normalized distribution, for obedience AR (1)-GJR yield (1, 1) model  $r_{i,t}$ , are:

$$\begin{aligned} c &= c_o + c_o r_{i,t-1} + e_{i,t} \\ e_{i,t} &= h_{i,t} \varepsilon_{i,t}, \varepsilon_{i,t} \sim Skewt-t(v_i, \lambda_i) \\ h_{i,t} &= \omega_{i,t} + \alpha e^2_{i,t-1} + \beta h_{i,t-1} + \gamma e^2_{i,t-1} I(e_{i,t-1} < 0) \end{aligned} \tag{6}$$

Where  $r_t$  is the logarithm yields the  $i$ -th industry index at time  $t$ ,  $e_{i,t}$  is the residual term,  $\omega > 0, \alpha > 0, \beta < 0$ , and  $\alpha + \beta < 1, I(e_{i,t-1} < 0)$  as an indicator function. Skewt density function is [13]:

B. Determine and Estimate on the Parameters of Copula Function

This paper selection becomes normality Copula, t-Copula time-varying and time-varying function of three SJC-Copula model fitting to choose the optimal dynamic Copula functions. In order to compare and static Copula, and also use a normal, t, Gumbel, Clayton, Frank and SJC six kinds of static Copula function fitting. Based on AIC, BIC and log-likelihood (LL) index, this paper selects the

optimal dynamic Copula functions.

Copula model combines the characteristics of a phase, we use a two-stage maximum likelihood method (IFM) to estimate the model parameters. First get the edge distribution function parameter estimation:

$$\hat{\theta}_1 = \arg \max \sum_{t=1}^l \ln f(x_t; \theta_1) \tag{7}$$

$$\hat{\theta}_2 = \arg \max \sum_{t=1}^T \ln g(y_t; \theta_2) \tag{8}$$

Then substitute into the Copula function to obtain the estimated value of  $\alpha$ :

$$\hat{\alpha} = \arg \max \sum_{t=1}^T \ln c(F(x_t; \theta_1), G(y_t; \theta_2); \alpha) \tag{9}$$

*C Calculate VaR by Monte Carlo Simulation Method*

Copula model parameters obtained after estimation, you can use the Monte Carlo simulation to generate random numbers in line with the given parameters Copula function to simulate actual industry index returns (assuming the holding period is one day), a combination of computing VaR assets. Monte Carlo simulation is repeated by a random process, making the estimated value converges to the true value. Step portfolio VaR calculation is as follows:

Step 1: generate pseudo random numbers (u, v) in accordance with the best Copula function, which is to produce two separate (0,1) uniformly distributed random number u and t:

$$V = C_U^{-1}(t) \tag{10}$$

$$C_U = \frac{\partial C(u, v)}{\partial u} \tag{11}$$

Where, (u, v) shall meet the best Copula function C (u, v) of a random number;

Step2: Anti solved

$$R_x = F^{-1}(u), R_y = G^{-1}(v) \tag{9}$$

Where X and Y denote the simulation yields two industry index, based on both the right weight  $\omega_1$  and  $\omega_2$ , find the combination yields  $R = \omega_1 R_x + \omega_2 R_y$ ;

Step 3: Repeat N times to get experience in the distribution of the portfolio of future earnings, the calculation for a given confidence level 1-  $\alpha$  quantile under obtains portfolio VaR.

IV. EMPIRICAL RESULTS AND ANALYSIS

*A Descriptive Statistical Time Series of Return on Assets*

This paper selects Chinese CSI 300 Index (HS300), US S & P index (SP500), Japan's Nikkei 225 (NKY), the UK FTSE 100 index (FTSE) the closing index build an international portfolio, examine the combination yields the risk of data selected time period April 1, 2005 to April 1, 2013, taking into account different national stock trading day of sync or holidays and other reasons, excluding trading day non-overlapping data, obtained after processing 7064 data that 1766 group

synchronization data. data sources for great wisdom database model to predict the effect of comparison, the 1766 data set into groups within the 1200 samples and 566-sample data set of sample data as foreign portfolio VaR prediction test samples.

First, the closing index of the number of treatment, based on the closing price of Pt for t day, the daily rate of return  $rt = 100 \times \text{HPt/Pt-i}$ -yields the treated data descriptive statistics are shown in Table 1.

Table 1 Descriptive statistics of yields

	average	Standard deviation	Skewness	Kurtosis	J-B	LM (2)
FTSE	0.0491	1.1838	-0.1566	4.9724	145.4203**	0.1529[0.000]
HS300	-0.0043	1.6439	-0.1701	4.9825	147.5074**	0.1527[0.000]
NKY	0.0369	1.4056	-0.5434	8.1207	999.0427**	0.0695[0.0623]
SP500	0.0734	1.2574	-0.2504	6.4429	441.2983**	0.3119[00.000]

From Table 1, the four sets of data were shown left side form (skewness coefficient is less than 0), and were more than the normal distribution kurtosis kurtosis 3, indicating that data exists obvious "fat tail" feature; JB statistic four sets of data show declined at 1% significance level of normal; visible, there is a significant "Rush fat tail" features comprehensive data .Arch effect on the test results to prove except LM NKY at 10% significance level denial does not exist ARCH effect null hypothesis, the other three sets of data are in the 1% significance level there is no ARCH effects reject the null hypothesis, so using Garch class model is reasonable.

*B. AR-GJR-Skewt Model Parameter Estimation Results*

By formula (1) to (3) constructed AR-GJR-Skewt model, using maximum likelihood estimation method to estimate the parameters of the results obtained are shown in Table 2.

Table 2 AR-GJR-Skewt Model Estimation Results

Estimated parameters	FTSE	HS300	NKY	SP500
$\alpha$	0.0286	0.1342	0.0309	0.0121
$\omega$	0.019	0.0305	0.0435	0.0107
$\alpha$	-0.006	0.0522	0.0264	-0.0431
$\beta$	0.9027	0.9415	0.8907	0.9451
$\gamma$	0.1901	0.0056	0.1279	0.183
$\nu$	9.2521	5.2578	10.0433	5.1446
$\lambda$	-0.1031	-0.1083	0.0374	-0.1473
L-BQ(5) Statistics	9.9085	9.8219	4.7678	4.1249
L-BQ(5) Probability value	0.0779	0.0804	0.4449	0.5316
K-S Statistics	0.0194	0.0184	0.0319	0.0301
K-S Probability value	0.7493	0.803	0.171	0.221

Seen from Table 2, p coefficient four sets of data were above 0.89, indicating that there are significant

fluctuations in the data aggregation; 7 coefficient four sets of data are not zero, confirming the existence of the data are leveraged .L-BQ (5) statistics and P values indicate that the residuals of the standard sequence of each set of sequences by GJR-skewt model fit after autocorrelation test, at 10% significance level, each sequence since there is no correlation, it is considered conversion after the sequence is independent; KS statistics and probability values indicate, for each set of data to make the probability integral transformation of the original sequence after sequence obtained at 1% significance level the null hypothesis should be accepted sequence of obedience "after change (0,1) uniform distribution"; Summing think through AR-GJR-Skewt model fit the data to meet the modeling requirements of each group Copula model.

*C. Dynamic VaR-sample Prediction*

In calculating portfolio VaR, such as paper, we consider the right of the four asset heavy case that formula (11) is called = 0.25 according to the portfolio VaR of 1.3 Monte Carlo simulation method to predict the future 566 rolling time window method day VaR trend.

First calculate the portfolio to meet the diverse T-Copula function rank correlation coefficient matrix. The sample is fixed at an estimated 1200 days, followed with the first 1200 days before t based on historical data, calculated Copula parameter and then calculate the correlation coefficient matrix, where t = (1201, ..., 1766), received a total of 566 groups of varying correlation matrix. Due to limited space, choose the first group and the second group of 566 rank correlation coefficient matrix is shown in Table 3.

Table 3 T-Copula rank correlation coefficient matrix

Index Group 1	FTSE	HS300	NKY	SP500
FTSE	1	0.1125	0.2286	0.4505
HS300	0.1125	1	0.1715	0.0667
NKY	0.2286	0.1715	1	0.1235
SP500	0.4505	0.0667	0.1235	1
Index Group 566	FTSE	HS300	NKY	SP500
FTSE	1	0.0968	0.2389	0.4164
HS300	0.0968	1	0.1584	0.0653
NKY	0.2389	0.1584	1	0.109
SP500	0.4164	0.0653	0.109	1

When calculated according to varying rank correlation coefficient matrix, using a Monte Carlo simulation randomly distributed into four groups of data. On the first day of forecast scenarios were simulated 40,000 times (each data 10,000 times), to get the first day 10,000 times may be distributed, and then calculated separately in accordance with section 1-3 of the calculation procedure to obtain a given level of confidence Dir day VaR predictive value, empathy was second and third in total 566 days of the VaR forecast. That is, for each given confidence level VaR value, for a total of 40000\*566=22640000 times scenario simulation calculations.

Where the actual yield from the portfolio 566-sample set of actual yields according to equation (11) is calculated from Figure 1 shows the predicted VaR

volatility generally fluctuate in line with the real rate of return, at the same time, the higher the confidence level is calculated VaR out bigger, larger VaR forecast indicates that fewer failures. Therefore, the actual application of choice depends on the confidence level of investment risk aversion or regulators, the higher the chosen confidence level of risk aversion the lower degree.

*D. Kupiec LR Test of Model Predict*

To obtain a more rigorous model predicted effect on the predicted VaR Kupiec LR more rigorous statistical tests, given Kupiec statistical failures and the failure rate of P values .P larger value indicates that VaR calculated under the assumption that the model the higher accuracy rate. If the examination of the actual number of failures too, said the model may overestimate risk, and vice versa, said the model may underestimate the risk, too much or too little of a corresponding number of failures will come to a low p-value.

Also, because the marginal distribution of the preset for VaR measure has important implications for a comparative study, the paper considered ordinary Garch selected class function Garch-Guassian, can portray the leverage effect of Garch class functions and can portray GJR-Guassian asymmetric distribution the GARCH-Skewt model as the marginal distribution model predicts VaR1 again predicted VaR actual number of failures in Table 4, P value Kupiec LR test results are shown in Table 5.

Table 4 VaR forecast Kupic T-copula function under different marginal distribution of test failures

model	99.5%		99%		97.5%		95%	
	expected	fact	expected	fact	expected	fact	expected	fact
GJR-Skewt	2.8	3	5.7	5	14.2	16	28.3	36
GARCH-Skewt	2.8	5	5.7	7	14.2	21	28.3	40
GJR-Guassian	2.8	1	5.7	1	14.2	1	28.3	2
GarchGuassian	2.8	0	5.7	0	14.2	4	28.3	5

Table 5 VaR forecast Kupic test P values for different marginal distributions under T-copula function

model	99.5%	99%	97.5%	95%
	P	P	P	P
GJR-Skewt	0.9201	0.7761	0.6255	0.1534
GARCH-Skewt	0.2435	0.5851	0.085	0.0332
GJR-Guassian	0.208	0.0152	3.90E-06	4.76E-11
Garch-Guassian	0.0172	0.0007	0.0013	3.78E-08

Secondly, under the assumption that the distribution of residuals obey Skewt, GJR and Garch VaR model predictive ability are superior model residuals obey normal distribution assumption, indicating that Skewt distribution assets to effectively portray the sequence of the fat tail of financial and asymmetrical features, and

then get better VaR prediction.

Again, Garch-Gaussian model predicted VaR and expected number of failures is too small compared to the number of failures, indicating a greater degree of risk deviate from this model and the actual market, there is a tendency to underestimate the risks.

Finally, in the discrimination of a large number of classification confidence level lower (95%, 97.5%, 99%), P values substantially higher confidence level of the test results obtained, the better the trend exists. The reason is that the higher the confidence level, the smaller the probability of occurrence of the corresponding event, the less the expected number of failures, the more difficult to find the system deviation. Thus, some regulators tend to choose a lower confidence level (e.g. 95%), so that a sufficient number of observed failures to reduce systematic bias. The empirical results of this paper show, GJR-Skewt model at the 95% confidence level, the Kupiec test result is still significantly better than the other three groups of models, indicating GJR-Skewt model even in the case of large systematic bias remains superiority.

#### V. CONCLUSION

This paper selected China, USA, Japan, the United Kingdom's as the most representative stock index to build an international portfolio, used Copula-GJR-Skewt model to depict a typical single asset fact (Stylized Fact) and the correlation between the portfolio. Use Monte Carlo method and rolling time window method to predict the dynamic portfolio VaR and strict Kupiec LR test. Meanwhile, the paper also use the above method compares the effect of several other volatility model for dynamic VaR forecasts.

Positive results can be seen: for the United States, Japan, Britain and the four countries most representative stock index, the yield sequences with significant volatility clustering, fat tail and biased skew characteristics; GJR-Skewt model can fit the sample these features stock index in the VaR sample predictive ability of international portfolio outstanding performance, superior to other groups of comparison model; the residuals follow a normal distribution assumption, the model can portray GJR leverage and exhibit no obvious advantages the ability to predict the general Garch VaR model, which shows the full description of the conditions and benefits of fat tail biased characteristics of the VaR prediction accuracy has a more significant impact, therefore, be able to describe the condition of earnings and biased fat tail characteristics. GARCH-Skewt model would be a relatively good model; Garch-Gaussian model predicted VaR and expected number of failures is too small compared to the number of failures, indicating a greater degree of risk deviate from this model and the actual market, there is a tendency to underestimate the risks. It also gives regulators and investors with a useful reference.

It should also be seen that the correlation between the portfolio of complex, distributed to more diverse between related assets to be further verification, which is the next problem to be solved.

#### REFERENCES

- [1] M. Sun, L. Song, T. Zhou, G.Y. Gillespie, R.S. Jope, *Biochimica Biophysica Acta*, 1813 (2011) 438-447.
- [2] Patton A J. Modeling Time-varying ExchangeRate Dependence Using the Conditional Copula. Working paper of Department of Economics, University of California, San, Diego, 2001.
- [3] Rosenberg J, Schuermann T. A General Approach to Integrated Risk Management with Skewed, Fat-tailed Risks. Federal Reserve Bank of New York, 2004.
- [4] Diebold F X, Gunther T, Tay A S. Evaluating Density Forecasts, with Application to Financial Risk Management. *International Economic Review*, 39 (1998)863-883.
- [5] Patton A J. Copula-Based Models for Financial Time Series. *Handbook of Financial Time Series*, 2009: 767
- [6] Singleton J C, Wingender J. Skewness persistence in common stock returns. *Journal of Financial and Quantitative Analysis*, 21(1986) 335-341.
- [7] Peiro A. Skewness in financial returns. *Journal of Banking & Finance*, 23(1999) 847-862.
- [8] Lambert P, Laurent S. Modelling financial time series using GARCH-type models With a skewed Student distribution for the innovations. Institut de Statistique, Universite Catholique de Louvain, Louvain-la-Neuve, Belgium, 2001.
- [9] Kupiec P H. Techniques for Verifying the Accuracy of Risk Measurement Models. *The Journal of Derivatives*, 3(1995)73-84.
- [10] Cherubini U, Luciano E, Vecchiato W. Copula methods in finance, England: John Wiley & Sons Ltd, 2004.
- [11] Lux T, Marchesi M. Volatility clustering in financial markets: A microsimulation of interacting agents. *International Journal of Theoretical and Applied Finance*, 3(2000)675-702.
- [12] Verhoeven P McAleer M. Fat tails and asymmetry in financial volatility models. *Mathematics and Computers in Simulation*, 64(2004)351-361.
- [13] Patton A J. Modelling Asymmetric Exchange Rate Dependence. *International economic review*, 47(2006)527-556.

# Analysis the Affection of Interaction in Teaching of Experiment

Zhu ke

Department of Educational Technology, Henan Normal University, Xinxiang, China

**Abstract**—In this paper , we take the experiment of using different interaction rate as single factor experiment , we get the equation of the interaction makes an effort to score by using the quadratic polynomial regression , which not only quantificational describe the affection of the interaction makes an effort to score but also getting the best degree of every interaction . Finally, our results fit the experiment data perfectly, and the model we constructed doesn't depend on any special conditions.

**Index Terms**— Data Mining, Experiment Teaching, Interaction

## I. INTRODUCTION

Over recent years, there has been a considerable growth of the size of data over the World .The data mining technology has become thoroughly entirely integrated in the too many field now [1]. The technology plays an important role in almost every aspect of human life such as industry, commerce, security domain. Learning analysis has appeared 5 years or more, but it has not given us too much surprise, what is the major challenge of the field learning analysis?

From an abstract point of view, a significant part of the activities that take place in any learning experience are interactions. Students interact with numerous resources (documents, forums, chats, specific tools), with the instructors, among themselves, etc. [2].

Interaction is identified as a crucial component of the learning process. Anderson and Garrison first categorized the different modes of interactions that can take place in a distance learning environment with two observations: deep and meaningful learning is supported if one of these forms of interactions is at its high level; and high levels of more than one of these modes will likely increase the quality of the experience although at a significantly higher cost [3]. Thus, following the equivalency statement we may assume that a successful learning experience has a high level of interaction in one of its aspects [4].

### A. Analysis problem

From the principle and experience of score to see, we can generally use multivariate polynomial regression model to describe and analysis the relationship between the output and the interaction rate, especially, when we discuss the general affect for output of K, G, C, in experiment and the other influencing factors that

knowledge, gender, cognitive load, and so on are in the equal level, we can use the ternary quadratic polynomial to construct the regression model:

$$E(W)=b_0+b_{NN}+b_{PP}+b_{KK}+b_{NNN2}+b_{PPP2}+b_{KKK2}+b_{NPNP}+b_{NKNK}+b_{PKPK} \quad (1)$$

Where W is output; K is the frequency of K; G is the frequency of G; C is the frequency of C; every b are the fraction, during (1), the last three parts are the cross terms of variable parameters, which apart reflect the cross effects of two different interactions [5].

In the design of experiment of this problem, when experiment uses different frequency of one of one interaction, keeping the other two interactions on the level of t, the method is called factor rotation method.  $n_0, p_0, k_0$  are the frequency which is the level of t of K, G, C, we move the origin of coordinates to the point of  $(n_0, p_0, k_0)$  and then carrying out coordinates transformation for model (1), the equation of the model doesn't change.

In the new coordinate system, all the experiment point are on the coordinate axis, namely, every experiment point has two zero coordinates at least, so all the cross terms are disappearing, accordingly, when estimating the form equation for regression coefficient, all the coefficient of  $b_{Np}$ ,  $b_{Nk}$ ,  $b_{pk}$ , are 0, so, we can't estimate the regression coefficient  $b_{Np}$ ,  $b_{Nk}$ ,  $b_{pk}$  through the experiment results.

As we use the experiment method, so we can't use the interaction effect [6]. As we can ignore the cross terms, so, model (1) becomes the apart model for three variable. If we see the ten experiments which every interaction has different frequency as a group of single factor experiment, thus, we can use regression model the which is constructed by three quadratic polynomial instead of the model(1) to simplify the problem.

## II. METHODOLOGY

### A. Assumptions

The experiment is carried out in the same and formal conditions, output changes as the length of interaction rate changes, so, there are some regulations between the output and interaction rate.

Curriculum has some K, G, C, in itself; so, it can make the score grow up without artificial interaction.

Every experiment is independent and there is no attachment with each other, we see the variable of K, G, C, without deviation.

B. Signal define

- W: the output of score
- X: interaction rate
- K,G,C: the frequency of K,G,C
- Tw: the value of score
- Tx: the value of interaction
- TN, TP, TK: the value of the interaction of K,G,C

C. Analysis problem

According to the experiment results, we write the unitary interaction domino equation and domino curve which reflect the relationship between interaction rate and output, using quadratic polynomial regression, we can get:

The domino equation of N to interaction between student and student:

$$W=14.74+0.197N-0.0034N^2 \quad (2)$$

The domino equation of N to education:

$$W=10.23+0.101N-0.00024N^2 \quad (3)$$

The domino curve of N (see figure 1 and figure2 ):

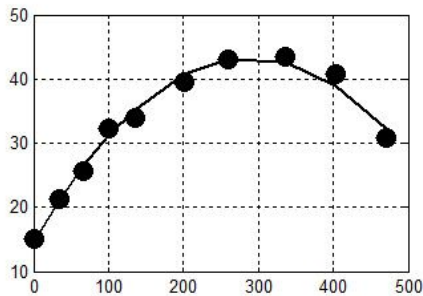


Figure 1. The domino curve of N to interaction between teacher and student

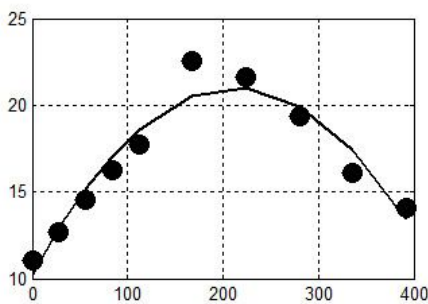


Figure 2. The domino curve of N to interaction between student and student

The domino equation of P to interaction between student and student:

$$W=32.9262+0.0718590P-0.00013783P^2 \quad (4)$$

The domino equation of P to education:

$$W=6.87566+0.0605913P-5.4527810\cdot 5P^2 \quad (5)$$

The domino curve of P (see figure 3 and figure 4):

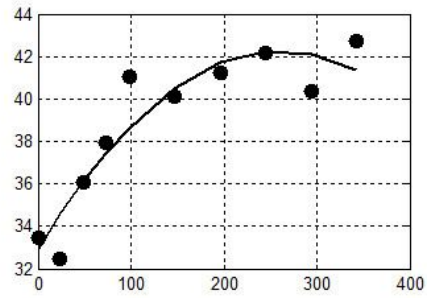


Figure 3. The domino curve of N to interaction between teacher and student

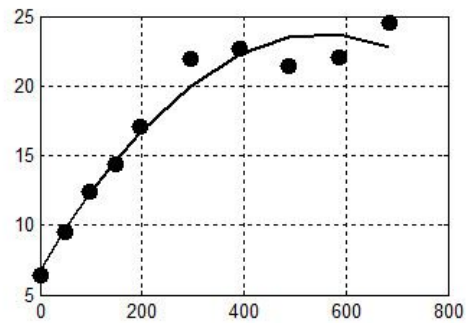


Figure 4. The domino curve of N to interaction between student and student

The domino equation of K to interaction between student and student:

$$W=24.4144+0.0749752K-6.99534\cdot 10^{-5}K^2 \quad (6)$$

The domino equation of K to education:

$$W=16.2396+0.00511548K-7.18972\cdot 10^{-7}K^2 \quad (7)$$

The domino curve of K (see figure 5 and figure 6):

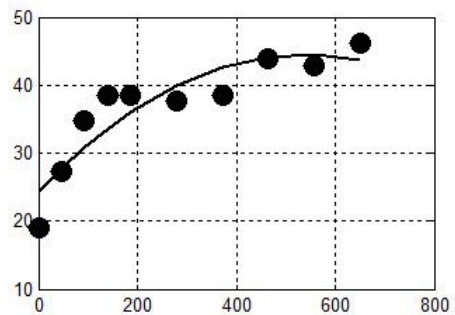


Figure 5. The domino curve of N to interaction between teacher and student

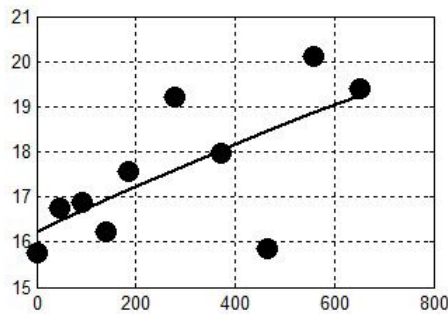


Figure6. The domino curve of N to interaction between student and student

### III. RESULT ANALYSIS

The model quantificational reflects the relationship between interaction rate and output, from the domino curve to see, superfluous N will make the score's output reduce, when the frequency of P overcome the fixed limit, it makes little affect, K has the similarity properties to P.

To calculate the best frequency of every interaction, we use the following equation:

$$\frac{d\omega}{dx} = \frac{T_x}{T_\omega}$$

In this time, when putting 1ton interaction, we get the best income.

Supposing the value of interaction are  $T_n$ ,  $T_p$ ,  $T_k$ , and used (2) we can get:

$$\frac{d\omega}{dN} = 0.197 - 0.00068 = \frac{T_n}{T_\omega}$$

used(3),we can get:

$$\frac{d\omega}{dN} = 0.101 - 0.00048 = \frac{T_n}{T_\omega}$$

So, we can get the best frequency of N to interaction between student and student.

Through (4) (5), we can get the best frequency of P to interaction between student and student, and interaction between student and teacher, and through the domino equation of interaction between student and teacher to K, we know, interaction between student and teacher need little K, even without K.

### IV. CONCLUSIONS AND FURTHER EXPLANATIONS

From the domino curve of every interaction, we can know, the model results fit experiment data very well, which shows the model is reasonable and has higher practical value, the model not only quantificational describe the effort of every interaction to score, but also we get the best frequency of every interaction, the model constructed depends nothing specially conditions and has widely applying, because, the experiment itself decide that we can't estimate the cross effect of interaction, thus, we can't calculate the best frequency of interaction, but to popularize the model, what we should do is only to improve the experiment equation.

### ACKNOWLEDGMENT

This work is supported by educational innovation project of Henan Province (No. 2014SJGLX026).

### REFERENCES

- [1] L. W. Murray and A. M. Efendioglu, "Valuing the investment in organizational training," *Industrial and Commercial Training*, vol. 39, pp. 372-379, 2007.
- [2] P. J. Goldstein and R. N. Katz, "Academic Analytics: The Uses of Management Information and Technology in Higher Education," *EDUCAUSE Center for Applied Research*, 2005.
- [3] Hwang, W.-Y., & Wang, C.-Y. A study of learning time patterns in asynchronous learning environments. *Journal of Computer Assisted Learning*, 20(4), 292-304, 2004.
- [4] Rourke, L., Anderson, T., Garrison, D. R., & Archer, W. Methodological issues in the content analysis of computer conference transcripts. *International Journal of Artificial Intelligence in Education*, 12, 8-22, 2001.
- [5] Kitamura, Y. Web information integration using multiple character agents. In H. Prendinger & M. Ishizuka (Eds.), *Life-like characters: Tools, affective functions and applications*. Berlin: Springer, 2004.
- [6] Hayt hornthwaite, C. Learning and knowledge networks in interdisciplinary collaborations. *Journal of the American Society for Information Science and Technology*, 57, 8, 1079-1092, 2006.

Zhu ke: born in 1982, His research interests include learning analysis, Computer education.

# The Allocation of Wheelchair at Airports Problem

Zhang jin

Department of Educational Technology, Henan Normal University, Xinxiang, China

**Abstract**—Epsilon Airlines faced the allocation of wheelchair problem. To minimize the cost of providing wheelchair assistance to its passengers, we analysis the trade-off between explicit costs (chairs and personnel) and implicit costs (losses in market share). Then, we develop Multi-Concourse Airport Model to simulate the interactions between escorts, wheelchairs, and passengers. In addition, the Airline Competition Model uses game-theoretic in seeking the maximum profits and configuration scheme based on the least cost airlines. To put these models into reality, we incorporate extensive demographic data and run a case study on 2005 Southwest Airlines flight data from Midland TX, Columbus OH, St. Louis MO.

**Index Terms**—optimization algorithm, carrying capacity, airport problem

## I. INTRODUCTION

### A. Problem statement

In practice, the airline company are equipped with air wheelchair in order to meet the transmit needs of the elderly, the disabled and the patient [1]. This is the international practice. The airline is responsible for providing the daily management and service, rather than the airport. When passengers are in need, they can apply for the airline company in advance; they will be served after handling the relevant formalities.

There are three approaches for wheelchair using application:

- a. Applying via the Internet.
- b. Booking application made by telephone to the airline.
- c. Or applying when reserving or ordering tickets.

After receiving passengers' application, the airline company will provide service according to their actual demands, allocating and arranging specific seats. Advance reservation request can be met, and in the interior of the airport services are free [2]. Of course, under special circumstances, subject to the given constrains, such as the number of wheelchairs and the attendant of the airport is limited, it may not guarantee the service in time, even cause passengers' flight delay[3]. We study the procedures used by airlines to shuttle passengers from arriving flight to connecting flight. With an aging population, more passengers need help. For boarding procedure, based on the above discussion, we

establish our two optimization models by the following steps.

**Multi-concourse airport model:** This model is based on multiple lounges including 2-50 situations in each different size of airport gates. We establish a minimum loss model, mainly by using the proportion of WP in the total during the decade from 1996 to 2005, as well as airline personnel and operating costs of accompanying data such as wheelchairs and so on. In the model, we not only consider the cost of the airline's wheelchair escort, but also notice flight delays due to improper management. The model calculates the effect of multiple airlines flight delays arising, through stochastic simulation to find the best airline wheelchair and three different settings operating strategy approaches, and were on different strategies to try to do a comparative analysis of the situation, assuming the operating costs and the effect of delay damages is as least as possible.

**Minimum cost model:** This model is the basis of the full analysis of the actual operation of the airline, the airline and the cost of providing wheelchair service entourage to WP generated mainly by the following aspects: the acquisition cost of a wheelchair, wheelchair maintenance costs, wheelchair at the airport and accompanying persons pay storage costs and so on. We first established a cost model related one single factor, including the cost of flight delays, WP waiting costs, service accompanying personnel wheelchair costs and the benefit model produced by working part time. We seek to devise a total cost model for solving the problem by exploring the new direction suggested by their investigations. The set of wheelchairs, the expenses in an accompanying shift are all in comprehensive consideration. Respectively a busy year with mild, moderate and severe cases busy and busy three periods calculated the total cost model.

### B. Key terminology

- Gate: A location where air passengers board flights. A given gate can be represented as an ordered pair, where indexes the concourse and indexes the gates in a concourse.
- Concourse: A collection of gates. Concourse contains gates and is represented as vector
- Airport: A collection of concourses, which we consider as a graph.
- Passenger: A traveler in an airport, associated with an arriving flight and with a connecting

flight. We distinguish WPs (wheelchair passengers) from non-wheelchair passengers.

- Traffic: The mass of passengers in an airport. The level of traffic affects the number of WPs needing transport between gates.
- Wheelchair depot: A location where wheelchairs are stored while not in use. In the strategy, there is a depot in each concourse
- Escort: An airline employee responsible for picking up WPs from arrival gates and transporting them to connecting gates.
- Missed flight: When a passenger arrives more than 15 min after the connecting flight's departure time, the flight leaves without them.
- Strategy: An algorithm for the flow of escorts and wheelchairs throughout the airport.

II. METHOD

A. Assumptions

The airline has a set policy that a plane will wait up to  $x^*$  min for a passenger heading toward the gate. If we increase  $x^*$ , the delay on account of missing flights will decrease, however, with the possibility of increasing delay for passengers waiting aboard planes accompany; similarly, lowering  $x^*$  favors boarded passengers at the expense of late passengers.

Therefore, it is necessary for the airline to seek an optimal value for  $x^*$  to balance the discomfort of waiting passengers against the probability that the late passenger will arrive in time.

Let disutility for small unexpected delays be linear in time, so if 120 passengers on a plane wait 15 min, the total utility loss is proportion to the 120=1,800 min of delay. Also, let the utility loss from missing a flight be  $-U_m < 0$  and set time  $t=0$  to be the flight's planned departure time. If a passenger is not at the gate at  $t=0$  but we know that they are on their way, then we wait up to  $x^*$  min for them.

Let L be a random variable for the lateness of our passenger; the probability of arrival after  $t=0$  is  $P(L \leq x^* | L \geq 0)$ . This means the late passenger benefits by  $U_m P(L \leq x^* | L \geq 0)$ , while the others expect to  $E[T | 0 \leq T \leq x^*]$  wait, since they will leave in at most 15 min.

With  $x^*$  chosen optimally, lost utility from waiting equals benefit to the late passenger. So, when  $N$  passengers are waiting, optimality is achieved when  $NE[T | 0 \leq T \leq x^*] = U_m P(L \leq x^* | L \geq 0)$ .

Given our past experience, we assume that  $x^* = 15$ , so that

$$U_m = \frac{N \times E[T | 0 \leq T \leq 15]}{P(L \leq 15 | L \geq 0)}$$

We determine average  $P(L \leq x^* | L \geq 0)$  and  $E[T | 0 \leq T \leq x^*]$  from our simulation results of an airport with a large enough supply of escorts and wheelchairs that every WP is immediately taken to their connecting flight (Table 4).

In 2000, according to the federal aviation administration statistics, an average flight delays and \$44 for 1 minute, make the cost of a passenger waiting for 1 minute approximately \$0.25. Due to the marginal cost of additional wait 1 minute has nothing to do with the total delay, so can get

$$C_A(t_{fd}) = 44t_{fd}, C_a(t_{pw}) = 0.25t_{pw}$$

$A(t_{fd})t_{fd}$  says all the flight delay of  $t_{fd}$  minutes and the total delay time. Therefore, the value of total time is  $A(t_{fd})t_{fd}$ . From the above definition, we can easily get the flight delay cost and passengers waiting cost, and can be expressed as:

$$T_{fd} = \sum_{t_{fd}} A(t_{fd})t_{fd}$$

Similarly, the total waiting time for passengers

$$T_{pw} = \sum_{t_{pw}=1}^{\infty} a(t_{pw})t_{pw}$$

$$C_D = 44t_{fd}, C_W = 0.25t_{pw}$$

The total cost of a flight service escort

All services within the airport flight attendants, complete with a work need the total cost for the

$$c = C_D + C_W + C_E + W_0 + C_K$$

The annual total cost airlines

The research is designed at reducing the whole year's costs as much as possible, apart from airlines daily operation prime cost. An increased attention has been paid to this important yet very difficult problem in the past decade. Airlines seem to adopt different strategies. Take the past three years for example, every day is 8 hours shift work, as a service escorts every 8 hours a day. Flight flow is distinctive in different period. Usually the flight traffic busy degree time period can be divided into three cases, and they are classified as mild, severe and moderate:

Mild busy. From 4 PM to midnight and from midnight to 8 am the next day two divisions, the two shifts at least make up 90% of the shipping day of the year has 329 days. Accounting for 60% of the 3 years (1095 days), both the 657 days. A conservative estimate flight flow in these time intervals is about half of the total flight.

Heavy busy. Heavy busy period is about 10%, which is about 110 days in accordance with the eight hour shift

rule. Relevant data shows that in these days of flight flow is about 2.5 times the average flow

Moderate busy. That belongs to either the above two cases period or moderately busy period of time (i.e., the remaining 328 days). Related data make clear that flight is about 1.5 times the average flow rate of the flow recently.

Here, the total cost function takes the airlines for a full year and annual different time weighted cost. We represent  $C_l, C_m, C_h$  as mild, moderate and severe busy period total cost respectively, airlines annual total cost can be given by

$$C_a = 657C_l + 328C_m + 110C_h$$

To take advantage of the airlines minimum cost model, we designed a dynamic deployment of wheelchair and escorts algorithm. The whole simulation process can be divided into six steps, which is shown in figure 1.

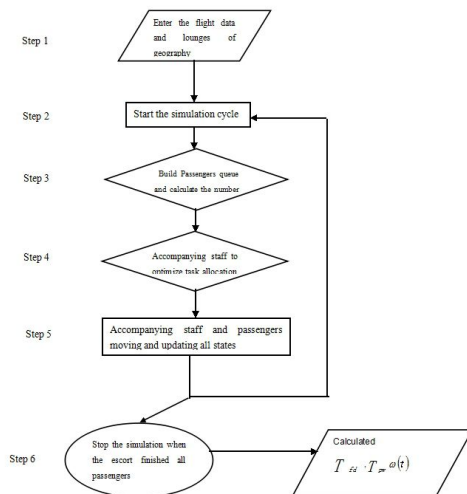


Figure 1. The whole simulation process

Step 1: Enter the basic data

The algorithm needs to know terminal layout of the airport and the schedules of the flight WP ride. Terminal layout includes desk position, the information about the transit gate location each WP arrives. If terminal have a two-story lounge, then also need an elevator. Flight Schedules including arriving flights and connecting flight information on the time and the corresponding gate and so on.

Step 2: The main loop

For each time step  $\Delta t$ , we determine WP queues and the appropriate retention time (minutes), and develop optimal allocation of accompanying persons.

Step 3: The establishment of the service queue WP

First, consider the possibility of a small part WP requiring wheelchairs but not booking in advance, which can be seen the part of the accounting WP who required in advance as a fixed ratio, where the wish to 5%, in other words, 5% of the WP no prior booking required wheelchair and escort service.

The time (minutes) is assigned for each WP (including advance booking and no prior booking), it is for them to transfer the flight before the flight take off. According to the lengths of the minutes to re-arrange the service queue,

giving priority arrangement to the WP who cost minimum duration, and insert new to WP, and arrange its services accompanying staff at the same time. This

feature will minimize the total delay time  $T^{fd}$  of flight, in order to reduce the loss of the airline.

Step 4: Optimize distribution service nursing staff

Here, we use Hamming distance  $| \Delta x| + | \Delta y|$  to represent the distance between two points, escort service personnel who is the nearest and also in free is assigned to the WP ranked in the top ranks of the passengers. After an escort service escort a WP, before being arranged in an escort mission, service nursing staff must return to the information desk in another services first.

Step 5: The movement and update status of service personnel accompanying

After determining an escort service personnel to each WP, the escort accompanying staff whose task is not yet complete will travel to accompany their destination within each time step  $\Delta t$ 's, each service personnel will move some distance  $\Delta d$ , which determines a natural velocity  $\Delta d / \Delta t$ . Here we may assume  $\Delta t = 1$  minute, escort service personnel's velocity is 2.5ft / s, mainly in view of there may be a number of other disorders and the affection from waiting passengers in the terminal, this assumption should be reasonable. Thus  $\Delta d = 150ft$  can be obtained.

When the service escort escorts a WP reaching a turnaround port, the state information of service accompanying persons will be updated accordingly. When a service of accompanying persons with wheelchairs reaches a WP's entry gate, but due to flight delays the WP may not arrive, indicating the possibility

of flight delays (probability) with  $P_d$ , in fact, according

to the relevant statistics, we can get  $P_d \approx 0.29$ . For the delayed flight, the length of the delay time obeys exponential distribution.

Step 6: Output calculation results

Loop simulation until all known WP on flight schedules are escorted to their connecting flight gate so far. Once this condition is satisfied, abort the cycle

calculation, then output all the waiting time  $T^{pw}$  of WP. Due to individual WP does not arrive interchange gate in time, the number of accompanying personnel services at time  $t$   $\omega(t)$  increased caused by the total number of totals flight delays time  $T^{fd}$ .

III. CONCLUSION AND DISCUSSION

In the model except that considering the airline wheelchair escort service we also consider that flight delays caused by unreasonable wheelchair-setting. The models calculate the effect of flight delays through multiple airlines actual data statistics. It find out the best airlines' wheelchair settings and three different kinds of operation strategies under the condition of reducing the

operation cost and delay loss effect as much as possible. It also has made a comparative analysis to applicable conditions of different strategies. In addition, this model is simple, considerable comprehensively and it notices all sorts of different situations and different schemes of comparative analysis based on the statistical analysis of actual data. Also it has advantages of pertinence, strongly practicability and operability. In the application of practical problems, it shows its superiority.

In reality, flight is affected by many uncertain factors, such as weather, air traffic and so on, as well as emergency incident. We ignore the impact of these factors in the model to make it simplified. Meanwhile it also makes effects on the model's rationality in the practical application.

With the minimum cost as the main target, although it considers customers' waiting time, it is not enough to set from reality. In fact, the rationality of the data and scheduling scheme that an airline configures wheelchair and ho service attendants in an airport or terminal shouldn't depend on airlines operating minimum cost at that time, but more should pay attention to how the

passengers' satisfaction. Because it directly affects the airline service quality and the potential changes in traffic.

#### ACKNOWLEDGMENT

This work is supported by soft-scientific project of Henan Province (No. 142400410425)

#### REFERENCES

- [1] Airline pricing data. [www.ecpedia.com](http://www.ecpedia.com), 2005.
- [2] Haythornthwaite, C. Online personal networks: size, composition and media use among distance learners. *New Media and Society*, 2, 2, 195–226, 2006
- [3] U.S. Department of Transportation. 2003. Nondiscrimination of the bases of disability in air travel. <http://airconsumer.ost.dot.gov/rules/rules/htm/>. n.d. Airline on-time statistics and delay causes. 2003

Zhang jin: born in 1983, Her research interests include Computer education.

# Design and implementation of Fire fighting robot

Yang. Guikao, Liu. Haibo, Zhang Qing  
Air Force Logistics College, Xuzhou, China

**Abstract**—This paper design a fire intelligent robot model, to the specified region of the rescue fire fighting work. The fire extinguishing robot based on ATmega16 microcontroller as the core, the use of infrared, optical sensor for detecting robot external environment, using pulse width modulation (PWM) method to control the speed of DC motor, steering through the I/O port to control the robot to avoid obstacles, find the fire and fan control on the robot for fire fighting. This system involves the SCM, automatic control, motor principle and drag, interface technology, electronic technology and other aspects.

**Index Terms**—ATmega16SCM; L298; infrared tube

## I. THE DESIGN IDEAS AND STANDARDS

The fire-fighting robot using high performance 8 bit microcontroller ATmega16 low power COMS based on AVR as the core, to simulate fire candle, randomly distributed in the site, In the fire area, when the robot from the starting region starting, advancing in the drive DC motor, using the obstacle detection sensor around obstacles, and in the process of moving the use of probe fire and control the fan light sensor to detect the fire, When the robot to the fire area fire fighting edge, region boundary is detected by a sensor, avoid out of the fire area, so as to control the robot to look for the source of fire, and so on for the whole fire area, and then return to the safe area.

## II. THE SYSTEM STRUCTURE AND PRINCIPLE

The hardware of this system mainly has the motor drive module, fire detection module, the software mainly completes the fire fighting robot program debugging and downloading functions. Through the ATmega16 single-chip microcomputer to control the output PWM signal to control the rotation of the motor, to achieve accurate control of the robot in the external environment under the different, for obstacle avoidance, fire extinguishing. The system structure diagram as shown in figure 1.

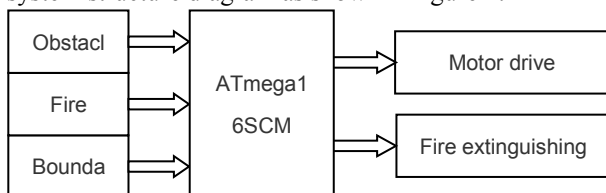


Figure 1 The system structure diagram

## III. THE MAIN HARDWARE CIRCUIT

### A. The Motor Drive Circuit

The circuit is integrated with internal special chip two bridge circuit of L298. Its main features are: high working voltage, maximum working voltage up to 46V; large output current, instantaneous peak current up to 3A, continuous working current of 2A; high voltage and large current containing two H bridge full bridge driver, can be used to drive the DC motor and stepper motor, relay inductive load; Using standard logic level control signal; Has two enable control end, without input signal under the condition of allowed or forbidden device has a logic input end of the power supply, so that the internal logic circuit part work under low voltage; Can be an external sense resistor, will change the amount of feedback to the control circuit. The four transistor is divided into two groups, alternating turn-on and turn off. Schematic diagram shown in Figure 2.

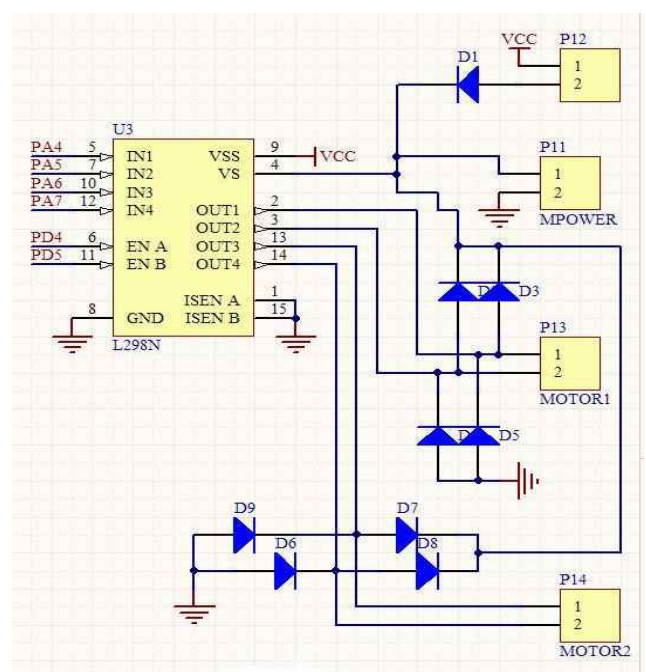


Figure 2 Schematic diagram

### B. Fire detection circuit module

When the receiving tube was found when the fire, its resistance changes, in the circuit is often reflected in the change of voltage and then through the LM339 circuit after shaping can output high level signal is not detected,

the light source is low, the detected light source: high level. SCM acquisition to the high or low level signal, to realize the control of robotextinguishing. Infrared tube itself to detect the distance between the light source is not big, but after this modification improved circuit, by adjusting the circuit diagram of the potentiometer, detection range can be reached from 5 centimeters to 2 meters.

IV. SOFTWARE DESIGN

The software of this system with the C language, the main program to complete the system hardware initialization, subroutine calls and other functions. The main program is shown in figure 3.

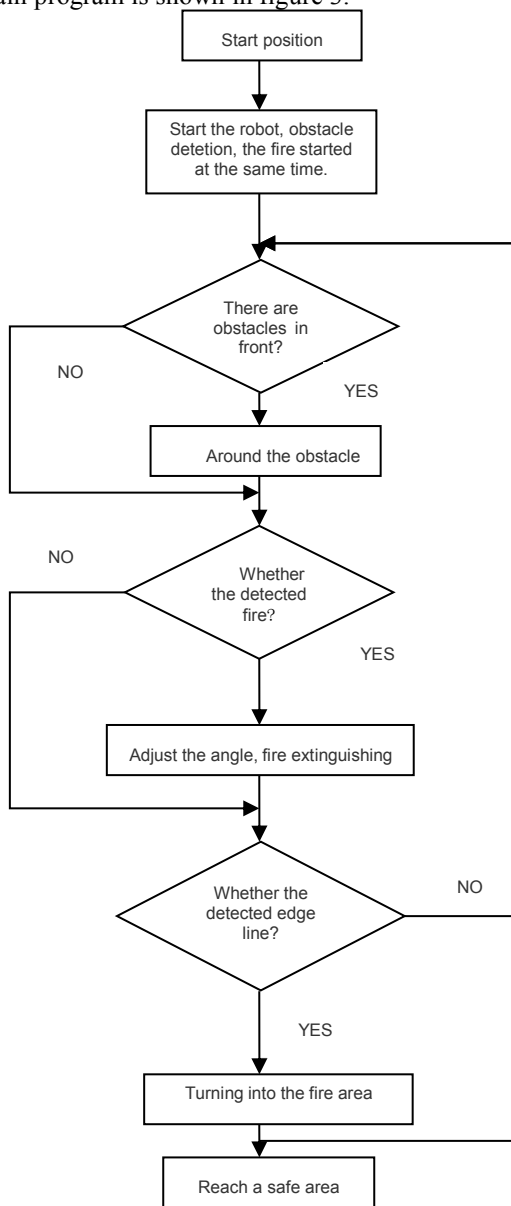


Figure 3 The flow chart of the main program

V. Conclusion

The practice proved that, this design and stable operation, good fire extinguishing robot can complete the task. Through the improvement of old mechanical structure, combined with the special debugging software can achieve the desired goal, the system hardware configuration is reasonable, the control scheme optimization, the realization of accurate control of the robot in the external environment under the different, for obstacle avoidance, fire extinguishing.

REFERENCES

- [1] Liu Guangrui, Robot innovative production, [M]. *Northwestern Polytechnical University press*, 2007.
- [2] Cheng Jirong, Intelligent electronic innovation - Robot making entry, [M]. *Science Press*, 2007.
- [3] Zhang Hongrui, 300 cases of sensor applications design, Beihang University press 2008.
- [4] Duan Xiufang, "How to Improve Teaching Ability Effectively", *Journal Reference of Basic Education*, 2013.
- [5] Ramon lopez.UGVs: making the objective. *Unmanned Systems*.2004.4.

**Yang. Guikao** was born in Tai Zhou, Jiangsu Province on January 2nd, 1981 and graduated from Shaanxi Normal University, Xi'an, China in 2008.

He has worked in Xuzhou Airforce Logistics College in Xuzhou, Jiangsu Province, China since 2008.

Mr. Yang has published more than ten papers in some famous magazines in China.

# Survey on Solving Large-scale Complex Optimization Problems

Fahui Gu<sup>1,2\*</sup>, Kangshun Li<sup>1</sup>, Lei Yang<sup>1</sup>, Yan Chen<sup>1</sup>

<sup>1</sup>School of Information, South China Agricultural University, Guangzhou, Guangdong 510006, China

<sup>2</sup>Department of electronic information engineering, Jiangxi Applied Technology Vocational College, Ganzhou, Jiangxi 341000, China

**Abstract**—The optimization problems widely exist in people's daily life, industrial design, process control and economic forecasting, involving many areas of industry, agriculture, communications, transportation, economic and others. In this paper, we put forward a new multi agent dynamic differential evolution algorithm to solve large-scale complex optimization problems through analysing the existing situation of research on solving large-scale complex optimization problems

**Index Terms**—Large-scale complex optimization problem; Multi-agent; Dynamic differential evolution algorithm

## I. INTRODUCTION

The optimization problems widely exist in people's daily life, industrial design, process control and economic forecasting, involving many areas of industry, agriculture, communications, transportation, economic and others [1]. Through optimization, operating efficiency of the system will be enhanced, all kinds of resources will be reasonable utilization, the energy consumption will be reduced, and the economic benefit will be improved obviously. But with the rapid development of society, the large-scale complex optimization problems are emerging in modern daily life and production, such as layout of sensor in internet of things, spacecraft design, layout of space pipeline, facilities layout in logistics park, resource scheduling in cloud computing, train scheduling and others optimization problems[2-4]. The optimization problems are always nonlinear, non-differential, multi peak and valley, non-convex, high complexity, large scale and high dimension, and the problems will become more complex with the environment.

It is often difficult for us to obtain satisfactory results, if we take the traditional optimization method and engineering experience to solve the large-scale complex optimization problems, even it is difficult to get effective solution.

Therefore, the large-scale complex optimization problems are difficult problems of our research.

## II. A CASE OF THE LARGE-SCALE COMPLEX OPTIMIZATION PROBLEM

In recent years, there are many of the domestic and foreign scholars who have put forward many methods to solve this lar

## III. RESEARCH PROGRESS OF THE LARGE-SCALE COMPLEX OPTIMIZATION PROBLEM

In recent years, there are many of the domestic and foreign scholars who have put forward many methods to solve this large-scale complex optimization difficult problems, such as the Japanese researchers Noman and Iba proposed the improvement using crossover different types of differential evolution algorithm [6]; Xingbao Liu proposed the immune evolutionary algorithm is applied to the high-dimensional optimization problems [7]; Finland scholar Matthieu proposed a new parallel differential evolution algorithm named SOUPDE [8]; Ke Tang et al. proposed a new differential evolution algorithm named GaDE [9]; Slovenia scholar Brest et al. put forward a new algorithm named jDElscop through combining three kinds of mutation and crossover operator parameter control strategy with mechanism of a new population changes [10]; Singapore put forward hybrid differential evolution algorithm [11]; and so on.

It is not doubt that these methods in solving large-scale complex optimization problems have achieved effective results. From the existing solution and the previous international competition in optimization, it is not difficult to find that the differential evolution algorithm is a very competitive method of solving large-scale complex optimization problems [5].

However, the existing differential evolution algorithms for solving large-scale complex optimization problems have the following several problems worthy of further study:

- (1) Local optimum problem. It is necessary to enhance the global search ability, for the results of the existing solving methods for the standard test problem are existing local convergence in different degree.
- (2) The efficiency of solution needs to be improved. The existing methods consume long time to solve the large-scale complex optimization problems, it is need to improve the convergence speed of the solving method.
- (3) The accuracy is not high. From the experimental effect of the existing methods, the general accuracy is not high. It is need for us to enhance the accuracy of the solving method.

- (4) The decomposition mechanism of large-scale complex optimization problems. How to reconstruct the solution space of the problem, and how to design a set of decomposition and transformation operation mechanism are important way of reducing the solution space size and the solving difficulty.

Therefore, the development of novel differential evolution model, solving itself existing question of the existing differential evolution algorithm, improving adaptability of differential evolution algorithm for solving all kinds of optimization problems, enhancing the algorithm's search efficiency, and solving more practical optimization problems in complex high dimension have important scientific significance and application value.

#### IV. MULTI-AGENT SYSTEMS

Multi-agent system (MAS) originated in distributed artificial intelligence research in twentieth century 70 years, is a kind of distributed autonomous system consisting of multiple agents, the system function is through the agent interaction with each other to achieve [12]. Because of its autonomy, distributed, collaborative, parallel, self-organizational characteristics ability, learning ability and reasoning ability, the MAS has natural advantages in describing the dynamics complex systems.

MAS express the structure, function and behavior of the system characteristics in solving complex system problems by communication, cooperation, mutual solution, coordination, scheduling, management and control between each other agent. It has high efficiency to solve dynamics complex optimization problems, and it has very strong robustness and dependability. It has been widely used, such as military, traffic and manufacturing, and achieved good results [13].

In recent years, some scholars feed the thought of multi-agent into evolutionary computation. The evolutionary algorithm can avoid premature through distributed multi-agent parallel structure, the neighborhood structure of the agent can improve population local exploration ability. Such as Weicai Zhong et al, put forward the multi-agent evolution algorithm to improve the solution accuracy through combining the agent structure with genetic algorithm, [14-15]; Xiaoping Zeng et al. add the dynamic chain agent network structure into the genetic algorithm, in order to reduce the occurrence of premature convergence because of the suboptimal individual premature obtaining "apical dominance" [16]; Dakuo He et al add differential evolution operator into multi-agent evolutionary algorithm to improve the updating speed of agent and keep the diversity of population [17]; Yongqing Huang et al introduce more interactive intelligent into evolutionary algorithm to improve the global convergence ability of the algorithm and the local search ability [18]. It is undoubted that Scholars introduce multi-agent into evolutionary computation to solve the prematurity, low precision, low efficiency problem, but most of the researches are limited to static function optimization,

very little researcher continue to improve the multi-agent ideas and introduce multi-agent ideas into the optimization algorithm to solve large scale complex dynamic optimization.

#### V. ANALYSIS OF THEORY AND FEASIBILITY

Based on decomposing large scale complex dynamic optimization problem into a small problem, to research on large-scale complex optimization problems solution in each small problem for the solution basis, just as most human activities involve multiple individuals constitute a social group, large and complex projects also need more professional personnel or organization and coordination to jointly complete.

Each agent in MAS has the ability of self-learning, characteristics of competition and cooperation between agents and agents, reacting to the environment and the agent itself, these characteristics make solving large-scale complex optimization problems become possible.

Agent sensing characteristic on the environment can reduce the hardware requirement and improve the efficiency of solution algorithm. The competitive and cooperative characteristics between agents and agents can coordinate the behavior of many agents to ensure the completion of the whole task collaboration. The self learning ability characteristics of agent can enhance the ability of the agent itself to improve intelligence the body's ability of adapt to the complicated and dynamic environment.

Differential evolution algorithm is put forward to solve the inequality problem with the characteristics of simple algorithm by Storn and Price, which has less control parameters. Scholars use DE algorithm in solving complex optimization problem to obtain certain result. It can be said to have a very good competitive advantage in solving large-scale complex optimization problems. In fact, DE algorithm is a kind of evolutionary algorithm and an intelligent system, the individual is an agent.

We take the individuals of differential evolution algorithm as agent, which can respond to environment, participate in the competition and cooperation, and has self learning ability. We solve large-scale complex optimization problems through the collaboration between agents and the environment, the competition between the agents and the agents.

Therefore, it is feasible that introducing multi-agent into differential evolution algorithm to solve large-scale complex optimization problems.

We will take the following methods to solve large-scale complex optimization problems.

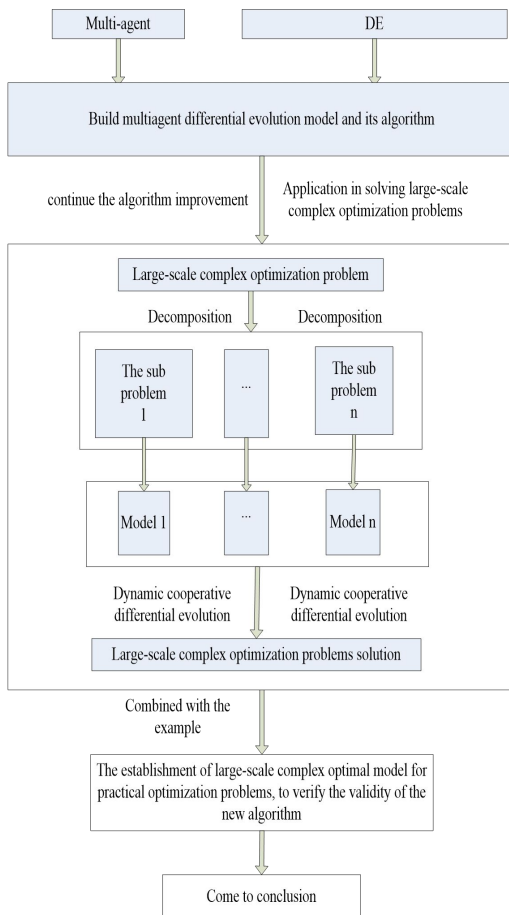


Fig.1. Research method

## VI. CONCLUSION

To sum up, to research on how to introduce the multi-agent thought into the differential evolution algorithm to optimize and improve, how to use multi-agent to enhance the solving ability of the algorithm; how to improve the optimization method for large-scale complex optimization problems, is the practical significance and value to the solution of real-life large-scale complex optimization problems.

## ACKNOWLEDGMENT

This work is financially supported by the Education Department of Jiangxi province science and technology research projects, China (No.GJJ14807)

## REFERENCES

- [1] Haibin Duan. Principle and application of ant colony algorithm. *Science Press*, 2009.[In Chinese]
- [2] Lee EK. Large-scale optimization-based classification models in medicine and biology. *Ann Biomed Eng*, 2007, 35(6):1095-1109.
- [3] Nasiri JA, Fard AM, Naghibzadeh M, Rouhani M. High dimensional problem optimization using distributed multi-agent PSO[C]. In Proceedings of the 2009 third UKSim European symposium on computer modeling and simulation, *IEEE Computer Society, Washington, DC, USA*:245-250.
- [4] Rojas, Yazmin, Landa, Ricardo. Towards the use of statistical information and differential evolution for large scale global optimization. *2011 International Conference on CCE*,1-6.
- [5] Li, X., Yao, X.. Cooperatively Coevolving Particle Swarms for Large Scale Optimization. *IEEE Transactions on Evolutionary Computation*, 2012, 16(2): 1-15.
- [6] Noman N, Iba H. Accelerating differential evolution using an adaptive local search. *IEEE Transactions on Evolutionary Computation*, 2008,12(1):107-125
- [7] Xingbao Liu, Zixing Cai and Yong Wang. Application in high dimensional optimization problems of immune evolutionary algorithm. *control and decision*, 2011,26 (1): 59-64. [In Chinese]
- [8] Matthieu Weber, Ferrante Neri, Ville Tirronen. Shuffle or update parallel differential evolution for large-scale optimization. *Soft Comput*. 2011,15: 2089-2107.
- [9] Zhenyu Yang, Ke Tang, Xin Yao. Scalability of generalized adaptive differential evolution for large-scale continuous optimization. *Soft Comput* ,2011,15:2141-2155.
- [10] Janez Brest, Mirjam Sepesy, Mauc̃ec. Self-adaptive differential evolution algorithm using population size reduction and three strategies. *Soft Comput*, 2011,11,15:2157-2174.
- [11] Shi-Zheng Zhao, Ponnuthurai Nagarathnam Suganthan, Swagatam Das. Self-adaptive differential evolution with multi-trajectory search for large-scale optimization. *Soft Comput*,2011,15:2175-2185.
- [12] KadarB, Monnstoril, SZelkeE. An object-oriented framework for developing distributed manufacturing architecture. *Journal of Intelligent Manufacturing*. 1998,9(2):173-179.
- [13] (US Andrew Ilachinski) Zhixiang Zhang et al. Artificial War: Based on combat simulation. Agent Beijing: *Electronic Industry Press*. 2010,08.
- [14] ZHONG W C, LIU J, XUE M Z, et al. A multi-agent genetic algorithm for global numerical optimization. *IEEE Transactions on Systems, Man, and Cybernetics, Part B: Cybernetics*, 2004, 34(2):1128 - 1141.
- [15] LIU J, ZHONG W C, JIAO L C. A multiagent evolutionary algorithm for constraint satisfaction problems. *IEEE Transactions on Systems, Man, and Cybernetics, Part B: Cybernetics*, 2006, 36(1):1128 - 1141.
- [16] ZENG X P, LI Y M, JIAN Q. A dynamic chain-like agent genetic algorithm for global numerical optimization and feature selection. *Neurocomputing*, 2009, 72(4-6): 1214 - 1228.
- [17] Dakuo He, Guangyu Gao, Fuli Wang. Multi agent differential evolution algorithm. *control and decision*, 2011, 26 (7), 962-972.[In Chinese]
- [18] Yongqing Huang, Qing Lu, Changyong Liang et al. Interactive multi-agent evolutionary algorithm and its application. *Journal of system simulation*, 2006, 18 (7): 2030-2055.[In Chinese]

# Introduction to the Training of Young Teachers' Teaching Ability

Liu. Haibo, Yang. Guikao Jiang Lin  
 Training Department, Air Force Logistics College, Xuzhou, China

**Abstract**—Young teachers are the main parts of teachers and the potential strength of the school. Young teachers' level of teaching will directly influence the overall quality of the teaching in school. So it is important to strengthen the training of young teachers in teaching ability and make them go through the transition from students to teachers smoothly. In the current status of training in teaching ability, some suggestions are given to the construction of teachers' teaching ability system.

**Index Terms**—young teachers; teaching ability; teaching level

## I. INTRODUCTION

Teaching ability is necessary to complete the teaching activities and it also directly influence the teaching quality and efficiency. It is one of the teachers' quality which is shown by teaching practice. The teaching ability of teachers not only affects the teaching efficiency, but also limits the ability structure of the educated men. Some scholars think that innovation ability, research ability and the ability of combining classroom teaching and scientific research are the characteristics of university teachers' teaching ability. Other scholars believe that teachers' ability are made up of the ability to master the basic theory of modern education, information ability as well as communication and cooperation ability. Young teachers are the main parts of teachers and the potential strength of the school. Young teachers' level of teaching will directly influence the overall quality of the teaching in school.

But many teachers in college schools do not graduate from normal colleges. So do the teachers who teach the core courses. Take the teachers majoring in mathematics, foreign language, physics, chemistry and computer in a certain college school for example (in Table 1). The total number of teachers in five staff rooms is 71, among which the number of teachers who are introduced from normal colleges is 19, taking up only 26.8%. Teachers graduating from non-normal colleges are not so skilled as those who are from normal colleges. Most of them do not receive systematic normal education.

TABLE I. INTRODUCTION OF SOME TEACHERS IN A CERTAIN COLLEGE

Majors	Maths	Eng-lish	Phy-sics	Chemis-try	Compu-ter	Total
From normal college	8	7	2	2	0	19

Total number	21	17	7	6	20	71
Proportion(%)	38.1	41.2	28.6	33.3	0	26.8

In order to accelerate the process of young teachers' growth and shorten the transition period from students to teachers, special training institutions must be set up and the training system should also be established which involves the basic teaching skills training, pre-job training, professional skills training and further education training (in Fig.1).

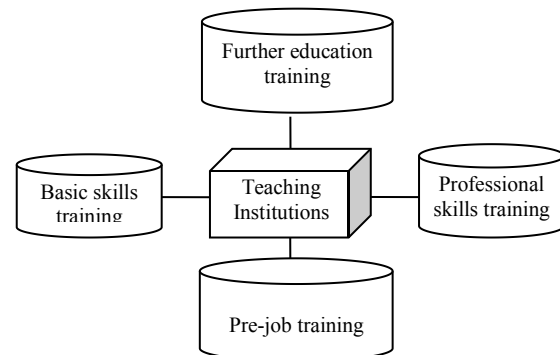


Figure 1 Training system for young teachers

## II. PRACTICE

### A. Combination Of Theory And Practice

To ensure the continuous improvement of young teachers' basic teaching skills, the teaching training institutions should make plan of the basic teaching skills every year. At the same time, they should employ the retired teachers who have rich teaching theory and enough practice as the full-time training teachers. The basic training platform for young teachers is built by various activities.

The contents of basic teaching skills are the basic teaching skills of classroom teaching, the skills of controlling the teaching process and the skills of using multimedia. Among them, the basic teaching skills of classroom teaching include teaching language skills, blackboard writing skills, evaluation skills, changeable skills, presentation skills, questioning skills and so on. The skills of controlling the teaching process involves import skills and strengthening skills.

Young teachers will teach in the future, so rehearsal is a necessary part. Young teachers should be fully prepared for their first rehearsal under the guidance of their tutors. While they are rehearsing, schools will be responsible for the evaluation according to the rules and make some records. On the one hand, the evaluation results provide a reference for young teachers in their future work. On the other hand, it can be used in the second rehearsal for comparison and reference.

Specialized professional skills training is the distinct characteristics of personalized training. It is also a teaching skills training carried out by combining disciplines, specialties and courses under the guidance of the training institutions. Every department should make specific professional skills training plan every year. The plan is made mainly according to the teaching process so as to make young teachers be familiar with the related courses and the contents, focuses as well as the difficulties. In order to give full play to the function of teachers who have rich teaching experience and skills, the schools should select qualified teachers and set up a platform for young teachers by a variety of forms to let them become quickly familiar with the course syllabus, textbooks, teaching tasks and requirements. In this way they can make better analysis in teaching materials and form a strong ability of teaching. The tutors should give the young teachers some guidance about teaching, including rehearsing, preparing the lessons, learning from others and participating the experiments. They should also make comments on the young teachers at the end of each semester, because each semester, young teachers' teaching and training contents are different. "Quality" and "quantity" are two important aspects for young teachers' training. In terms of "quantity", it is required that all the training should be completed according to the teaching plan. In terms of "quality", the second rehearsal is needed and then it should be compared with the first rehearsal to find out if the teaching skills are improving.

#### B. Combination Of Macro And Micro

Pre-job training is to let the young teachers have a better understanding towards the characteristics and requirements of the teaching job, as well as the working conditions, working environments and working targets, so that they can be fully prepared for the better performance in the future.

Dedication is the core of the teachers' ethics construction. With the professional spirit, young teachers will abide by professional ethics and will be ready to delve into the business. Dedication is also the virtue of teachers. Young teachers must set up a strong sense of mission, a sense of responsibility and selfless dedication for the education career. They should be loyal to the education career and be kind and helpful to students,

especially caring for students, understanding students and respecting students. Therefore, the first task of training is to guide young students to establish correct outlook on world, life and values, making them realize that teaching job is a sacred profession and the devotion to education career is a noble choice. So the pre-job training of young teachers must pay attention to professional moral education.

#### C. Training Participation

Enlarging the platform for further training should pay attention to the combination of internal training and external training. Establish and improve the education system with the aim of improving young teachers' teaching ability. Insist on giving priority to working with various forms and strengthening practice to achieve a goal of clear purpose and strong pertinence. Select good young teachers to study in the well-known universities and research institutions at home and abroad. Participate in academic lectures and academic conferences. To fully arouse the enthusiasm of young teachers to attend the training, schools should formulate measures for the management of young teachers' training, provide learning opportunities, giving training funds and keep related benefits while young teachers are receiving the training, so that they can encourage young teachers to participate in further training.

#### REFERENCES

- [1] Jiang Weijin, Guo Xiuqin and Jiang Wen, "Study of College Teachers' Quality," [J]. *Journal of Higher Education Research*, pp. 78-79. 2003.
- [2] Feng Xuchen, "The Theory of Multi-level Construction of Young University Teachers' Teaching Ability Training System," [J]. *Journal of Teaching Education and Profession*, pp. 57-58, 2009.
- [3] Sue Home Linsky, "Tips to Teachers", 2000.
- [4] Duan Xiufang, "How to Improve Teaching Ability Effectively", *Journal Reference of Basic Education*, 2013.
- [5] Dai Jinchu, "The Innovation of Teaching Ability", *Middle School Teaching Reference*, 2013

**Liu. Haibo** was born in Si Ping, Jilin Province on June 18th, 1979 and graduated from Changchun University of Technology, Changchun, China in 2002. He got a master's degree majoring in Computer Application in Xuzhou Airforce Logistics College, Xuzhou, Jiangsu Province, China in 2009.

He has worked in Xuzhou Airforce Logistics College in Xuzhou, Jiangsu Province, China since 2002.

Mr. Liu has published more than ten papers in some famous magazines in China and has completed four National Social Science Fund Projects and National Science Education Programs.

# Study On Heating System By Using Water-Source Heat Pump To Recycle Waste Heat In Power Plants

Bin Yang, Lin Wang, Degong Zuo, Chengying Qi

(School of Energy and Environment Engineering, Hebei University of Technology, Tianjin 300401)

**Abstract:**Based on the water-source heat pump(WSHP) data monitoring system, the author collected and analysed the operating data of heat season in 2012-2013. Therefore, it could have intuitive and comprehensive understanding of the actual operation of WSHP. Results showed the change regulation of the system's COP ,with the supply and return water temperature from the pump and user. And we can also learn that the regulation of the exergy is same as the COP, from the relationship of the Cold and heat source temperature and the system exergy.

**Key words:**Water-source heat pump ; The heating system ; Recovery of waste heat

## I. INTRODUCTION

Waste heat is heat energy not being used or discharged directly. Heat is mainly contained in the gas and water .It , treated and discharged into the environment, will cause thermal pollution. And it also can make the urban heat island effect .With the low efficiency ,the heat from cooling circulating water of power plant with large accounts for more than half of the waste heat The power plant total heat will make ,only one third, into electricity [1].The other will disperse to the surrounding, environment ,through the flue gas, cooling water and other ways .For a long time, it would make negative effects on the environment. Water source heat pump cooling circulating water heat recovery technology can provide heating source for the effective recovery of power plant waste heat .And it also saves the resources of coal and reduce emissions of CO<sub>2</sub>, SO<sub>2</sub> and dust .So we should promote technology of recovery heat pump to solve the current serious energy and environmental problems. Under background, the research provides certain reference for the improvement and development of waste heat recovery heat pump technology of cooling water of power plants[2].

## II. RESEARCH OBJECTS AND METHODS

### A project overview

This topic comes from the heating project of Tangshan Iron industrial waste heat .The system is located in the east of Tangshan City Gangyao Road in Tangshan City , to provide heating in winter for Heshun Park, taoranju, and Gaogezhuang projects. Heating areas 2000000 m<sup>2</sup>.The project adopts 4 Trane centrifugal type water source heat pump unit. Unit type: CDHG2250, nominal cooling / heat: 8790kW/10300kW; nominal cooling / heat input power: 827.1kW/694.6 kW; heat pump rated supply and return water temperature is 50 °C/45°C. Circulating cooling water of power plant is taken by two heat pump units that rated flow rate is 3000t/h, and rated power is 200kW pumped[3] .heat user side circulating water is taken by two circulating water pumps that rated flow rate is 3000t/h and the power of circulating water pump for supplying heat for user 583kW. During the stage of trial operation 2012-2013 year in the stage of trial operation, the heating area is 150000 m<sup>2</sup>, respectively Heshunyuan and Dongfanghong districts. And Heshunyuan residential occupancy rate is 98%.The Dongfanghong area occupancy rate is 37.5%. The heating process only open a heat pump and a circulating water pump[4].

### B The main data monitoring

The main monitoring datas as follows: ① the power plant cooling water supply / return water temperature TH、 T2, instantaneous flow G1, cumulative flow Σ G1, cumulative heat Σ Q1; ② the heat pump supply and return water temperature TL、 T2', instantaneous flow G2, cumulative flow Σ G2, cumulative heat Σ Q, the total energy consumption Σ Nj; ③ the heat pump instantaneous power Pj, the total energy consumption Σ Nj; ④ the temperature of the environment T0. The COP value and the exergy loss rate formulas as follow:

$$COP = \frac{\Sigma Q_2}{\Sigma N_j} \tag{1}$$

$$R' = \frac{1}{\frac{T_0 - T_0}{T_H - T_L} \left(1 - \frac{1}{COP'}\right) - \frac{T_0}{T_c COP'}} \tag{2}$$

(Parameter units: temperature °C , instantaneous flow m<sup>3</sup>/h, and cumulative flow m<sup>3</sup>/h, accumulated heat kWh, instantaneous power kW, total power consumption kWh, area m<sup>2</sup>).

III EXAMPLES OF APPLICATION AND ANALYSIS

Based on the analysis of the working properties , it helps know the working performance of waste heat power plant cooling water recycling heating system[6]. Recording parameters of water source heat pump in the heating period, it can analyze the influence of COP change and exergy loss.

A the affecting factors of COP

The data source, from 2012 ~ 2013 the first heating season, have a frequency of about once every 5 Minutes. Because the user heat load demand is not big, open a heat pump and a circulating water pump. Because of the large amount data, figure 1 and Figure 2 are given to test the period January 11th 9:00 to January 13th 9:00 the two day[7] . The curve are shown water side and user side day supply and return water temperature and heat pump COP respectively.

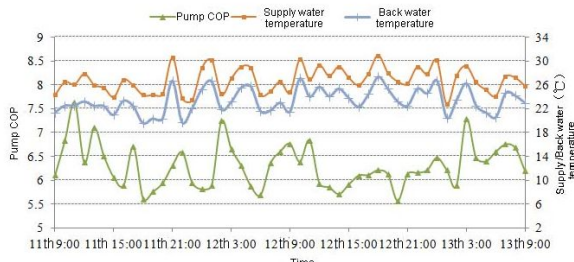


Figure 1. Source heat pump COP changes with the variation supply and return water temperature

From the chart ,we can see that the water temperature will remain basically unchanged, at about 17.2 °C . The return water temperature changes between 13.1 to 14.8 °C ; And the user side of the supply water temperature changes between 39.5 to 41.5 °C and return water temperature is maintained at 35.5 °C . Data show that, at the same time, increasing the user side of the water temperature is inevitably lead to decreased water side return water temperature . Both temperatures and heat load is closely related to the demand of user[8].

As you can see from Figure 1, the power plant circulating cooling water temperature is relatively stable. The supply water temperature changes between 23 °C to 30 °C , and the backwater temperature changes between 20 °C to 26 °C . The COP of heat increases with the increasing temperature of circulating cooling water of power plant. And there is certain lag. The heat pump unit COP was affected by the heat pump significantly. And it increases with the water inlet of low-temperature heat source temperature rise.

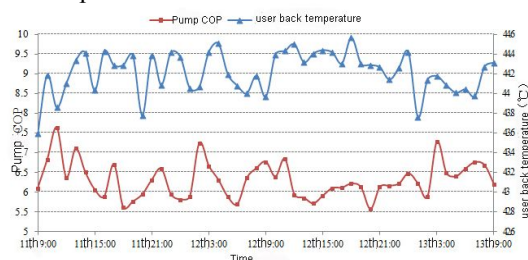


Figure 2. Source heat pump COP changes with the variation user side return water temperature

Because the heat pump water temperature is 50 °C , it can think heat pump water temperature constant. We can be seen from Figure 2, group COP was affected by the heat pump water temperature significantly, and if the pump water temperature increased, the COP will be decrease .There also is a certain lag[9].

The average of heat pump COP throughout the test period was 6.35.And the average COPs of the system is 5.31. The mean value of the compression type heat pump under the same working conditions COP is about 5.So the heating system with heat pump COP is obviously higher than the average current compression type heat pump COP value ,As a result, the heating system of heat pump is more energy saving[10].

B The influence factors of exergy loss of heat pump heating system.

According to the relevant principles of the second law of thermodynamics ,it is proposed that the exergy loss rate of heating heat pump system energy is a index to evaluate the heat pump working efficiency[11].

From the Formula, the factors which most effective compression type heat pump unit exergy loss rate are: hot user heating temperature, temperature of low temperature heat source, heat pump performance parameter COP value. As following analysis of these influencing factors.

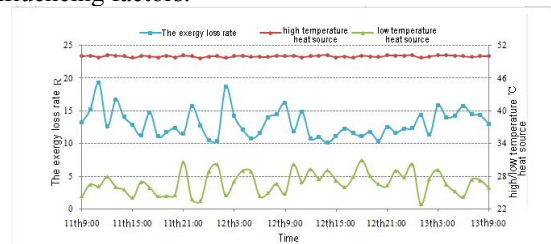


Figure 3. The exergy loss rate of heating changes with the variation high and low temperature heat source temperature .

It can be seen from Figure 3, the high temperature heat source temperature (heat pump water temperature) changes little.It can think the high temperature heat source temperature keep constant. Low temperature heat source (temperature of circulating cooling water of power plant) strongly change. It changes between 25.3 to 28.5 °C . The heating unit exergy loss rate increased with the temperature of heat pump low-temperature heat source increase . In the condition of heat pump heat source temperature remains unchanged , heat pump low-temperature heat source temperature is high. The heating unit exergy loss of the heat pump rate is higher, the thermal economy of the heat pump heat pump heating system operation is betterand the more favorable[12].

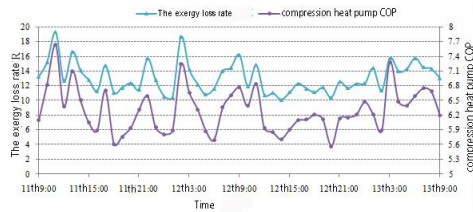


Figure 4. The exergy loss rate of heating changes with the variation COP of the pump

It can be seen from Figure 4 that the heating unit exergy loss rate of heat pump heat pump increases with COP increasing. When the system operate, reducing the return water temperature not only can increase the heat pump cop, but also can make the heating unit exergy loss rate of increase of heat pump. In the heat pump operation process, meeting the requirement of the operation of the unit, temperature differences between supply and return water should increase[13].

IV CONCLUSION

1) Base on water source heat pump heating system, operating at 2012-2013 year, the first heating season, data was sampled and analyzed[14]. And there is a more intuitive understanding of the operation performance of the heat pump system and the situation of energy consumption. In the whole heating season, the influence of heat pump system COP value of water is measured by the user side of supply and return water system. With the increase of supply and return water temperature increases, heat pump COP increases.

2) The unit exergy loss rate of heating heat pump system as evaluation performance index of performance. If increase the supply and return water temperature difference and improve the heat pump COP, it can effectively reduce the exergy loss of heat pump and improve the economic effect.

REFERENCE

[1] M.k.Drost. Air to air heat exchanger performance. *Energy and Buildings*. [J].2009(10): 215~220.  
 [2] B.Sanner, C.Karytsas. Current Status of Ground Source Heat Pumps and Underground Thermal Energy Storage in Europe. *Geothermics*, 2013 (32): 579-588

[3] Narodoslowsky M, Otter G, Moser F. Thermodynamic criteria for optimal absorption heatpump media. *Heat Recovery Systems & CHP*, 2008, 8(4):221~233  
 [4] R.E.Cook. Water Storage Tank Size Requirement for Residential Heat Pump/Air-Conditioner Desuperheater Recovery [C]. *ASHRAE Transactions*, Vol. 96(2)2012, 715~719.  
 [5] W.M.Ying. Performance of Room Air Conditioner Used for Cooling and Hot Water Heating [C]. *ASHRAE Transactions*, Vol. 95(2): 441~444.  
 [6] Keay D.A. Heat pump research and development in USA. *J Heat Recover System*, 1999, 3(3): 165.  
 [7] Uddholm H, Setterwall F. Model for dimensioning a falling film absorber in an absorption heat pump. *International Journal of Refrigeration*, 2012, 11(1):41~45  
 [8] O. Ozgener, L. Ozgener, J.W. Tester A practical approach to predict soil temperature variations for geothermal (ground) heat exchangers applications *Int J Heat Mass Transf*, 62 (2013), pp. 473–480  
 [9] O. Ozgener, L. Ozgener, D.Y. Goswami Experimental prediction of total thermal resistance of a closed loop EAHE for greenhouse cooling system.  
 [10] S. Carlino, R. Somma, A. Troiano, M.G. Di Giuseppe, C. Troise, G. De Natale  
 [11] The geothermal system of Ischia Island (southern Italy): critical review and sustainability analysis of geothermal resource for electricity generation *Renew Energy*, 62 (2013), pp. 177–196  
 [12] C. Steins, A. Bloomer, S.J. Zarrouk Improving the performance of the down-hole heat exchanger at the Alpine Motel, Rotorua, New Zealand. *Geothermics*, 44 (2012), pp. 1–12  
 [13] A.Galgaro, E. Destro, F. Mion STRIGE project – final report University of Padua, Department of Geo-sciences, for the Veneto Region Environment Protection Agency (ARPAV) (2010) [in Italian]  
 [14] D. Banks An introduction to thermogeology – ground source heating and cooling (2nd ed.) Wiley-Blackwell, Chichester (2012)  
 [15] A. Galgaro, J. Boaga, M. Rocca HVSR technique as tool for thermal-basin characterization: a field example in N-E Italy *Environ Earth Sci* (2013)

**Bin Yang** received the M.S degree in Tianjin University of commerce China, the PH.D degree in Tianjin University. He is currently a lecture with the school of Hebei University of Technology, China. His areas of research include renewable energy. His latest research focuses on clean combustion theory and technology and solar thermal storage heating new energy technologies.